CHALMERS
UNIVERSITY OF TECHNOLOGY

Multidisciplinary Optimisation of Geometric Variation and Dynamic Behaviour for Squeak & Rattle

Master's Thesis in Product Development

ASWIN DHANANJAI KRISHNASWAMY
CHIDAMBARAM SATHAPPAN

Department of Industrial and Materials Science
CHALMERS UNIVERISTY OF TECHNOLOGY
Gothenburg, Sweden 2020

MASTER'S THESIS 2020

Multidisciplinary Optimisation of Geometric Variation and Dynamic Behaviour for Squeak & Rattle

ASWIN DHANANJAI KRISHNASWAMY
CHIDAMBARAM SATHAPPAN

Department of Industrial and Materials Science
CHALMERS UNIVERSITY OF TECHNOLOGY
Gothenburg, Sweden 2020

Multidisciplinary Optimisation of Geometric Variation and Dynamic Behaviour for Squeak & Rattle

ASWIN DHANANJAI KRISHNASWAMY
CHIDAMBARAM SATHAPPAN

Supervisor: Mohsen Bayani, Volvo Car Corporation (VCC)
Examiner: Lars Lindkvist, Department of Industrial and Materials Science (IMS)

Master's Thesis 2020
Department of Industrial and Materials Science
Chalmers University of Technology
SE–412 96 Gothenburg, Sweden
Telephone: +46 31 772 1000

Printed by Chalmers Reproservice
Gothenburg, Sweden 2020

Multidisciplinary Optimisation of Geometric Variation and Dynamic Behaviour for Squeak & Rattle

ASWIN DHANANJAI KRISHNASWAMY
CHIDAMBARAM SATHAPPAN
Department of Industrial and Materials Science
Chalmers University of Technology

Abstract

Squeak & Rattle (S&R) are undesired sounds that are caused when two components come in contact with each other. They give the user a feeling of the possibility of a quality issue. In modern premium cars, user comfort is of utmost importance and these undesired sounds must be eliminated. There are various reasons that cause the S&R of which geometric variation is a major contributors. The variation and deviation in the assembly lead to undesired gaps between the components making them come in contact with each other. This also influences the dynamic behaviour of the components leading to resonance. However, varying the location of the attachment points could impact the cause of S&R and requires an optimisation.

A benchmark study was done with various cars in different segments from different manufacturers. Assemblies that are prone to have high Squeak & Rattle were identified and a simpler version of the assembly was modelled. The simplified models were categorized into different model configurations and the optimisation was carried out. A modified Incremental Space Filler program was written to generate Design of Experiments based on certain requirements of the work. The program was created by including all the constraints making the DOE design generation faster. A two-stage genetic algorithm-based optimisation approach was used to identify the right attachment scheme between components. The findings were documented, and the methodology was also applied for some industrial cases with models from real industrial applications like Instrument Panel assembly and Side door assembly.

Keywords: Squeak and Rattle, Multidisciplinary Optimisation, Geometric variation, Dynamic response, Resonance

Acknowledgements

Firstly, we would like to thank our supervisor, Mohsen Bayani from the Solidity group at Volvo Car Corporation (VCC) for his continuous support throughout this thesis work. He has been instrumental throughout the course of work right from the framing of the conceptual idea for the work.

Secondly, we would like to thank Sandeep Shetty from Vehicle Structure Integration at VCC for his suggestions and all other people working in the Solidity Department at VCC for their help and support during our time at VCC. Furthermore, we would like to thank our examiner Lars Lindkvist for his support during the thesis work.

Last but not the least, we would like to thank our parents, friends and family for their constant support and making our time at Chalmers a memorable one.

Aswin Dhananjai Krishnaswamy & Chidambaram Sathappan,
Gothenburg, Sweden
September 2020

Nomenclature

Abbreviations

BSR	Buzz, Squeak & Rattle
CAD	Computer Aided Design
CAT	Computer Aided Tolerancing
DOE	Design of Experiments
FE	Finite Element
GA	Genetic Algorithm
IP	Instrument Panel
ISF	Incremental Space Filler
MAC	Model Assurance Criterion
MDO	Multi-Disciplinary Optimisation
MOGA-II	Multi-Objective Genetic Algorithm – II
NVH	Noise, Vibration, Harshness
RBE	Rigid Body Elements
RD&T	Robust Design & Tolerancing
RSM	Response Surface Method
S&R	Squeak & Rattle
SDO	Single Disciplinary Optimisation
STD	Standard Deviation
VCC	Volvo Car Corporation

Table of contents

List of Tables

1. Introduction

This chapter explains the background of the work carried out along with the research questions. Literature study was carried out and the chapter also includes details about similar works carried out in this area.

1.1 Background

Buzz, squeak, and rattle (BSR) is the automotive industry term for the audible engineering challenges faced by all vehicle and component engineers [1]. Sounds inside a car can be from different sources like engine, tire, etc., but unanticipated noises in the form of squeak and rattle creates an irritating feeling to the passengers and are therefore undesired. NVH engineers deploy different methodologies to reduce these unwanted noises and enhance user comfort.

Squeak & Rattle are nonstationary sounds that occur when adjacent parts come into contact, either impacting or sliding. Geometric variations in the assembly is the top contributor to the sounds and several practices are available to minimize the variations. Some of the methods include optimisation of the attachment points, adjusting the tolerance levels and assembly procedure optimisations. However, the optimisation of the attachment points of the assembly also lead to other problems like affecting the dynamic response of the assembly. This requires a multi-disciplinary optimisation of the geometric variations and the dynamic behaviour of the assemblies. The main aim of this thesis work is to perform a multi-disciplinary optimization on simpler models that would represent assemblies within the car and comparing them with some industrial models thereby resulting in greater understanding of the optimisation behaviour.

1.2 Company

The Master's Thesis has been performed in collaboration with Volvo Car Corporation (VCC) at Gothenburg, Sweden. Volvo Cars is a Swedish car manufacturer which manufactures cars in SUV, station wagon and sedan segments. The headquarters is located at Torslanda in Gothenburg, and is a subsidiary of the Chinese automotive company, Geely Group.

The master thesis work was performed in the Solidity department of Volvo cars. Solidity, as an important attribute within Craftsmanship and Durability Centre of Volvo Cars, is responsible for the solid feeling in the car and reducing the Squeak & Rattle sounds (S&R). The main scope is setting requirements and verification of S&R problems from early phases to after-production launch. One of the major challenges is to improve the competence for using robust design concepts in early phases to shorten lead time by avoiding the late phase changes and reducing the need for physical complete vehicle prototypes.

1.3 Aim

The main aim of the work is to expand the method developed during the previous year at Volvo Car Corporation by performing a multidisciplinary optimization by defining the objective function in a way to satisfy both the dynamic response and static geometric variation. The work will focus on improvements in the following areas:

- To improve the design objectives in postprocessing and optimization.

- To improve the optimization scheme, as a suggestion to expand the used method to a multistage GA optimization.
- To empower generalization of the findings by using wider range of geometry types or more generic geometries.

1.4 Research questions

The work was carried out to answer the following research questions that are within the scope of the project:

- With the aim of S&R prevention by geometric variation and dynamic response analyses, how different the results of a decoupled or multidisciplinary optimization are?
- For different geometries (and assemblies), how the above difference varies? Can the findings be clustered for different types of geometries and attachment schemes?
- What would be the effect of having tolerances in the planar tolerances on measures in normal directions?

The results and findings for the above research questions are explained in Chapter 6.1 - Conclusion.

1.5 Literature Study

Literature study was performed on the optimization of squeak and rattle and relevant literatures and researches were studied.

1.5.1 Geometric variation

Assembled parts usually involve some kind of joining methods like welding, fastening or riveting. The parts that are joined may not be as desired due to the variations in the manufacturing processes. These variations could lead to undesired gaps between the parts and this affects the assembly both functionally and aesthetically. Geometric variation simulations aim to reduce this variation and evaluate different parameters that influence them. The variation simulation is usually supported by other evaluations such as stability analysis to evaluate the positioning systems and contribution analysis to evaluate the tolerances, [2]. An illustration of the robust positioning system is shown in Figure 1.1. Monte Carlo Simulation is used in most variation analysis where the statistical distribution of parameters affects the dimension of interest, [3].

CAT software like RD&T is used to perform variation simulation and it is possible to model connection points as spot weld points or fasteners. The sequence in which the assembly is spot-welded can also be simulated and Wärmefjord, K. [4] has proposed a method for identification and sequence optimization of the weld points within a geometry assurance digital twin. Different strategies for optimization of spot-welding sequence are verified and compared in [5] and the effect of the spot-welding sequence in geometric variation in sheet metal parts is also discussed.

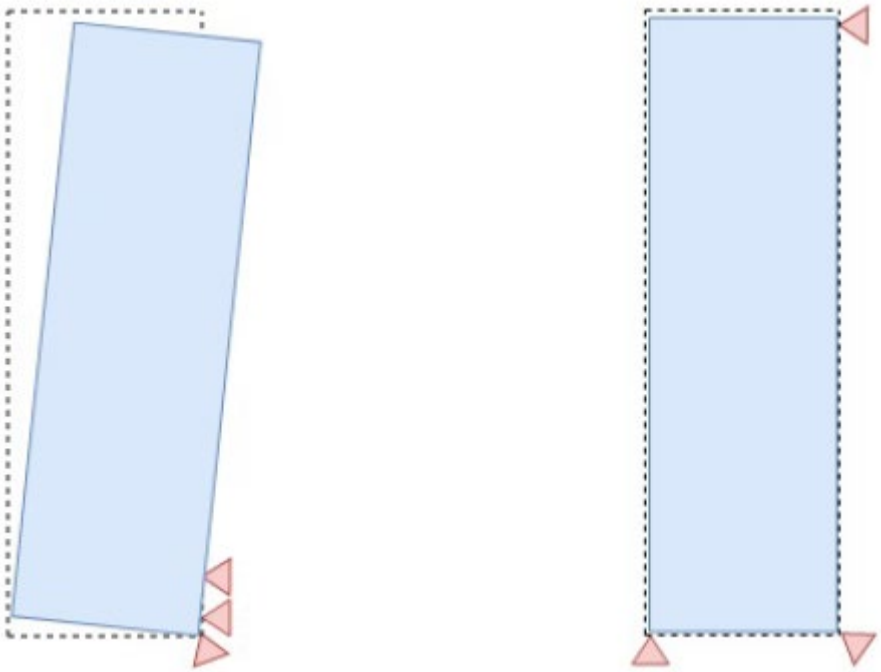

Figure 1.1: An illustration of a robust positioning system [6]

1.5.2 Geometric variation with rattle

In a very demanding industry like Automotive, high quality products are vital to be able to perform better. The comfort and the quality of the product is an important element. One such factor is the squeak and rattle noises.

Squeak are friction-induced noise caused by relative motion resulting from slip stick phenomenon between interfacing surfaces. The squeak could be due to a number of different parameters like the material, coefficient of friction, interface to tangential forces, environmental conditions, lubricants present and so on [1].

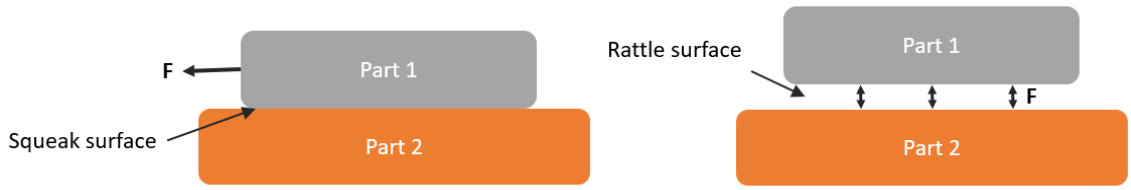

Figure 1.2: Squeak and Rattle occurrence in components

Rattle is an impact induced phenomenon that occurs when there is a relative motion between components/ parts with a short loss of contact. Rattle occurs due to a number of reasons like insufficient attachments, insufficient structural strength, inadequate tolerances, excessive vibrations and so on [1]. The phenomenon of rattle and squeak is illustrated in Figure 1.2.

Trapp and Chen [1] also conclude in their work that one of the effective design practices to avoid S&R is optimized distribution of the fastener positions.

1.5.3 Modal analysis

Her, J et al. [7], describe a case study of a Glove compartment where modal analysis is used to determine rattle performance with the help of a sensitivity analysis.

Fabian Anselmet [8] proposes identification of experimental resonance frequencies in the form of a formula to compare calculated and measured frequencies.

1.5.4 Optimization with geometric variation and modal analysis to reduce rattle

A Multi-disciplinary optimization on the geometric variation and the dynamic response behaviour of the model and its impact on the squeak and rattle would be interesting to evaluate. Previous related work on using optimization study to reduce rattle has used different methodologies and techniques to evaluate rattle.

Naresh Chaudhari [9] has performed a simulation driven S&R Development for Glove box assembly. An FE model was used for the evaluation with force as input excitation from real track data. Different rubber bump stops were evaluated, and the best rubber stop was chosen based on the Pre-tension force and the dynamic force values. The methodology proposed could be used in the initial design to drive the glove box bump stop design.

A similar study done at PSA [10] also proposed a simulation driven design process for S&R in interior assemblies. The mode shapes in which the Relative Modal Contribution are high is identified and an optimization problem is formulated with minimizing the magnitude of the mode shapes as the objective. The gap is measured to evaluate the possibility of rattle occurrence and tolerance data is inputted to the optimization. The optimization also involves a 1-D topology optimization with different possible attachment points.

Most previous works in the S&R rattle reduction studies have involved components like the glovebox assembly, tailgate assembly, side door assembly, cockpit assembly and the roof systems indicating the common S&R occurrence places.

2. Methodology

This chapter explains the methodology in detail in which the work was conducted. The thesis work has three components: Geometric variation, Dynamic response and Multi-disciplinary Optimization. The methodology for each is discussed in this chapter.

2.1 Geometric variation

Geometric variation, being one of the major contributors to S&R is simulated using the software RD&T [11]. Mean shift and Sigma values at required measure points is obtained by simulating the assembly of the components. The attachment points are varied based on the design using a model script. The single disciplinary optimization was performed in two stages: Optimization in the rattle direction and Second Optimisation stage with fasteners in planar directions.

2.1.1 Stage 1: Optimisation in rattle direction

In the first stage of the optimisation, only the fasteners in normal rattle direction is involved. However, two planar fasteners in the form of a dummy is activated for all the designs in the first stage. The dummy fasteners were included in order to fully constraint the components and create a robust boundary condition. The influence of these dummy planar fasteners on the results that were in rattle normal direction was evaluated by performing a study as explained in Section 2.1.1.1. The Optimisation problem can be formulated as:

Objectives: Minimize Six sigma value (Variation), Minimize Mean shift value (Deviation)

Design variable: Coordinates of the Attachment point

Constraints: Number of attachment points

Parameters: Material, Part Topology

The optimisation is done using the software modeFRONTIER. Evolutionary algorithms in the software was used as the optimisation algorithm. For the stage one, an initial population of size 50 which includes some user-inputted EXTREME designs and system-generated ISF designs. The ISF algorithm used to generate the initial population is explained in detail in Section 2.4.2. The number of generations was 50 and hence the total number of designs that were run were 2500. The objectives were plotted to determine the designs that form the pareto front. It was made sure that no designs from the last 5 generations was a part of the pareto front. This was done to understand whether the algorithm was still in the process of finding the global optimum. The pareto points was then plotted in a pictorial form to visualize the attachment point positions. From the different configurations, the best design was chosen.

2.1.1.1 Study on dummy planar fasteners

The study was performed to understand the influence of the presence of dummy fasteners in the objective values in normal rattle direction. A set of 50 designs involving a mix of ISF and EXTREME cases was chosen for the study. The designs were simulated in RD&T with two dummy fasteners in planar directions and the objective values (Mean shift and Six sigma in normal and planar directions) were tabulated. The same designs were again simulated by deactivating the dummy fasteners in planar directions and the results were tabulated.

Table 2.1: Percentage difference in mean shift values with and without dummy planar fasteners

Design ID	Weighted Mean shift normal			Weighted Mean shift planar		
	With dummy	Without dummy	% difference	With dummy	Without dummy	% difference
0	0.0176	0.0170	3%	2.2106	0.4679	372%
1	0.0185	0.0229	-19%	1.7817	0.4688	280%
2	0.0165	0.0155	6%	3.7358	0.4722	691%
3	0.0594	0.0757	-21%	5.0866	0.5282	863%
4	0.0181	0.0178	2%	1.5788	0.4741	233%
5	0.0165	0.0170	-3%	1.3861	0.4682	196%
6	0.0599	0.0463	29%	2.3607	0.4815	390%
7	0.0341	0.0362	-6%	2.0245	0.4787	323%
8	0.0124	0.0163	-24%	2.6981	0.4763	466%
9	0.0324	0.0328	-1%	1.5116	0.4669	224%
10	0.0617	0.0791	-22%	2.0087	0.4931	307%
		Absolute Mean	**13.6%**		**Absolute Mean**	**395%**

The %change in the results for each output was calculated and the results were compared. It was noted that the there was little to no differences in the objectives in the normal direction whereas the difference was very high in the objectives in planar direction. The results for one of the models are tabulated in Table 2.1. The study was performed on different models and the results are shown in Table 2.2.

Table 2.2: Percentage difference in mean shift and six sigma values for different models in planar and normal directions

Model No.	Mean shift normal	Mean shift planar	Six sigma normal	Six sigma planar
1	13.6%	496%	29%	612%
2	58%	67%	47%	71%
3	28%	101%	18%	89%
10	43%	626%	3%	623%
13	4%	41%	7%	47%
14	81%	148%	0.04%	0.12%

2.1.2 Stage 2: Second optimisation stage – planar

The best design chosen from the first stage of the optimisation forms the base for the second stage optimisation. The dummy fasteners are deactivated and the number of attachment points in the planar direction is decided. Objectives were also activated in the planar direction. The attachments points were activated in planar directions and a full factorial DOE is possible given the smaller number of total designs. The results are then plotted and again visualized in the pictorial form. Thus, the design from the stage one optimisation is made fully constrained by choosing the optimum planar fasteners. The schematic representation of the assembly with measure points and design space is shown in Figure 2.1.

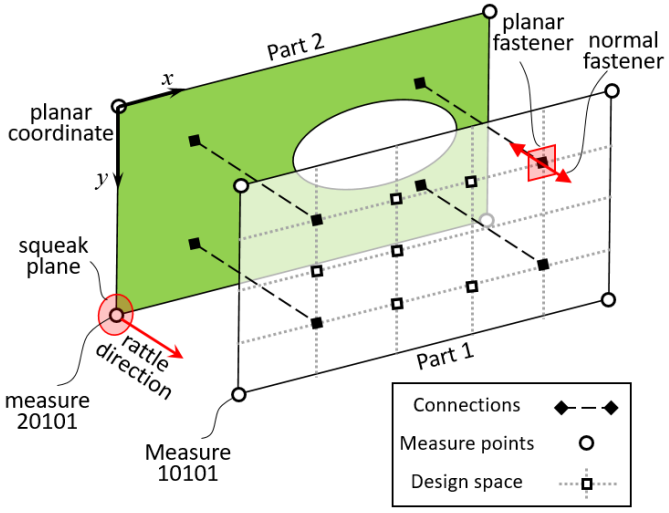

Figure 2.1: Schematic representation of the assembly with the design points and measure points [12]

2.2 Dynamic response

A similar two stage approach for the Dynamic response was followed. The two objectives for the optimisation are resonance occurrence risk and mode shape similarity. The Optimisation problem can be formulated as:

Objectives: Minimize Resonance risk, Minimize Mode shape similarity number

Design variable: Coordinates of the Attachment point

Constraints: Number of attachment points

Parameters: Material, Part Topology

For the first stage optimisation, attachment points in the form of CBUSHs is activated only in the rattle direction. This is done by changing the stiffness in the required direction. Two planar CBUSHs serves as the dummy fasteners in this case. A MATLAB code changes the stiffness of the CBUSHs as per the design. The two objectives for the optimisation are Resonance occurrence risk and mode shape similarity. Mean line factor and Percentile values are the two parameters with which the Resonance occurrence risk is calculated. A study was performed to determine the right mean line and percentile values. The study performed is explained in Section 2.2.1.

In addition to the displacement, velocity and acceleration, phase data for each frequency was also outputted and used in the calculation of number of resonances to account for the phase shift. The mode shape similarity number is obtained as a MAC number from 0 to 100.

In the second stage of optimisation, the best design from the stage 1 was optimized for different positions of planar fastener. The fasteners were activated in the planar directions by modifying the stiffness of the CBUSH in the X and Y direction. A full factorial DOE was performed in this second optimisation. The pareto was plotted and the best design was chosen. Unlike RD&T, simultaneous Nastran simulations could be run, and hence concurrent designs are possible thereby reducing the time taken for the optimization.

2.2.1 Sensitivity analysis of Mean line factor and Percentile values

The study was performed to identify the mean line factor and percentile values for the calculation of total resonance occurrence. The Displacement is plotted against the frequency for both the parts as shown in Figure 2.2Figure 2.2: Dynamic Stiffness Vs frequency plot for resonance frequency identification. The thick black line represents part 1 and the thick green line represents part 2. The thin black line and black dashed line represents the mean line and percentile value of part 1 respectively. Similarly, the thin green line and green dashed line represents the mean line and percentile value of part 2 respectively.

The mean line is the average value of the displacement over the frequency span, for all node point, per part. This mean line was also multiplied with a factor ranging from 0.3-1.0 to experiment with, seeing how the number of resonance changes with varying mean line factor. The percentile line is calculated by the percentile of each curve per node and part. Thus, if a percentile of 80 is used, only the top 20% of the eigenfrequencies can contribute to resonance. This threshold/percentile can vary between 10^{th} – 90^{th} percentile.

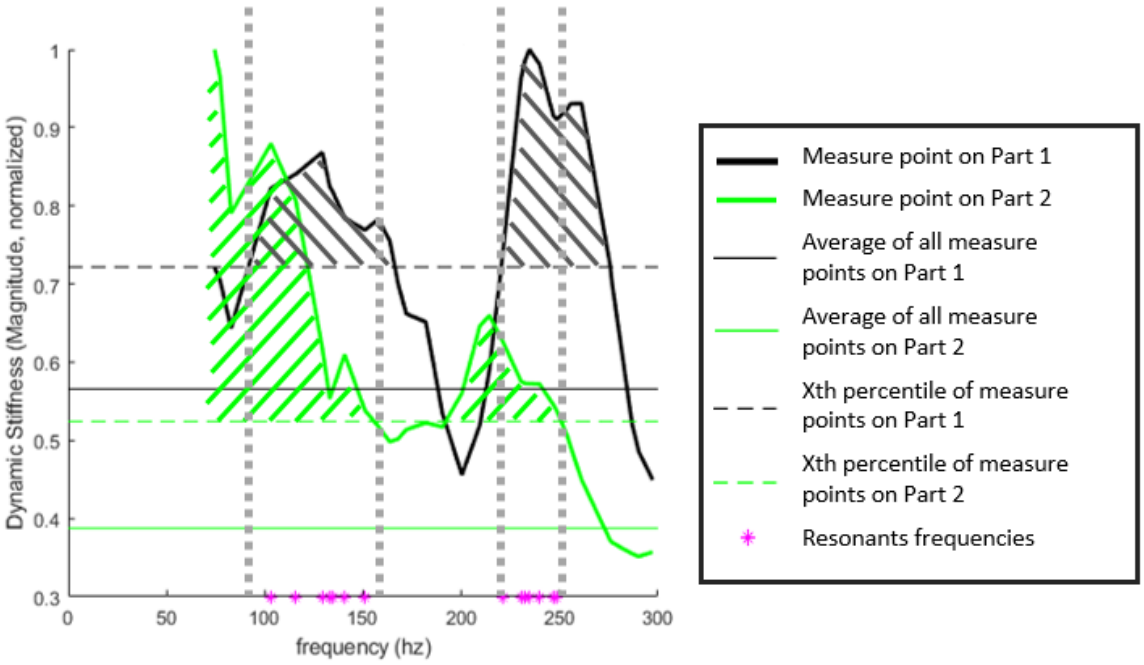

Figure 2.2: Dynamic Stiffness Vs frequency plot for resonance frequency identification

The plot shows which eigenfrequencies can contribute to resonance. For an eigenfrequency to count as a resonant contributor, the dynamic stiffness value of the curve must be above the mean line and percentile line. The black and green hatched portions in the plot indicates the regions where the dynamic stiffness value for both the parts falls above their respective percentile and mean line values. The frequencies in this area are significant with respect to resonance. If the given frequency is significant for both the parts, it can cause resonance. In the

plot, the resonance frequencies are marked with a purple asterisk (*). The total number of resonances is the sum of all resonance frequencies identified.

With the help of displacement data, velocity data and the total number of resonance for each measure point, the resonance risk number can be calculated. This number provides an indication on the severity of the resonance. To calculate the resonance risk in normal direction, the total number of resonance in normal direction is multiplied with rattle factor. The rattle factor is the product of relative displacement and the relative velocity in normal direction. To calculate the resonance risk in planar direction, the total number of resonance in planar direction is multiplied with the squeak factor. The squeak factor is the product of relative displacement in normal direction, relative displacement in planar direction and relative velocity in planar direction.

The sensitivity analysis was done using MATLAB by iterating the mean line factor and percentile values for each design cases. The design cases were extreme cases of each configuration selected. For each design case, the mean line factor was iterated from 0.3-1 and percentile value was iterated from 10-90. Hence, a total of 72 iterations were run and the total resonance occurrences were identified. To compare the sensitivity, the standard deviation and mean of the total Resonance occurrence risk was calculated.

The ratio between the standard deviation and the mean was chosen as the metric to identify highly sensitive areas (STD/MEAN). A sample table for some of the iterations is shown in Table 2.3. These values were then plotted in a 3D plot to visualize the sensitive areas as shown in Figure 2.3.

Table 2.3: Sample table depicting the calculation of mean, standard deviation and the mean/STD metric for some of the iterations

Percentile	Mean line	Design 1	Design 2	Design 3	Design 4	Design 5	Mean	STD	STD/Mean
10	0.3	2309	4628	4628	2309	2309	2889	1003.99	0.35
10	0.4	2309	4628	4628	2309	2309	2889	1003.99	0.35
10	0.5	2309	4628	4628	2309	2309	2889	1003.99	0.35
10	0.6	2309	4628	4628	2309	2309	2889	1003.99	0.35
10	0.7	2309	4628	4628	2309	2309	2889	1003.99	0.35
10	0.8	2309	4628	4628	2309	2309	2889	1003.99	0.35
10	0.9	2309	4628	4628	2309	2309	2889	1003.99	0.35
10	1	1942	4628	4628	1942	1942	2614	1162.70	0.44
20	0.3	2051	3427	3427	2051	2051	2395	595.80	0.25
20	0.4	2051	3427	3427	2051	2051	2395	595.80	0.25
20	0.5	2051	3427	3427	2051	2051	2395	595.80	0.25
20	0.6	2051	3427	3427	2051	2051	2395	595.80	0.25
20	0.7	2051	3427	3427	2051	2051	2395	595.80	0.25
20	0.8	2051	3427	3427	2051	2051	2395	595.80	0.25
20	0.9	2051	3427	3427	2051	2051	2395	595.80	0.25

The analysis was performed for all the different model configurations and the sensitive portion was identified. The common sensitive areas for all the configuration was identified and the resulting mean line factor and percentile values were chosen for the identification of the total Resonance occurrence risk objective. The values are summarized in Table 2.4.

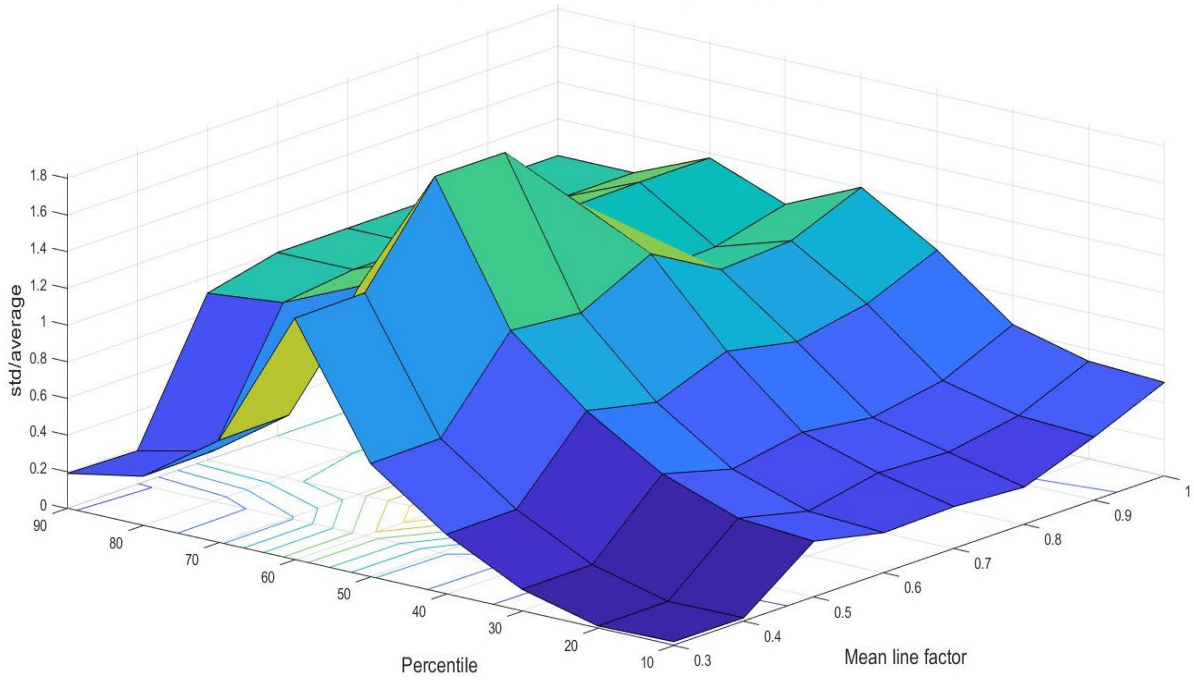

Figure 2.3: 3D plot of the metric (STD/mean) Vs mean line factor and percentile values

Mean line factor value of 0.7 and 70th percentile lied in all the sensitive portions of all the configurations and hence these values were chosen.

Table 2.4: Table depicting the sensitive portions for different model configurations

Config number	Mean Line factor	Percentile
1	60-80	0.3-1
2	50-70	0.3-1
3	70-90	0.3-1
9	60-70	0.3-1
	80	0.5-1
	90	0.3-0.5
10	50-60	0.3-1
	70-80	0.3-0.7
12	50-70	0.3-1
	90	0.6-1
13	70-90	0.3-1
	60	0.7-0.9
14	80-90	0.6-1

2.3 Constraints

Constraints are necessary to bound the input variables generated. For this optimisation, three constraints were used.

2.3.1 Gap elimination constraint

This constraint is used to avoid having designs with attachment points that are not a candidate in the model. The candidates are in the form of a grid like 8 X 5 and for model configurations where the attachment points can only be on the outer edges or if there is not a possibility to have a fastener in that particular position, the candidates must be neglected. This constraint eliminates the possibility of creating such designs.

2.3.2 Number of attachment point constraint

This constraint is used to limit the number of attachment points in a design. The number of attachment points is determined by the total number of input variables. However, if two or more input variables generates the same value, the number of attachment points activated in that design would be less than the desired number of attachment points for that model. Thus, the constraint always makes sure that the values of the input variables are always unique values.

2.3.3 Sorting constraint

This constraint is used to make sure that there is always only one way of writing one design. A design with 8 attachment points can be written in 8! different ways as shown in Figure 2.4. The two designs showed in the figure activates the same attachment points but according to the optimiser, they are two different designs and runs the same design again. This constraint sorts the design in ascending order such that the value of any input variable is always smaller than the value of the next input variable.

Figure 2.4: Design comparison in sorting constraint

The sorting helps in the reducing the time taken for the optimisation and identifies the global optimum much quicker. Without the constraint, the same attachment point configuration would be run multiple times by the optimiser and could feature in the population multiple times.

2.4 DOE & Optimisation algorithm

2.4.1 Incremental Space Filler

Incremental Space filler or ISF is a DOE algorithm which was used to create the initial DOE population for the optimisation. It is an augmenting algorithm which sequentially adds new design configurations to a database by maximizing the minimum distance from the existing points (optimization of the maximin criterion) [13].

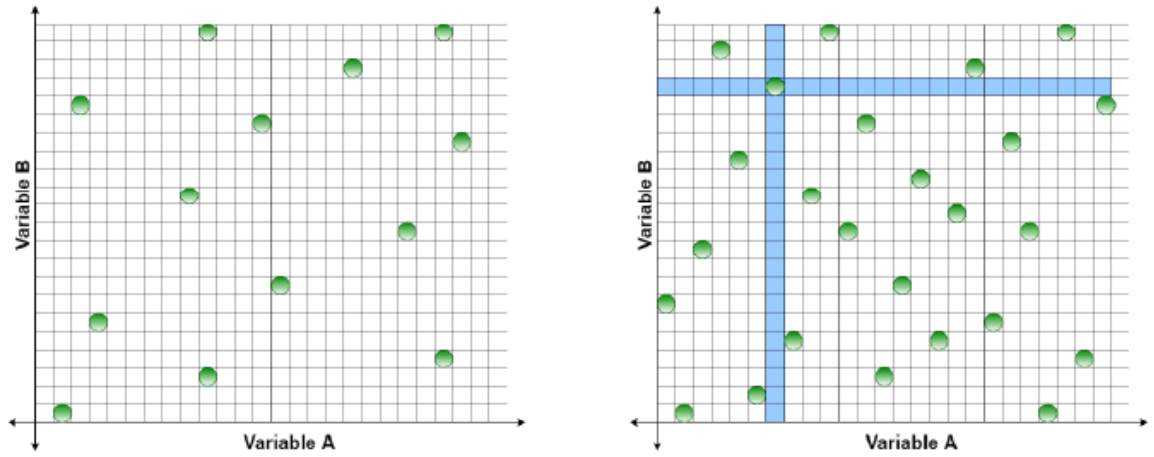

Figure 2.5: Incremental Space Filler algorithm [14]

Incremental space filler is useful for generating a uniform distribution of points in the input space. It considers the existing points in the database, and it adds new points in order to fill the space in a uniform way as shown in Figure 2.5. This algorithm is particularly suited for Response Surface training as it increases the RSM approximation quality and reliability [15].

2.4.2 Modified Incremental Space Filler

ModeFRONTIER has a limitation of generating 256000 designs in the DOE and hence DOE cannot be generated more than that number even though a lot of designs would be unfeasible due to the constraints. To overcome this, a modified ISF was programmed using MATLAB that will generate a DOE by satisfying all the constraints and equally spaced just like a conventional ISF algorithm. These designs could then be fed into modeFRONTIER and the optimisation could be run.

The modified ISF was programmed in such a way that the values assigned to each variable is equally spaced across the design space. To achieve this, input parameters such as the total number designs required, total number of attachment points, maximum number of attachment points in X-direction and maximum number of attachment points in Y-direction is obtained from the user. The program then calculates the maximum number of times the same value can be assigned to an input variable. This is done by calculating the total design slots (number of designs * number of variables) and dividing it by the number of discrete values possible for the variable.

For example, if we require a total of 10 designs with 4 input variables and if each variable can be assigned a value between 1 to 8, then the maximum number of times a value can be assigned to any input variable is calculated by (10*4)/8 = 5. One single value cannot be repeated more than 5 times in the design space. This value is the threshold limit of each value.

The program initially creates a base value set for X-direction and Y-direction that consists of all possible values that can be assigned to a variable. For the first design, the values are assigned on a probabilistic manner such that the first value in the base set has a greater probability of being assigned to the first input variable. This is to make sure that there are enough values available to be assigned to the rest of the input variables. This method also ensures that the designs will always be sorted in ascending order. The probability factor is calculated with the total number of input variables and the total number of discrete values the variables can be assigned. Each value will have a probability factor range and the value is selected if the random number generated falls within its range.

Once all the input variables in X-direction are assigned a value, input variables in Y-direction is assigned a value from the Y base set. Since the value of the variable in the X-direction is known, it is possible to choose a respective Y base set, thereby complying with the gap elimination constraint. In case of configurations where the attachment points are only around the edges, Y value could only have the minimum value and maximum value in the base Y set for all X values except the first and last value.

The design is then passed through a X counter and Y counter which counts the total number of times each value is assigned. The whole process is repeated to generate the following designs. At the end of each design, the X and Y counter is updated. If any of the value reaches the threshold limit, the value is removed from the base set. For the next design, it is not possible to assign this value to a variable since it is not available in the base set.

At the end of each design, the design is checked if it satisfies all the three constraints previously explained in section 2.3. The process is repeated until the required number of DOE is reached and all the design space has been assigned a value.

2.4.3 Genetic Algorithm

Genetic algorithm is an evolutionary algorithm and is preferred to solve multi-objective problems. The convergence rate to reach the global optimum is better in this type of algorithm. MOGA-II or Multi Objective Genetic Algorithm - II in modeFRONTIER is the proprietary version of the multi-objective genetic algorithm that uses a smart and efficient multi-search elitism which is able to preserve excellent (Pareto or non-dominated) solutions without converging prematurely to a local optimum [16]. It uses directional crossover and elitism in addition to classical crossover, mutation and selection. The following are the steps followed in MOGA:

1. The algorithm starts with an initial population with an empty elite set. The following generation population is created by using different MOGA operators like
    a. **Selection:** A design is copied to the next generation without any changes
    b. **Mutation:** The genes are mutated randomly to create a new design as shown in Figure 2.6

Figure 2.6: Mutation

    c. **Classical crossover:** Two parents are selected, and the genetic material are exchanged to form an offspring as shown in Figure 2.7. Classical crossover aims to produce better characteristics in the offspring than the parents.

Figure 2.7: Classical crossover

    d. **Directional crossover:** This is based on the assumption that the direction of improvement could be found by comparing the fitness of the individuals. The new design in the next generation is created by moving in a randomly weighted

direction computed based on the direction vector of the parent individuals as shown in Figure 2.8.

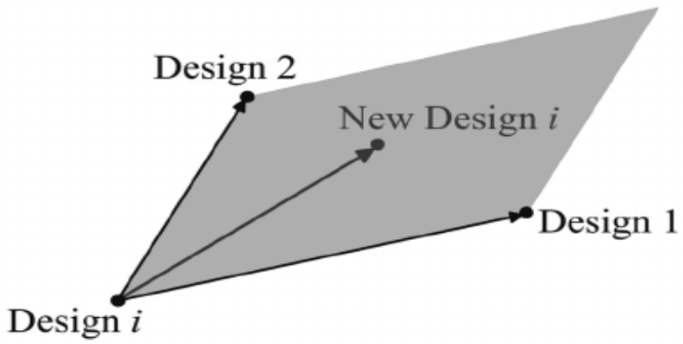

Figure 2.8: Directional crossover [16]

The MOGA operator to create a new design is chosen on a probabilistic manner and vary from generations to generations.

2. The objective fitness function is calculated after creating the population of the generation. Fitness scaling and fitness sharing techniques are performed to avoid premature convergence or convergence to a local minimum.
3. All non-dominated designs are moved to an elite set. The elite set is constantly updated, and repeated designs are removed.
4. Designs from the elite set and designs created by the MOGA operators form the population of the next generation.
5. The process is repeated until the specified maximum number of generations is reached.

2.5 Multi-Disciplinary Optimisation

Similar to the single disciplinary optimisation, a two-stage optimisation was performed for the MDO as well. The two objectives for the optimization was Geometric variation and Dynamic response. The Optimisation problem can be formulated as:

Objectives: Minimize Dynamic response, Minimize Geometric variation

Design variable: Coordinates of the Attachment point

Constraints: Number of attachment points

Parameters: Material, Part Topology

The mean shift was also multiplied by a multiplier to normalize the value with the six sigma. Similarly, in the dynamic response objective, the resonance occurrence risk and the mode shape similarity were summed. A multiplier was multiplied to the mode shape similarity to normalize it with the total resonance occurrence. The optimisation was run in MOGA and the results were plotted to form the pareto. The best design was chosen to perform the second stage of planar simulations. Planar fasteners were activated and the best design with the combination of normal and planar fasteners were obtained. The flowchart is represented in Figure 2.9.

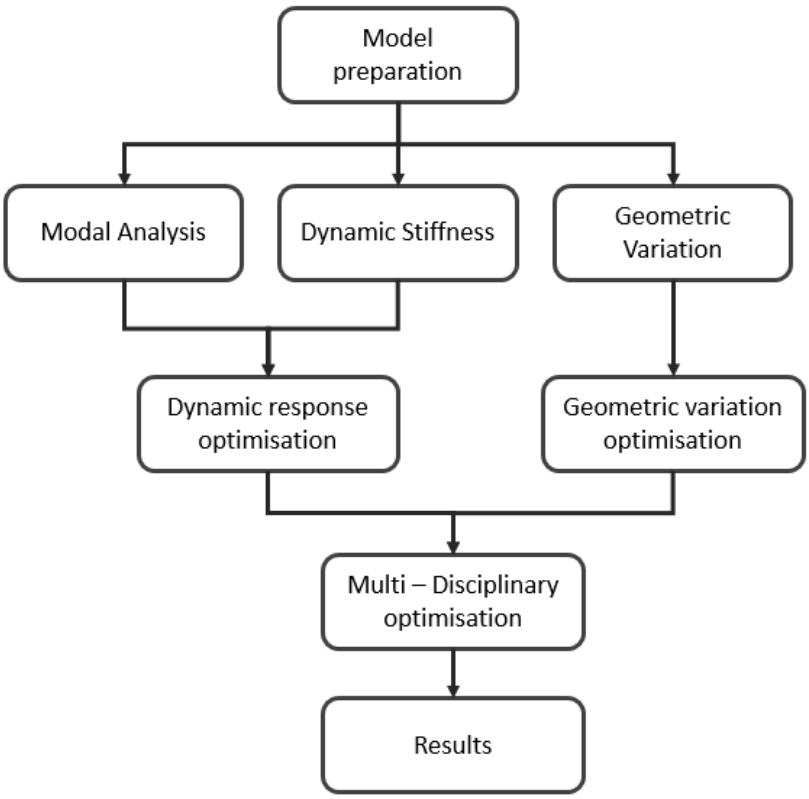

Figure 2.9: Flowchart of the optimisation methodology

3. Modelling

3.1 Model Selection

A study was performed to identify assemblies that were potential candidates for squeak and rattle across all car segments of VCC, for which a tool called A2MAC1 was used. A2MAC1 is a powerful automotive benchmarking tool which offers the most comprehensive and detailed documentation of vehicles, equipment, systems and parts of manufacturers worldwide. They are delivered in an intuitive user interface via a web accessible software where the possible components which can be subjected to squeak & rattle behavior were identified. The components are listed in Table 3.1.

Table 3.1: Table containing the components prone to squeak and rattle

S.No.	Component
1	Front Bumper, license plate and inner frame
2	Central re-inforcement under tunnel console
3	Hood and insulation
4	Hood and seal hood
5	Side mirror front shell and shell
6	Sunroof and headliner filler
7	Pedals and pedal support
8	Transfer box
9	Tunnel console
10	Seat rail

A benchmarking study for the type of fastening and number of attachment points for the above components in different models was carried out using A2MAC1. The models chosen for the study included VCC's car models and from VCC's competitors. The models are listed below:

1. Compact luxury crossover SUV – Volvo XC40
2. Compact luxury crossover SUV – BMW X3
3. Mid-size luxury crossover SUV – Audi e tron
4. Mid-size luxury station wagon – Volvo V60
5. C segment/small family car – Mercedes A – Class

Factors such as type of fastening, number of attachment points, location of attachment points, type of material and their shape were thoroughly studied and compared with VCC's solution.

The identified assemblies were complex models and they were categorized into several categories based on their type of structure (for example plane-plane, structure-panel so on) These models were modelled into simplified geometries using CAD. The Table 3.2 shows the list of geometries and their attachment types.

Table 3.2: Table containing the details of geometry type, measure and the type of attachments for each model configuration

Config	Category	Component 1	Component 2	Attachment	Measures
1	Plane - Plane	Flat Panel	Flat Panel	Attachment Outside	Measures Outside
2	Plane - Plane	Flat Panel	Flat Panel	Attachment Outside	Measures Inside
3	Plane - Plane	Flat Panel	Flat Panel	Attachment Inside	Measures Outside and Inside
4	Plane - Plane	Curved Panel	Curved Panel	Attachment Outside	Measures Outside
5	Plane - Plane	Curved Panel	Curved Panel	Attachment Outside	Measures Inside
6	Plane - Plane	Curved Panel	Curved Panel	Attachment Inside	Measures Outside and Inside
9	Beam - Panel	Flat panel	Beam	Attachment along the beam	Measures along the beam
10	Structure - Panel	Structure	Flat Panel	Attachment Outside	Measures Outside and Inside
11	Structure - Panel	Structure with one side open	Curved Panel	Attachment Outside / Hinged at one end	Measures Outside and Inside
12	Structure - Panel	Structure	Flat Panel with hollow centre	Attachment Outside	Measures Outside
13	Structure - Structure	Structure	Structure	Attachment Outside	Measures Outside
14	Panel - Panel	Flat Panel	Flat Panel perpendicular to component 1	Attachment in both components	Measures at the intersection

The geometries were of free size and the dimensions for each configuration is shown below.

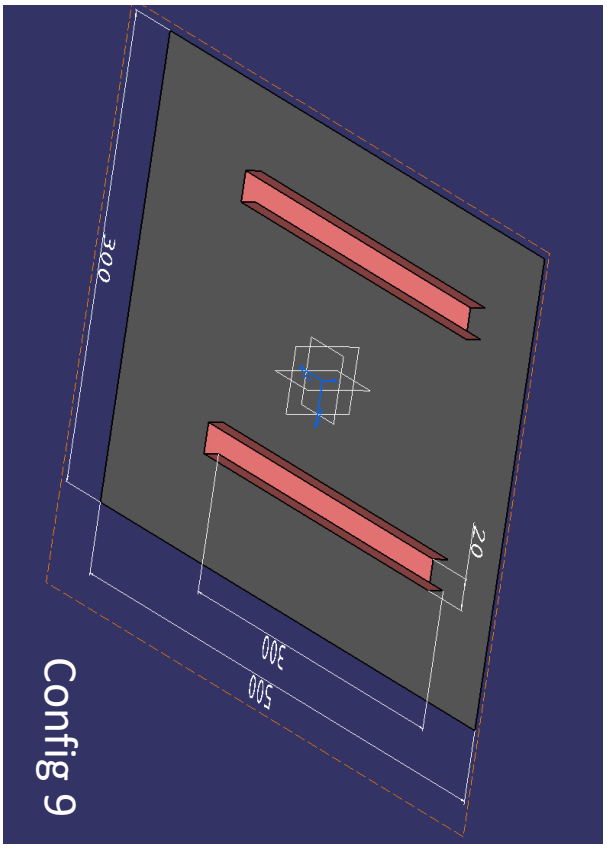

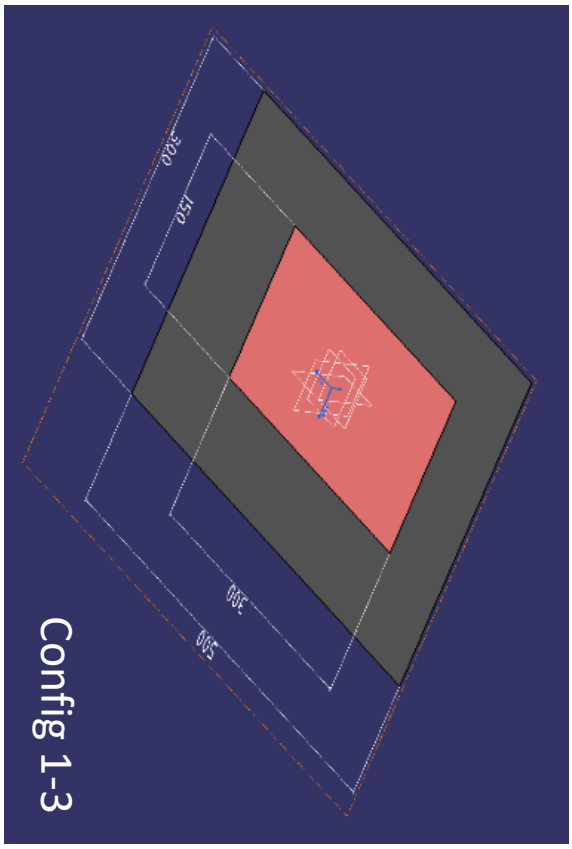

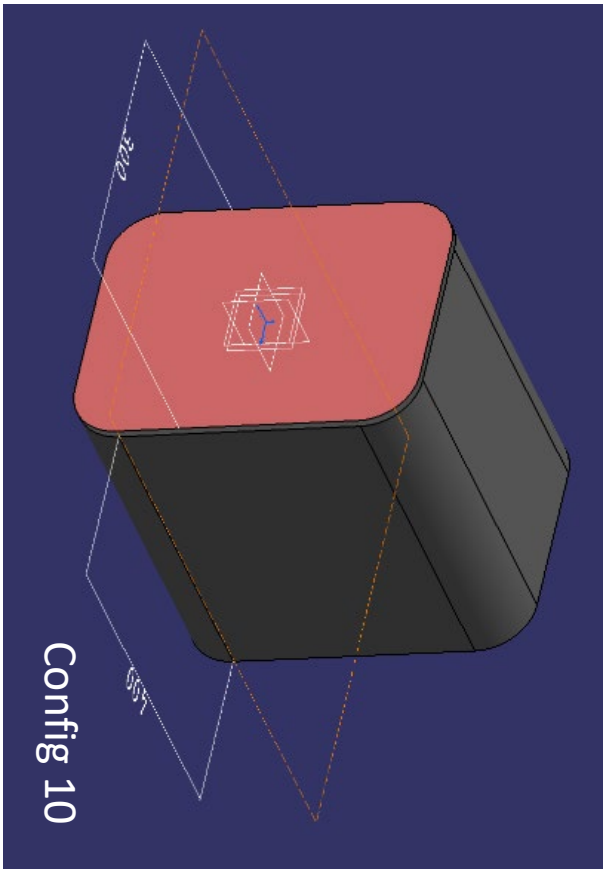

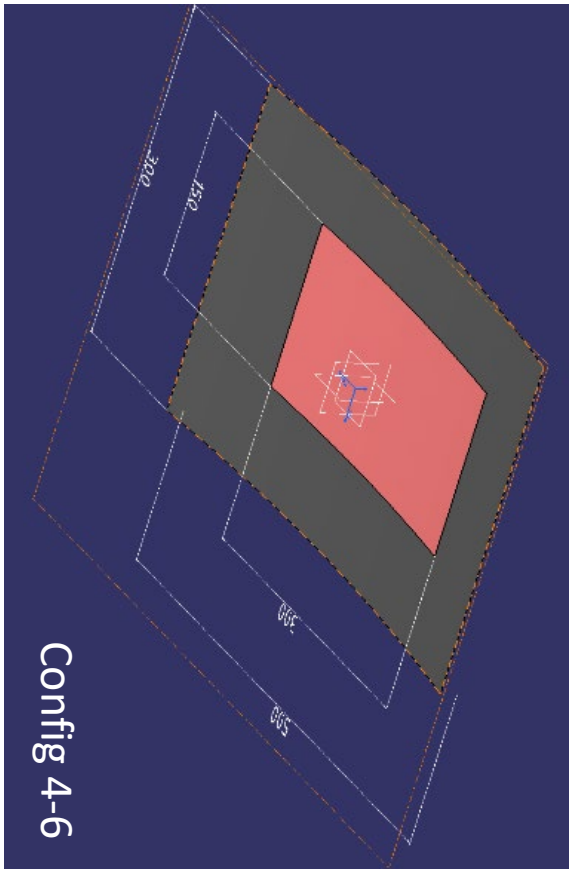

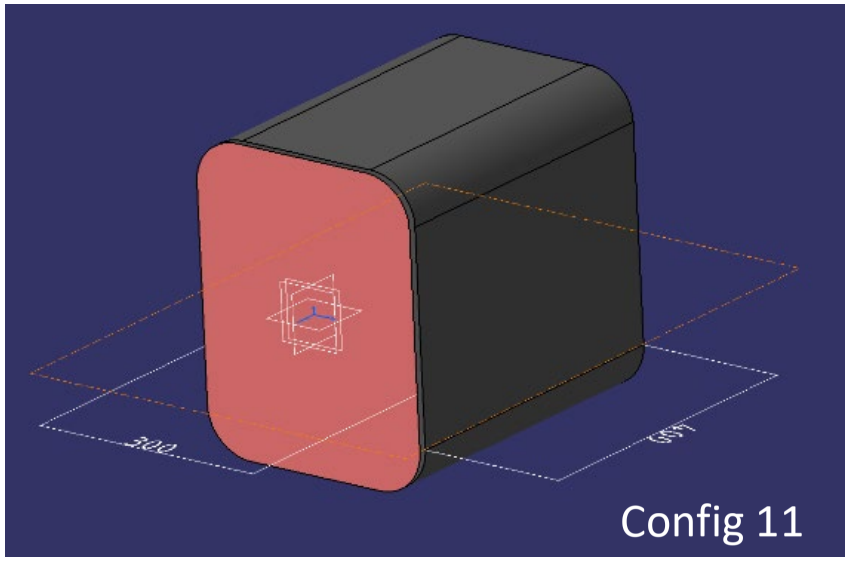
300
450
Config 11

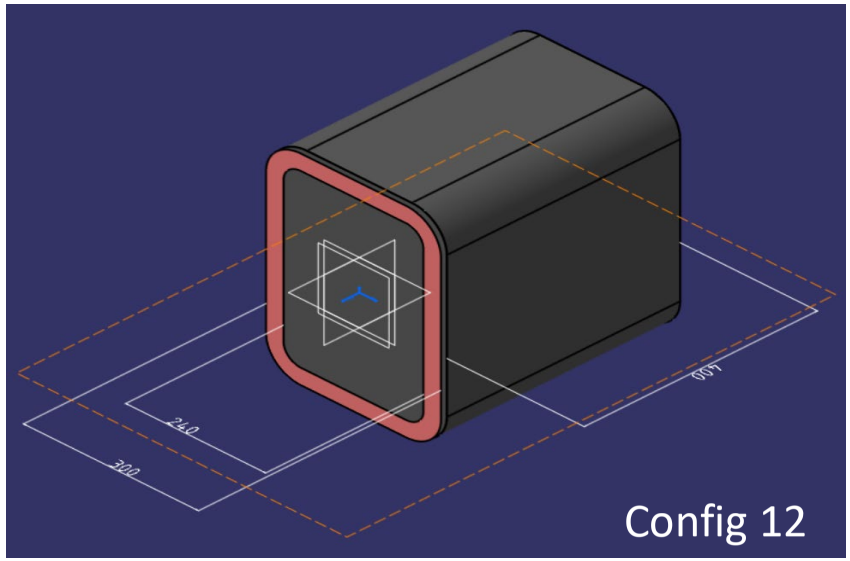
240
300
400
Config 12

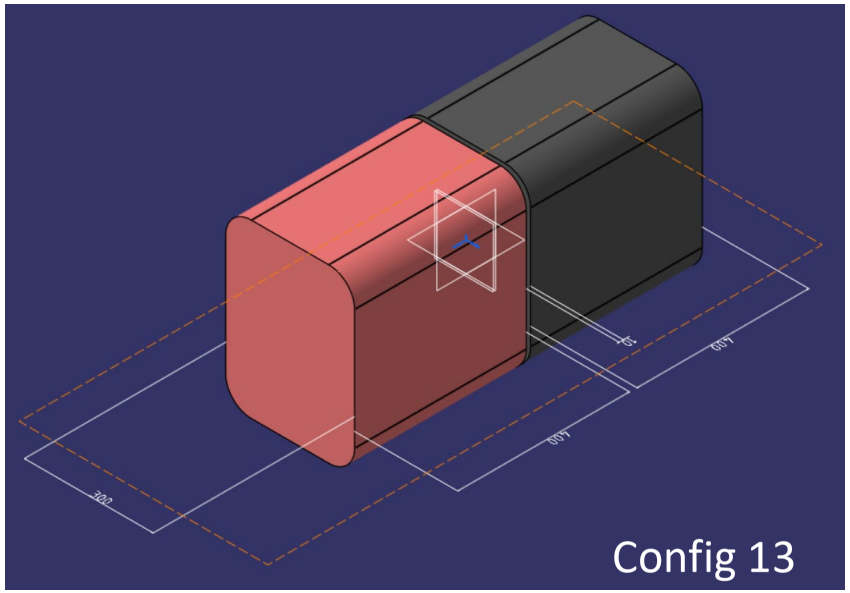
25
400
400
300
Config 13

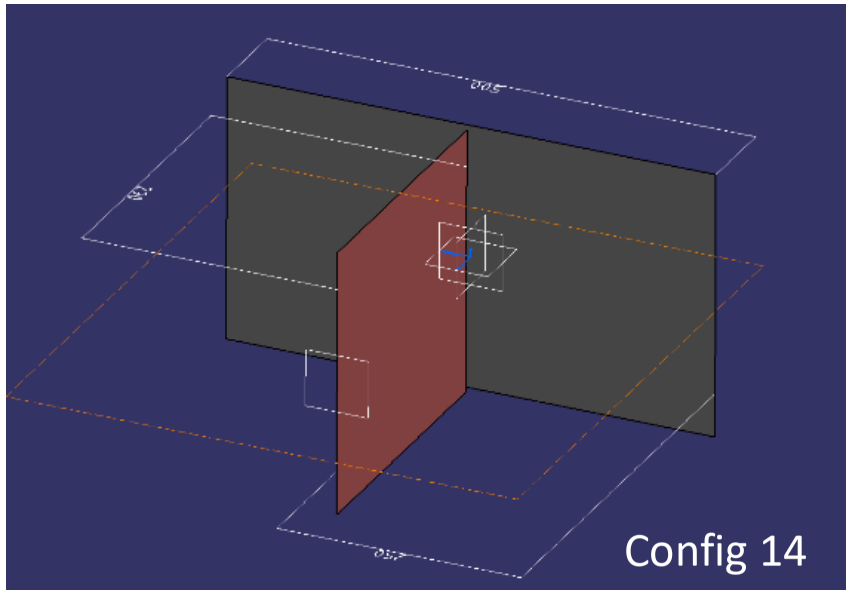
500
150
Config 14

Outside represents measure points or attachment points around the edges of the geometry and inside represents the points that are present in the middle of the geometry. Each configuration represents a part which is identical in either the type of attachment or other factors. The relevant examples associated with each configuration is shown in Table 3.3. Out of the 12 geometries, 8 geometries were prioritized for the research work.

Table 3.3: Table showing relevant examples for each configuration

Config	Component
1	Tailgate door and cover
2	Sunroof, Side door cover
3	Deco Panel, Side door
4	Config 1 with curved panels
5	Config 2 with curved panels
6	Config 3 with curved panels
9	Seat rail
10	Dashboard side cover and dashboard
11	Glovebox
12	Chrome rail and tunnel console, Side mirror front shell and shell
13	Gearbox housing, transfer box housing
14	Tunnel console

3.2 Mesh model preparation

The CAD models done using CATIA were imported into ANSA. The number of parts were verified, and the material properties and thickness were assigned for each part. Depending on the requirement, mesh type and size was determined, and the mesh was created in ANSA. Table 3.4 shows the type, size of mesh. Table 3.5 shows the material and thickness for each component.

Table 3.4: Table showing the type of mesh, mesh size, element size and materials

Config	Category	Material	Mesh type	Mesh size	No. of elements
1	Plane - Plane	Steel-Plastic	Quad	5 mm	7230
2	Plane - Plane	Steel-Plastic	Quad	5 mm	8352
3	Plane - Plane	Steel-Plastic	Quad	5 mm	8352
9	Beam - Panel	Steel-Steel	Quad	5 mm	9246
10	Structure - Panel	Plastic-Plastic	Quad & Tri	5 mm	30612
12	Structure - Panel	Plastic-Plastic	Quad & Tri	5 mm	26977
13	Structure - Structure	Plastic-Plastic	Quad	5 mm	50956
14	Panel - Panel	Plastic-Plastic	Quad	5 mm	9480

Table 3.5: Table showing the material and thickness of each component

Config	Component 1	Component 2	Material Component 1	Material Component 2	t1	t2
1	Flat Panel (Outer)	Flat Panel (Inner)	Mild Steel	NFPP 1250 Natural fiber	1	3
2	Flat Panel (Outer)	Flat Panel (Inner)	Mild Steel	NFPP 1250 Natural fiber	1	2
3	Flat Panel (Outer)	Flat Panel (Inner)	Mild Steel	Stamax 30YK270 (PPLGF30)	1	3
9	Flat panel	Beam	Mild Steel	Mild Steel	1	2
10	Structure	Flat Panel	PPLGF20 20YK270	PPLGF20 20YK270	1.47	2.2
12	Structure	Flat Panel with hollow centre	PPLGF20 20YK270	PPLGF20 20YK270	2.2	3.3
13	Structure	Structure	PPLGF20 20YK270	PPLGF20 20YK270	2.2	2.2
14	Flat Panel	Flat Panel perpendicular to component 1	PPLGF20 20YK270	PPLGF20 20YK270	2.2	2.2

* t – thickness in mm.

The material name and its properties such as young's modulus, Poisson ratio and mass density were listed in the table 3.6 below

Table 3.6: Table showing the material name and its properties

Material	Youngs Modulus	Poissons ratio	Mass density
Mild Steel	210000	0.03	7.85E-09
NFPP 1250 Natural fiber	3500	0.25	8.3E-10
Stamax 30YK270 (PPLGF30)	4052	0.4	1.12E-09
PPLGF20 20YK270	3160	0.4	1.4E-09

RBE2 elements were created for measuring the squeak and rattle behavior and they served as the measure points. The coordinate systems were set up on the measure points as a reference for selecting the target point. The RBE3 elements which serves as the location of attachment points were created. RBE3 elements in two parts were connected by CBUSH element and PBUSH properties were created depending up on the type of fasteners required i.e. normal or planar direction. Total number of fasteners, measure points, active normal fasteners per design, active planar fasteners per design is shown in the **Error! Reference source not found.**

Table 3.7: Table showing the possible fasteners, number of measure points, number of active normal and planar fasteners

Config	Number of candidates for attachment points	Number of active normal fasteners per design	Number of active planar fasteners per design	Number of measure points
1	38	8	2	12
2	38	8	3	15
3	28	8	3	25
9	56	4		10
10	28	8	2	14
12	28	8	3	14
13	28	8	4	14
14	33	6		10

Boundary conditions were assigned, and mesh quality was analyzed. The model was exported as a .nas file and this file was used to run Nastran simulations. Also, each individual part was exported as .nas file along with mesh which will be used for geometric variation analysis.

A commercial software package, RD&T was used for performing geometric variation analysis. A new part was created in RD&T by importing the bulk data mesh of ANSA part. The parts were positioned using 3-2-1 location schemes and support points were also included. The super part was created by including the imported parts and fasteners in both normal and planar direction was created. Tolerances of linear type and a range of 1 mm were specified at the fastener points. The tolerances were specified only in the direction of the fastener. Fasteners constraining in rattle normal direction only had tolerances in normal Z-direction and the planar fasteners had tolerances in X and Y directions. The measure points were defined, and the simulation were carried out.

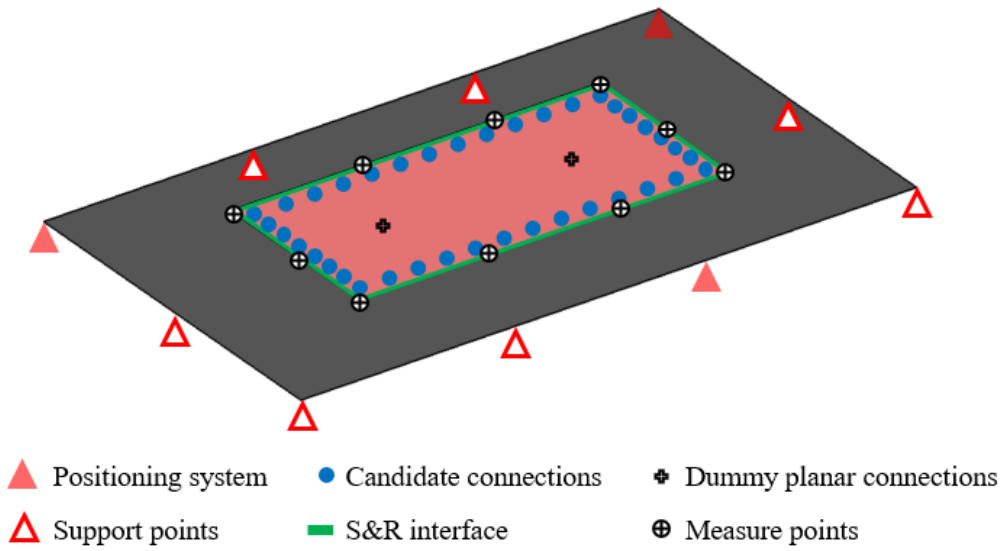

Figure 3.1: Pictorial representation of the Configuration 1.

The model with all the measure points, boundary conditions, attachment points and dummy planar connections is shown in a pictorial form in Figure 3.1. The positioning system is a 3-2-1 location scheme with additional support points represented in solid and hollow triangles. The Squeak & Rattle proximity places represented in a green line, are places where the S&R occurs. The measure points are indicated by a plus with a circle and the dummy planar connection position is indicated by a plus sign. The blue circles represent the possible positions for having an attachment point.

4. Results and Discussions

In this chapter, the results of the optimisation for all the model configurations are described.

4.1 Results

The models were prepared for the selected model configurations, and the workflow was created in modeFRONTIER. The two-stage optimisation methodology explained in Chapter 2 was applied for all the model configurations. All the configurations were optimised for only Dynamic response, only geometric variation and both geometric variation & dynamic response. The results of the optimisations are detailed below.

4.1.1 Configuration 1 (Panel – Panel)

4.1.1.1 Geometric Variation Optimisation

For the first stage of optimisation, the attachment points in the rattle direction were involved and two dummy attachment points in planar direction was activated. The optimisation was run for 50 generations and the initial population contained 50 designs that were a mix of ISF and EXTREME designs. The objectives were plotted against each other and it resulted in a pareto. It was made sure that there are no designs in the pareto that were part of the final 5 generations. The results are represented in Figure 4.1. The optimum design in rattle direction that was chosen for the next stage of the optimisation process is represented as Opt_rattle. The designs that formed the pareto is represented in the form of a connection configuration in Figure 4.3.

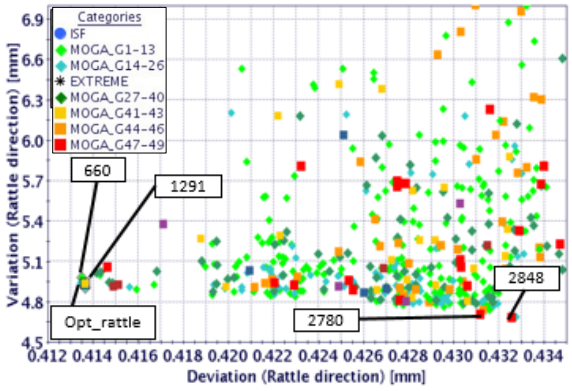

Figure 4.1: Scatter plot of objective function of Variation and Deviation for Configuration 1, Geometric Variation stage one optimisation

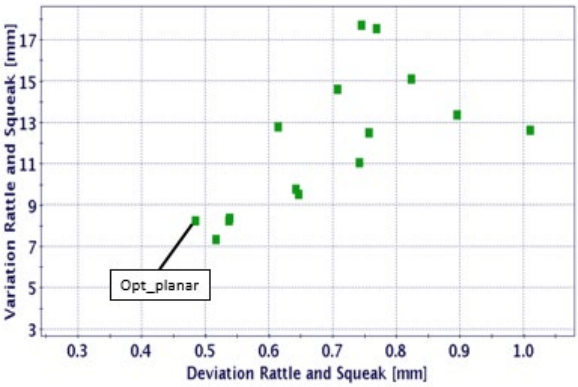

Figure 4.2: Scatter plot of objective function of Variation and Deviation for Configuration 1, Geometric Variation stage two optimisation

In the second stage of optimisation, the dummy attachment points in planar direction was deactivated and the attachment points that needs to be constrained in the planar direction (both X and Y directions) in the Opt_rattle design was identified. A full DOE optimisation was possible due to the smaller number of possible combinations and the results are shown in Figure 4.2. The best design in the planar optimisation is also indicated in the connection configuration (see Opt_rattle design in Figure 4.3).

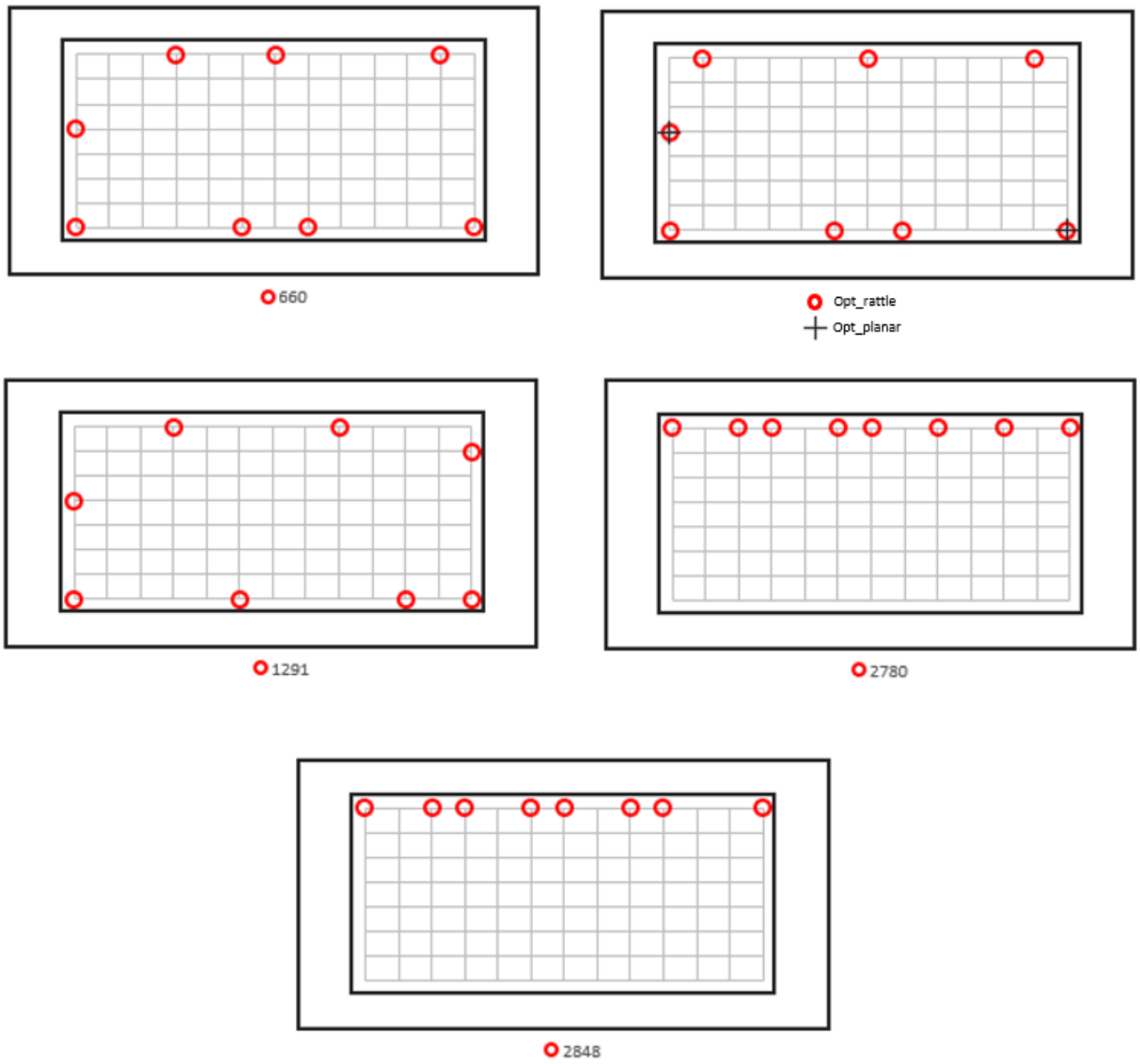

Figure 4.3: Schematic connection configuration for the designs that form the Pareto of Figure 4.1 in Configuration 1.

4.1.1.2 Dynamic Response Optimisation

A similar two stage optimisation was done for the Dynamic response as that of Geometric variation. The difference was the change in objectives: Resonance risk and Mode shape similarity. For the first stage of optimisation, the attachment points in the rattle direction were involved and two dummy attachment points in planar direction was activated. The objectives were plotted against each other and it resulted in a pareto. The results are represented in Figure 4.4. The optimum design in rattle direction that was chosen for the next stage of the optimisation process is represented as Opt_rattle.

There was only one design in the pareto indicating that the optimisation has converged to one optimum solution for the problem. The connection configuration of the optimum design in rattle direction is represented in the form of a connection configuration in Figure 4.6 and marked as Opt_rattle.

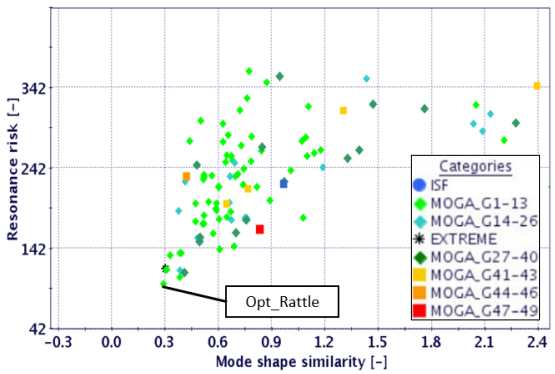

Figure 4.4: Scatter plot of objective function of Mode Shape Similarity and Resonance risk for Configuration 1, Dynamic response stage one optimisation

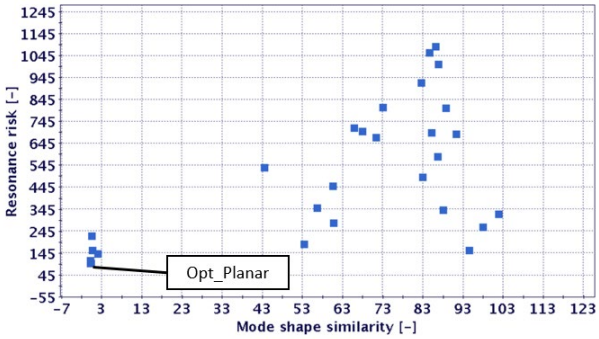

Figure 4.5: Scatter plot of objective function of Mode Shape Similarity and Resonance risk for Configuration 1, Dynamic response stage two optimisation

In the second stage of optimisation, the attachment points in Opt_rattle design that needs to be constrained in the planar direction was identified. A full DOE optimisation was done, and the results are shown in Figure 4.5. The optimum planar attachment points configuration is also indicated in the connection configuration plot.

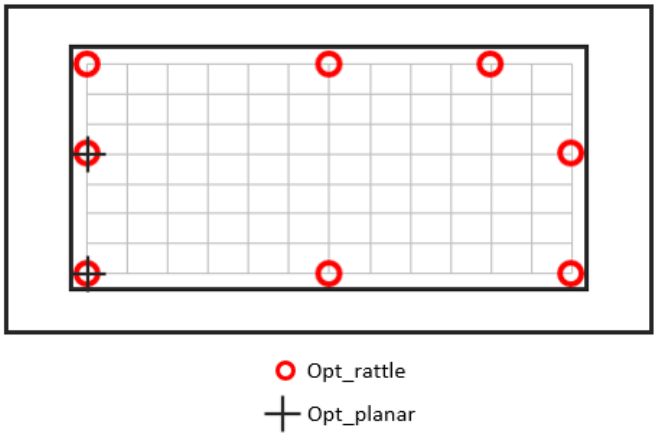

Figure 4.6: Schematic connection configuration for the designs that form the Pareto of Figure 4.4 in Configuration 1.

4.1.1.3 Multi-Disciplinary Optimisation

An MDO was performed to optimise the designs for both Dynamic response and Geometric variations. The two objectives that needs to be minimised in the optimisation are Dynamic response and Geometric variation. Dynamic response objective is the sum of resonance risk and mode shape similarity whereas geometric variation is the sum of variation and deviation. A suitable multiplier was calculated for each objectives and included in the objective so that the values are normalised when summing the two values. For the first stage of optimisation, the attachment points in the rattle direction were involved and two dummy attachment points in planar direction was activated. The objectives were plotted against each other and it resulted in a pareto. The results are represented in Figure 4.7. The optimum design in rattle direction that was chosen for the next stage of the optimisation process is represented as Opt_rattle and the pareto designs are shown in Figure 4.9.

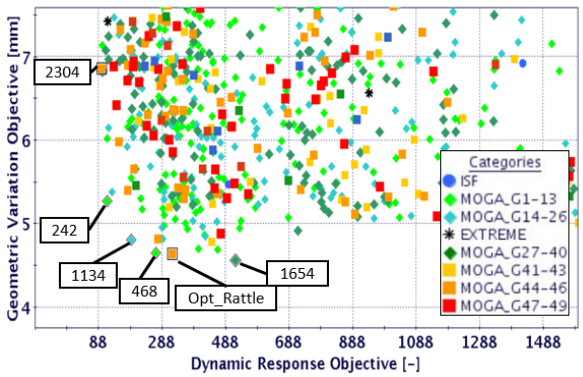

Figure 4.7: Scatter plot of objective function of Geometric Variation and Dynamic response for Configuration 1, MDO stage one optimisation

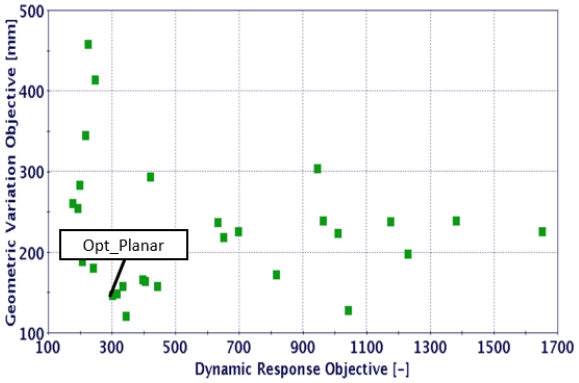

Figure 4.8: Scatter plot of objective function of Geometric Variation and Dynamic response for Configuration 1, MDO stage two optimisation

In the second stage of optimisation, the attachment points that needs to be constrained in the planar direction was identified. A full DOE optimisation was done, and the results are shown in Figure 4.8. The optimum planar attachment points are also indicated in the connection configuration plot.

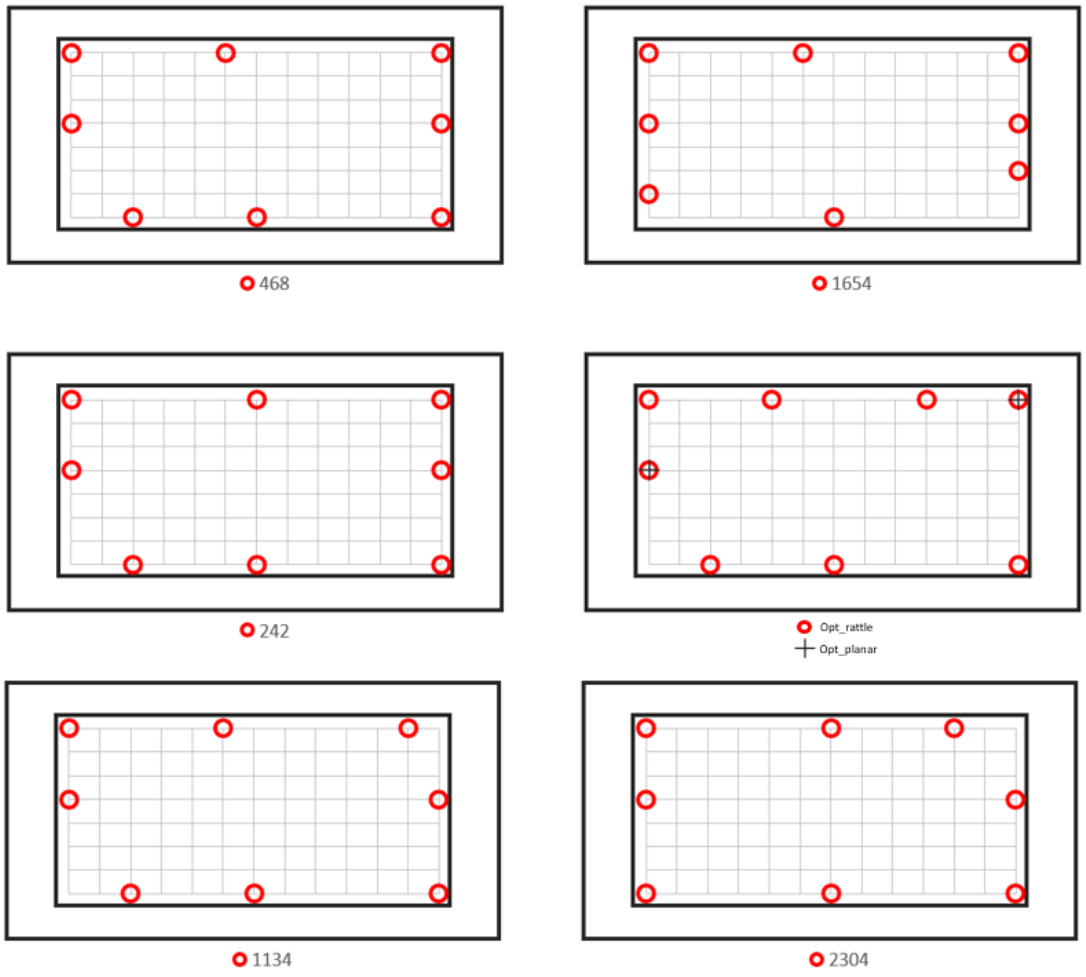

Figure 4.9: Schematic connection configuration for the designs that form the Pareto of Figure 4.7 in Configuration 1.

4.1.2 Configuration 2 (Panel – Panel)

The same two stage optimisation methodology was followed for this configuration and the results are shown below.

4.1.2.1 Geometric Variation Optimisation

For the Geometric variation optimisation, the results in the form of a pareto is shown in Figure 4.10 and the connection configuration is shown in Figure 4.12. The second stage optimisation involved identification of the attachment points constrained in planar direction and the results is shown in Figure 4.11.

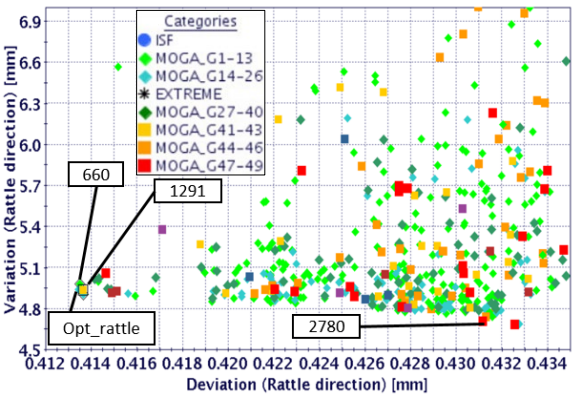

Figure 4.10: Scatter plot of objective function of Variation and Deviation for Configuration 2, Geometric Variation stage one optimisation

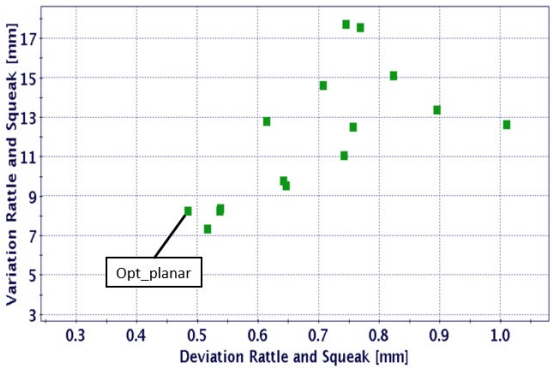

Figure 4.11: Scatter plot of objective function of Variation and Deviation for Configuration 2, Geometric Variation stage two optimisation

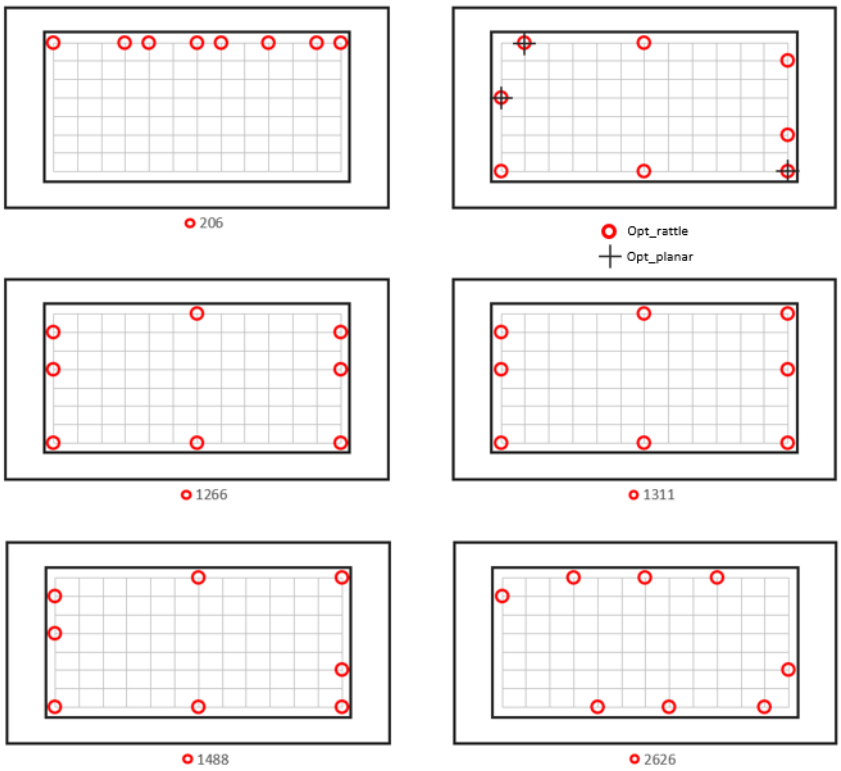

Figure 4.12: Schematic connection configuration for the designs that form the Pareto of Figure 4.10 in Configuration 2.

4.1.2.2 Dynamic Response Optimisation

For the Dynamic response optimisation, the results of the first stage optimisation in the form of a pareto is shown in Figure 4.13 and the connection configuration is shown in Figure 4.15. The pareto chart of the second stage optimisation is shown in Figure 4.14.

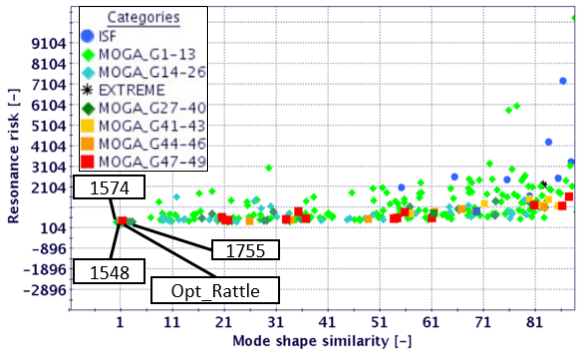

Figure 4.13: Scatter plot of objective function of Mode Shape Similarity and Resonance risk for Configuration 2, Dynamic response stage one optimisation

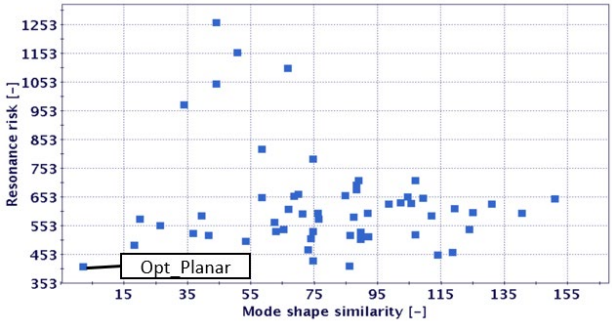

Figure 4.14: Scatter plot of objective function of Mode Shape Similarity and Resonance risk for Configuration 2, Dynamic response stage two optimisation

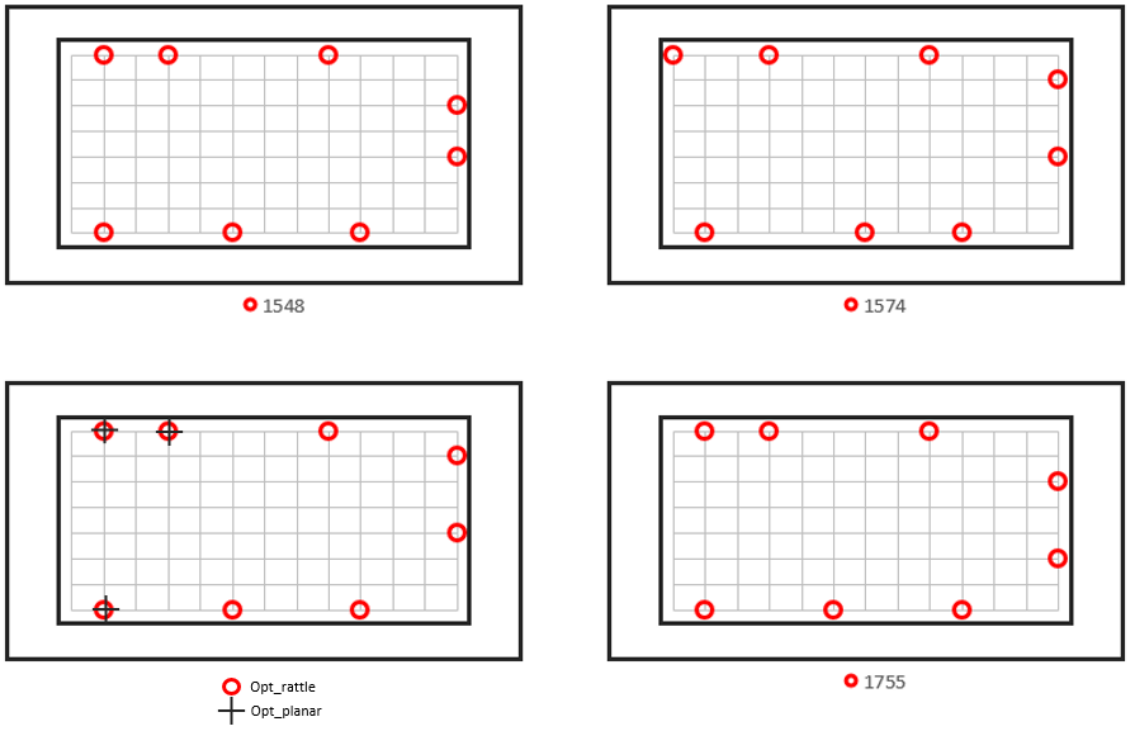

Figure 4.15: Schematic connection configuration for the designs that form the Pareto of Figure 4.13 in Configuration 2.

4.1.2.3 Multi-Disciplinary Optimisation

For the Multi-disciplinary optimisation, the results of the first stage optimisation are shown in Figure 4.16 and the connection configuration in Figure 4.18. The results of the second stage planar attachment point optimisation is shown in Figure 4.17.

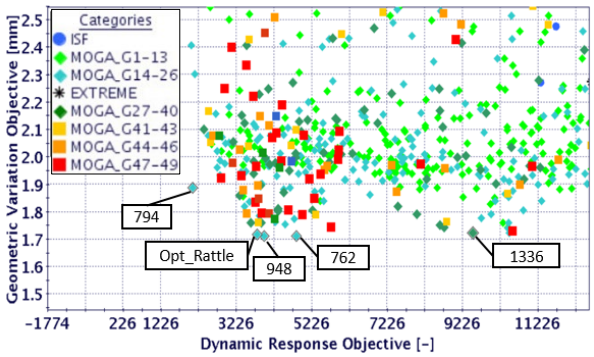

Figure 4.16: Scatter plot of objective function of Geometric Variation and Dynamic response for Configuration 2, MDO stage one optimisation

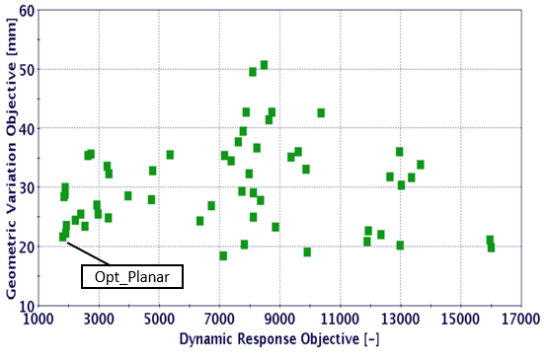

Figure 4.17: Scatter plot of objective function of Geometric Variation and Dynamic response for Configuration 2, MDO stage two optimisation

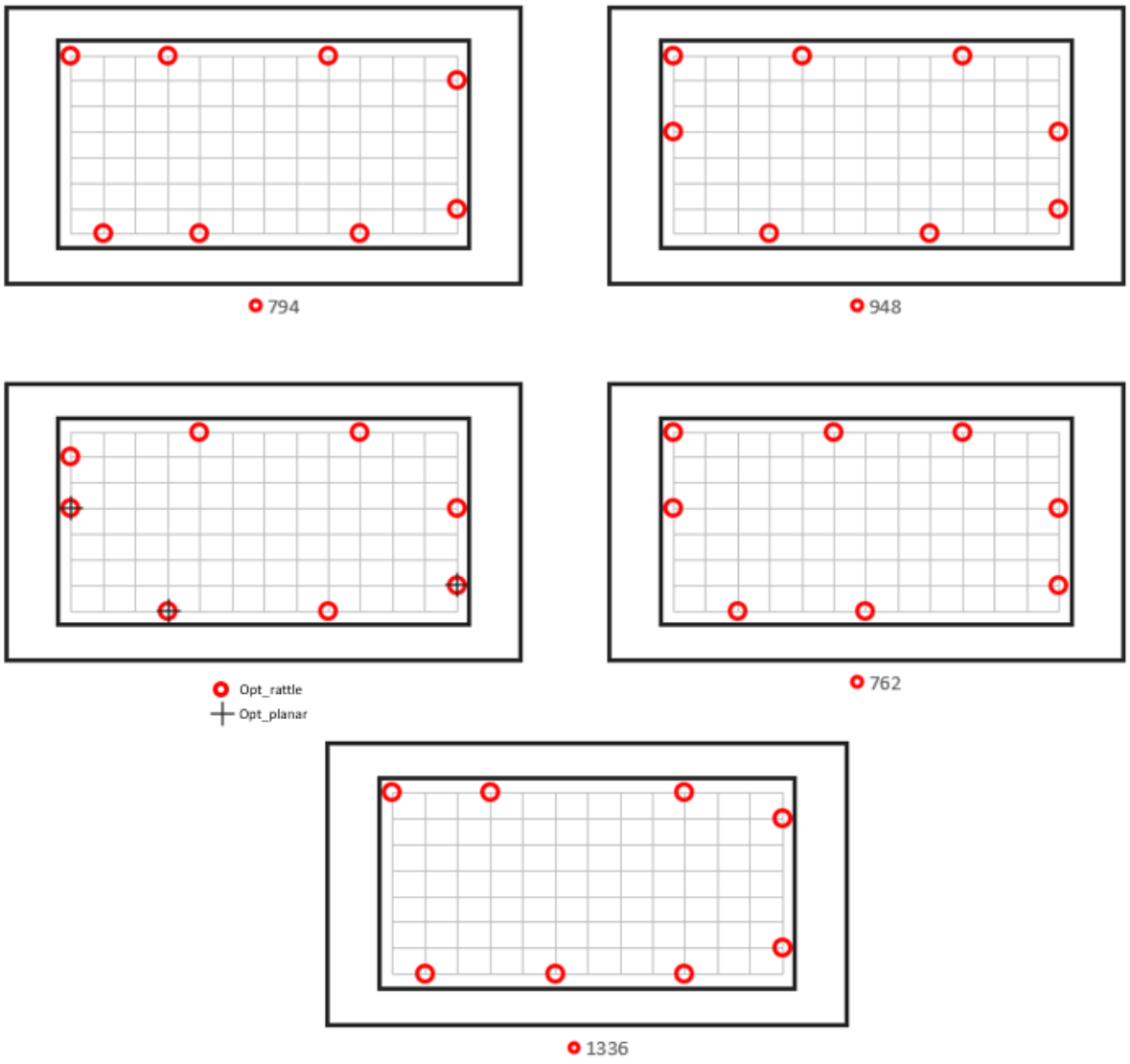

Figure 4.18: Schematic connection configuration for the designs that form the Pareto of Figure 4.16 in Configuration 2.

4.1.3 Configuration 3 (Panel – Panel)

The configuration 3 shared the same model as the previous two configurations but had differences in the measure and attachment points. The two-stage optimisation was also followed for this configuration.

4.1.3.1 Geometric Variation Optimisation

The results of the first stage optimisation in the form of a pareto is shown in Figure 4.19and the connection configuration is shown in Figure 4.21. The second stage optimisation involved identification of the attachment points constrained in planar direction and the results is shown in Figure 4.20.

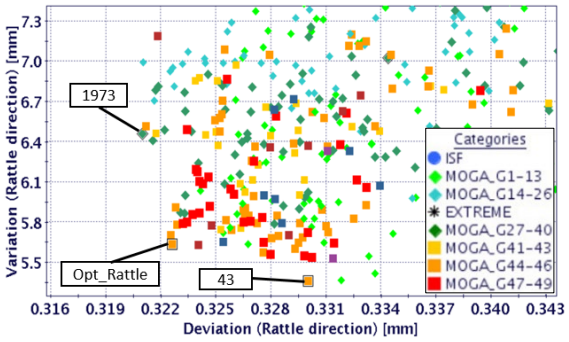

Figure 4.19: Scatter plot of objective function of Variation and Deviation for Configuration 3, Geometric Variation stage one optimisation

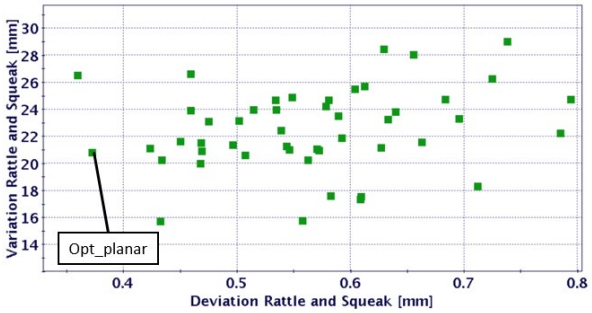

Figure 4.20: Scatter plot of objective function of Variation and Deviation for Configuration 3, Geometric Variation stage two optimisation

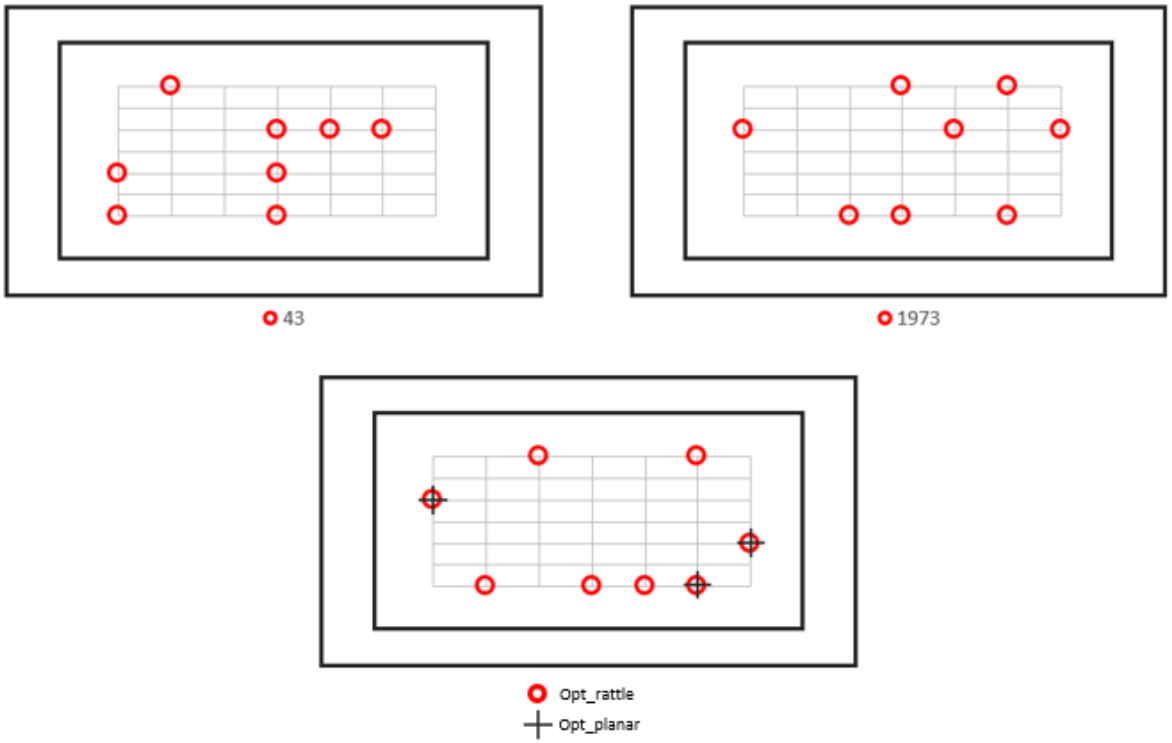

Figure 4.21: Schematic connection configuration for the designs that form the Pareto of Figure 4.19 in Configuration 3.

4.1.3.2 Dynamic Response Optimisation

For the Dynamic response optimisation, the results of the first stage optimisation in the form of a pareto is shown in Figure 4.22 and the connection configuration is shown in Figure 4.24. The pareto chart of the second stage optimisation is shown in Figure 4.23.

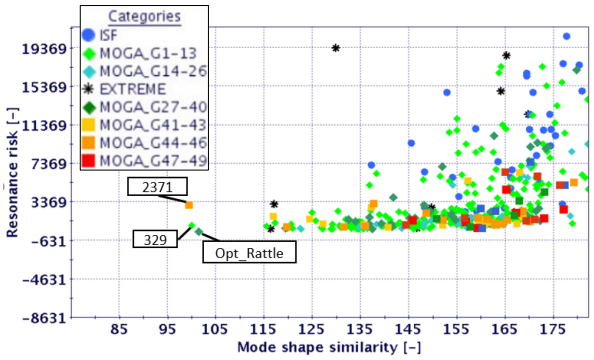

Figure 4.22: Scatter plot of objective function of Mode Shape Similarity and Resonance risk for Configuration 3, Dynamic response stage one optimisation

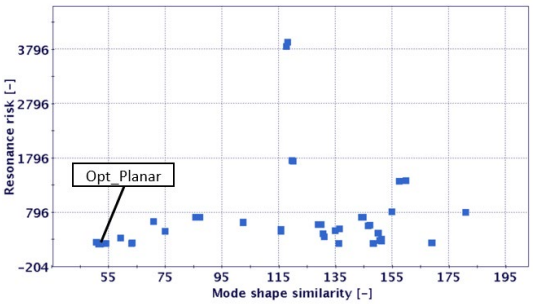

Figure 4.23: Scatter plot of objective function of Mode Shape Similarity and Resonance risk for Configuration 3, Dynamic response stage two optimisation

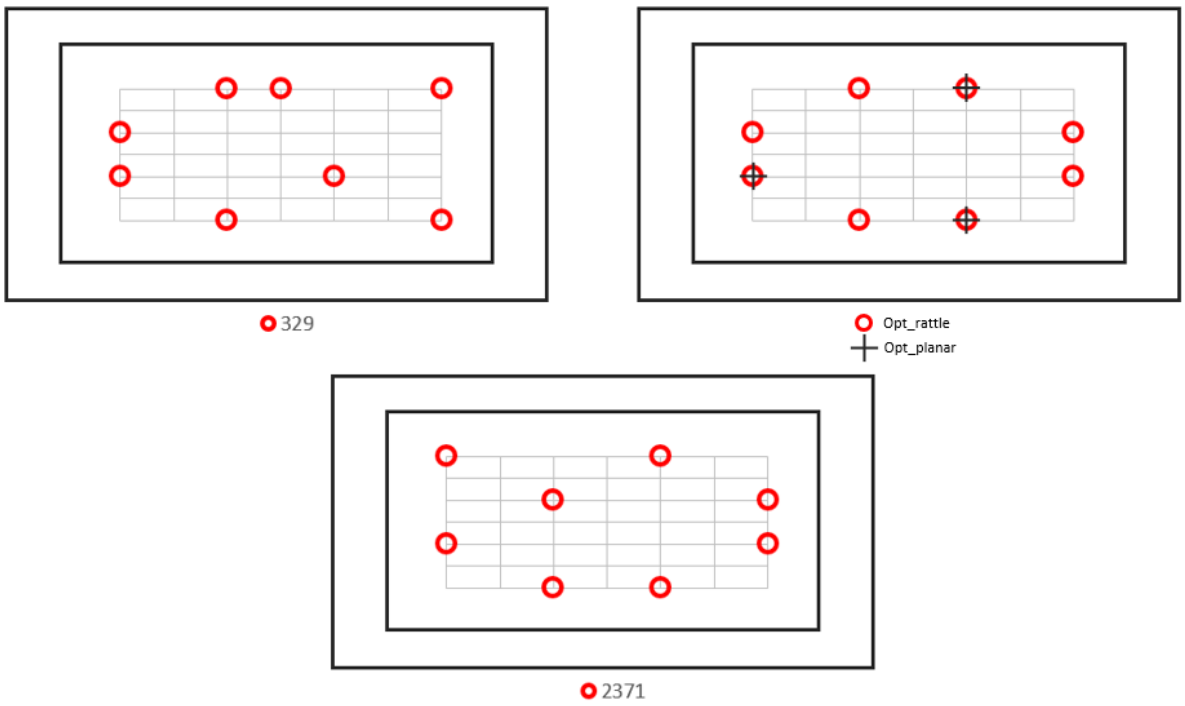

Figure 4.24: Schematic connection configuration for the designs that form the Pareto of Figure 4.22 in Configuration 3.

4.1.3.3 Multi-Disciplinary Optimisation

The results of the first stage MDO optimisation is shown in Figure 4.25 and the connection configuration in Figure 4.27. The results of the second stage planar attachment point optimisation is shown in Figure 4.26.

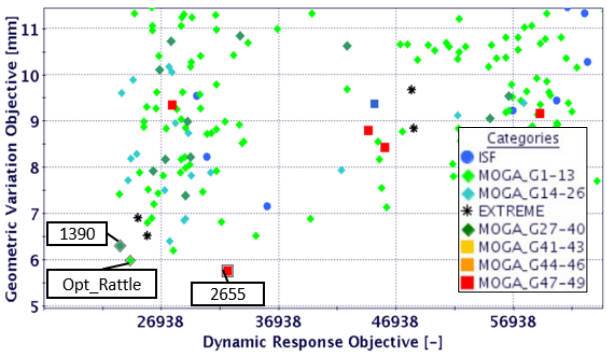

Figure 4.25: Scatter plot of objective function of Geometric Variation and Dynamic response for Configuration 3, MDO stage one optimisation

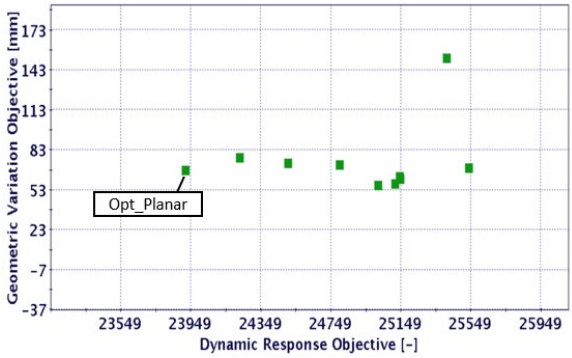

Figure 4.26: Scatter plot of objective function of Geometric Variation and Dynamic response for Configuration 3, MDO stage two optimisation

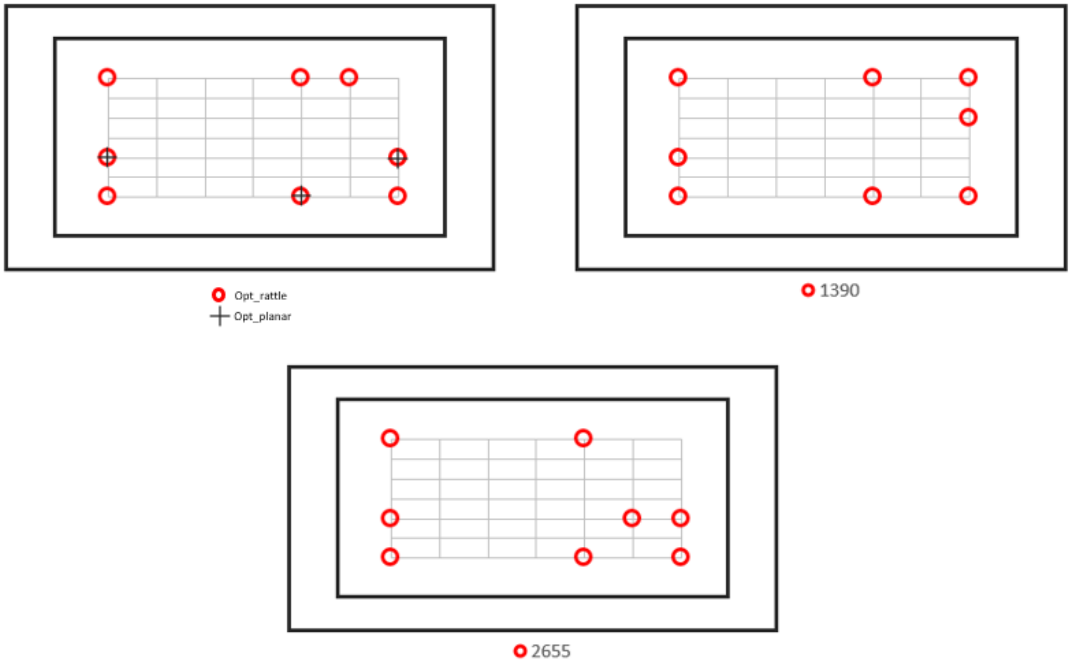

Figure 4.27: Schematic connection configuration for the designs that form the Pareto of Figure 4.25 in Configuration 3.

It is evident from the plots that for geometric variation, the attachment points are spread out as much as possible and the planar attachment point evenly spaced out. Although the designs are spaced out for dynamic response, the planar attachment points are found to be closer to each other in the side where there are more attachment points. No major common traits could be found in designs between Geometric variation and Dynamic response. The results of the MDO seemed to be a trade-off for both the objectives and the designs are more evenly spaced out with planar attachment points evenly spaced on two edges.

4.1.4 Configuration 10 (Structure – Panel)

The Configuration 10 includes a structure model along with a panel. The same two stage optimisation was followed for this configuration.

4.1.4.1 Geometric Variation Optimisation

The results of the first stage optimisation in the form of a pareto is shown in Figure 4.28 and the connection configuration is shown in Figure 4.30. The second stage optimisation involved identification of the attachment points constrained in planar direction and the results is shown in Figure 4.29.

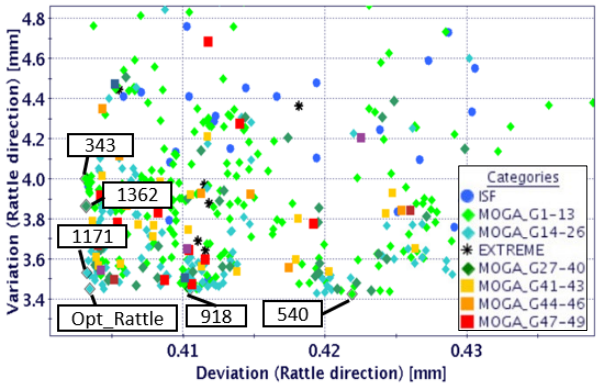

Figure 4.28: Scatter plot of objective function of Variation and Deviation for Configuration 10, Geometric Variation stage one optimisation

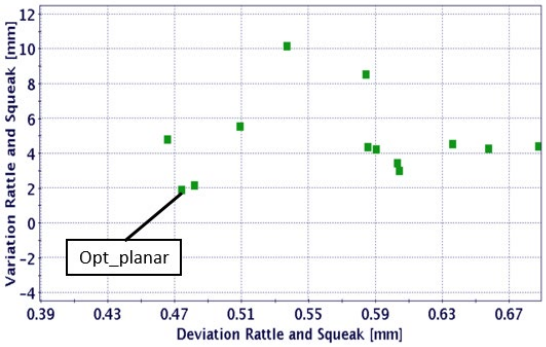

Figure 4.29: Scatter plot of objective function of Variation and Deviation for Configuration 10, Geometric Variation stage two optimisation

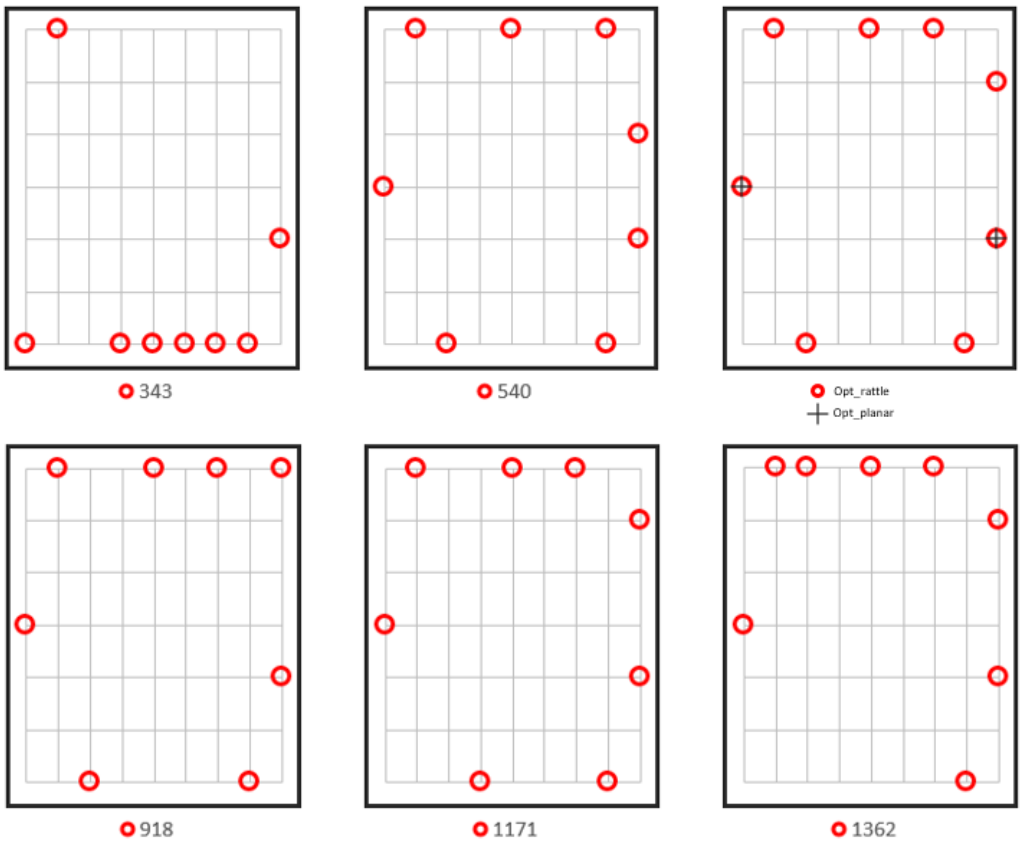

Figure 4.30: Schematic connection configuration for the designs that form the Pareto of Figure 4.28Figure 4.32 in Configuration 10.

4.1.4.2 Dynamic Response Optimisation

For the Dynamic response optimisation, the results of the first stage optimisation in the form of a pareto is shown in Figure 4.31 and the connection configuration is shown in Figure 4.35. The pareto chart of the second stage optimisation is shown in Figure 4.32.

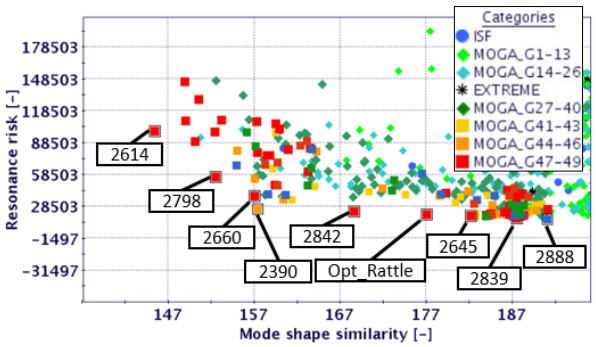

Figure 4.31: Scatter plot of objective function of Mode Shape Similarity and Resonance risk for Configuration 10, Dynamic response stage one optimisation

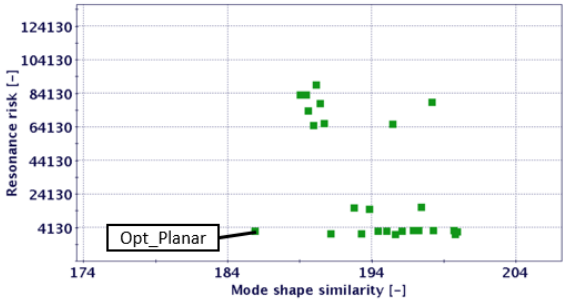

Figure 4.32: Scatter plot of objective function of Mode Shape Similarity and Resonance risk for Configuration 10, Dynamic response stage two optimisation

4.1.4.3 Multi-Disciplinary Optimisation

The results of the first stage MDO optimisation is shown in Figure 4.33 and the connection configuration in Figure 4.36. The results of the second stage planar attachment point optimisation is shown in Figure 4.34.

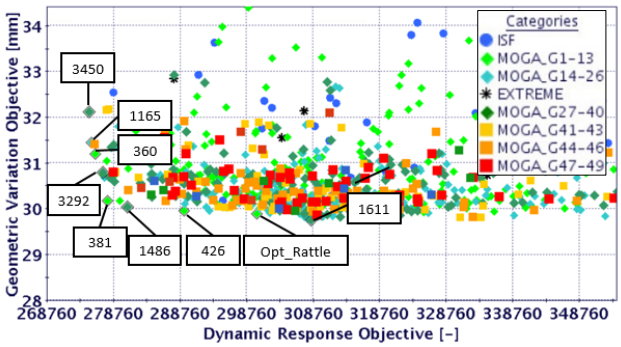

Figure 4.33: Scatter plot of objective function of Geometric Variation and Dynamic response for Configuration 10, MDO stage one optimisation

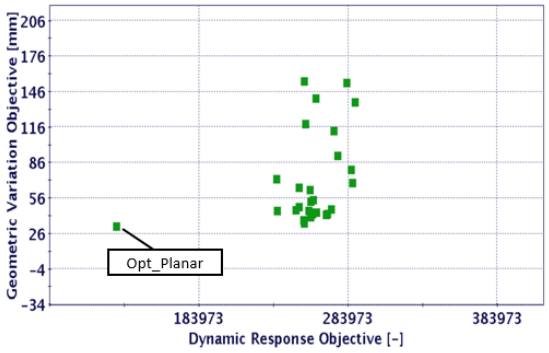

Figure 4.34: Scatter plot of objective function of Geometric Variation and Dynamic response for Configuration 10, MDO stage two optimisation

The optimum design for the geometric variation optimisation resulted in an evenly spaced out design with the two planar attachment points in the right and left side. A clustered design was achieved in the dynamic response optimisation on the top and bottom edge. The designs which did not have an attachment point on any of the corners were from the ends of the pareto curve.

MDO was found to be similar to the geometric variation design with a spaced-out design and planar points on the left and right edges. Similar to the dynamic response optimisation, the designs that were not evenly spaced out were from the ends of the pareto curve.

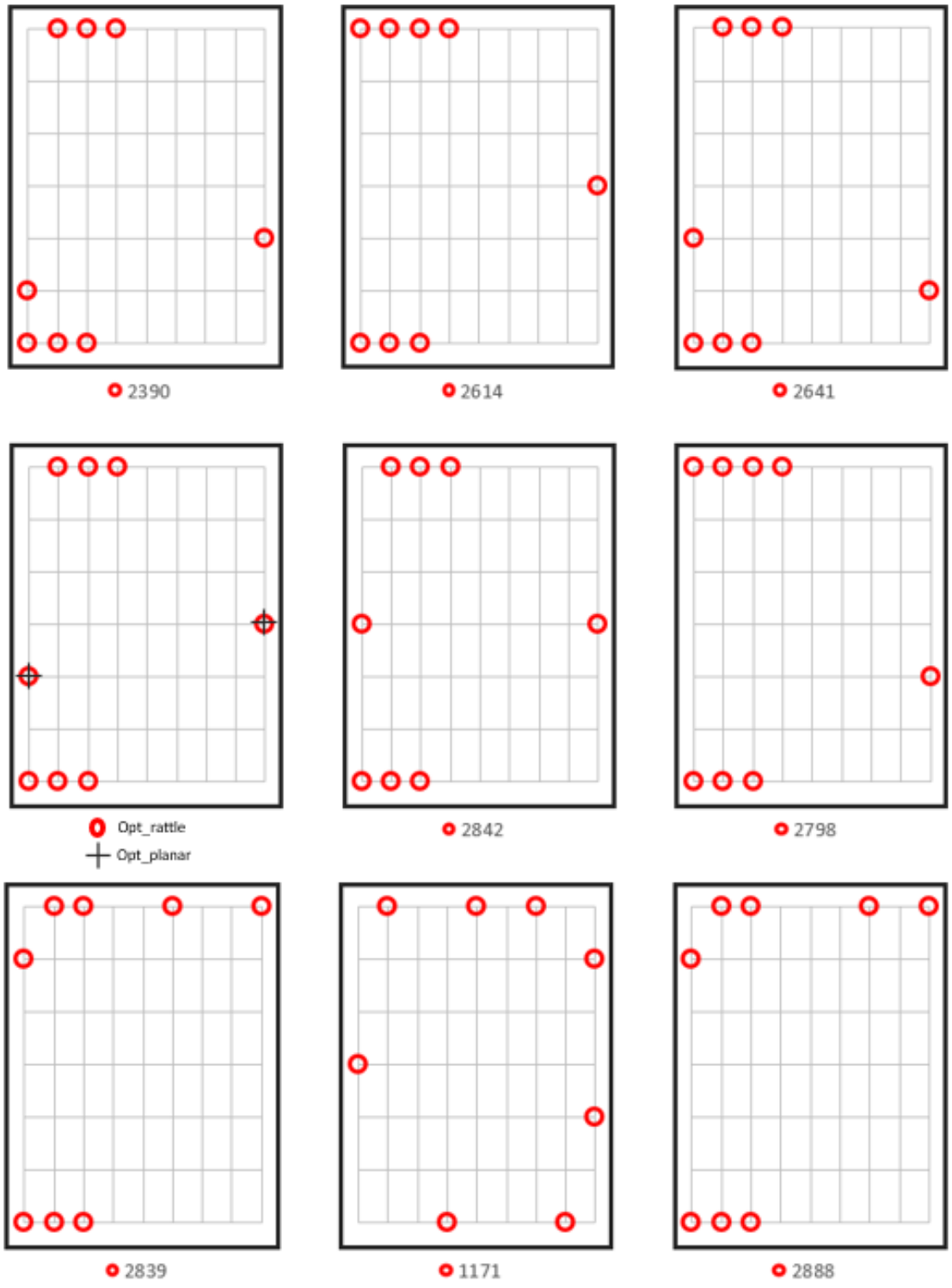

Figure 4.35: Schematic connection configuration for the designs that form the Pareto of Figure 4.31 in Configuration 10.

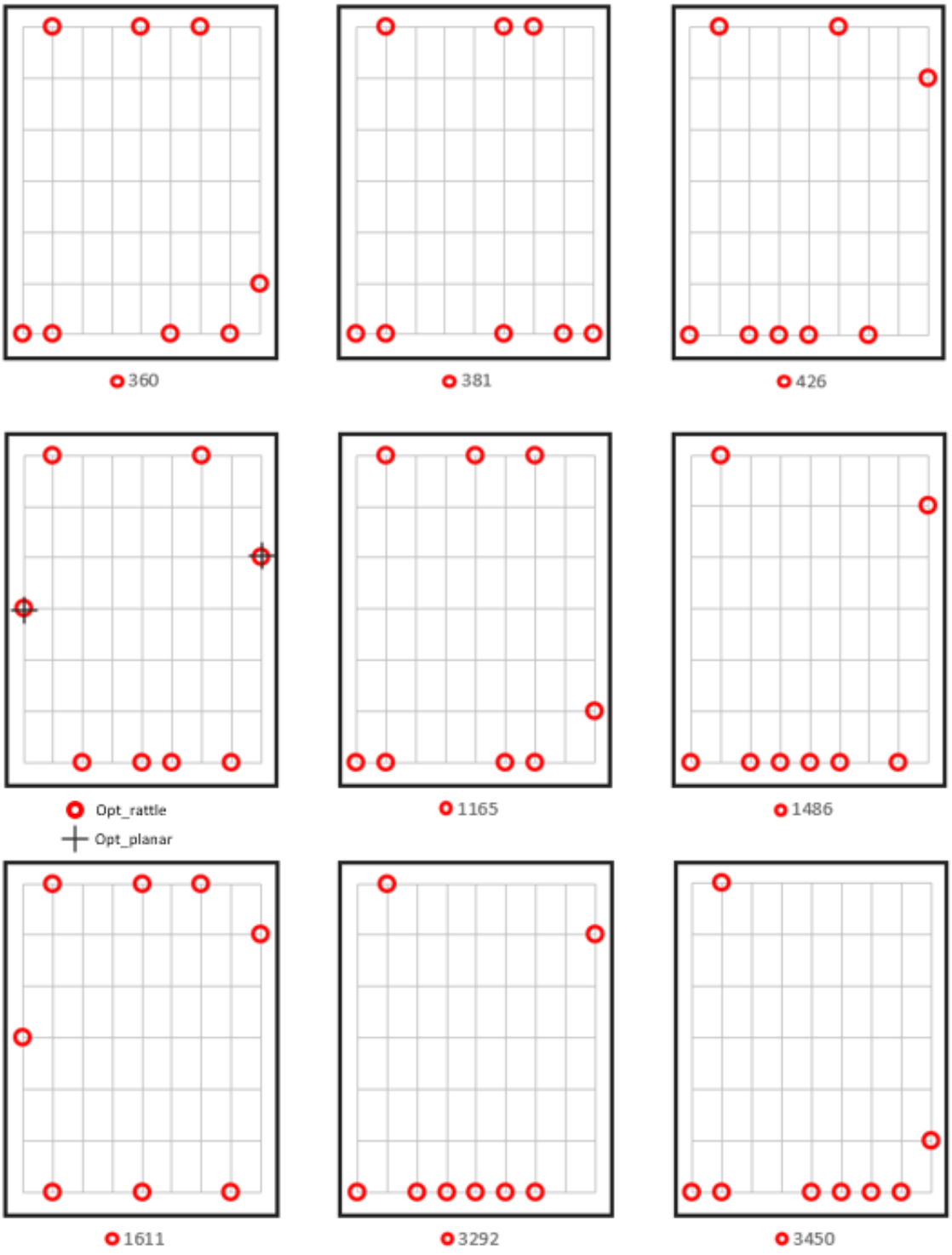

Figure 4.36: Schematic connection configuration for the designs that form the Pareto of Figure 4.33 in Configuration 10.

4.1.5 Configuration 12 (Structure – Panel)

Configuration 12 is same as the configuration 10 except that the panel is made hollow in this configuration. The optimisation methodology is the same as the previous one.

4.1.5.1 Geometric Variation Optimisation

The results of the first stage optimisation in the form of a pareto is shown in Figure 4.37 and the connection configuration is shown in Figure 4.41. The second stage optimisation involved identification of the attachment points constrained in planar direction and the results is shown in Figure 4.38.

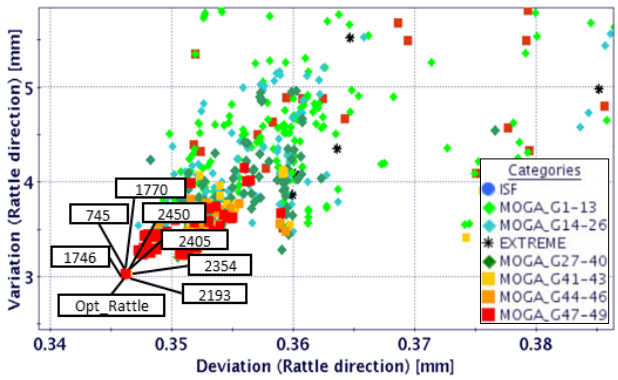

Figure 4.37: Scatter plot of objective function of Variation and Deviation for Configuration 12, Geometric Variation stage one optimisation

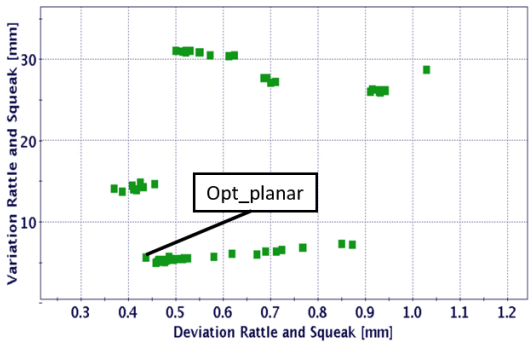

Figure 4.38: Scatter plot of objective function of Variation and Deviation for Configuration 12, Geometric Variation stage two optimisation

4.1.5.2 Dynamic Response Optimisation

For the Dynamic response optimisation, the results of the first stage optimisation in the form of a pareto is shown in Figure 4.39 and the connection configuration is shown in Figure 4.42. The pareto chart of the second stage optimisation is shown in Figure 4.40.

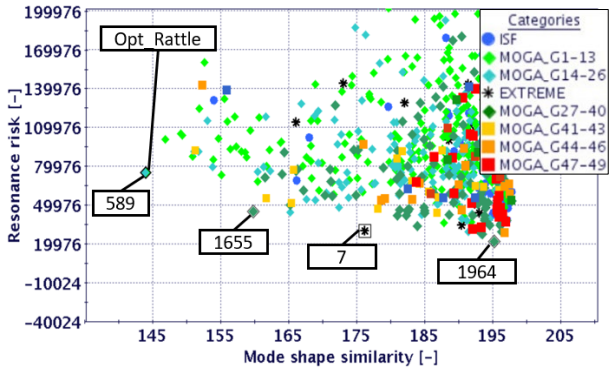

Figure 4.39: Scatter plot of objective function of Mode Shape Similarity and Resonance risk for Configuration 12, Dynamic response stage one optimisation

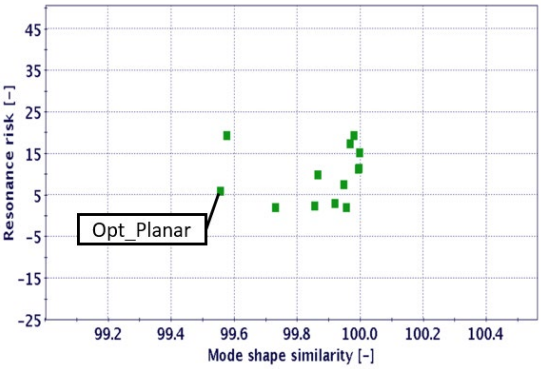

Figure 4.40: Scatter plot of objective function of Mode Shape Similarity and Resonance risk for Configuration 12, Dynamic response stage two optimisation

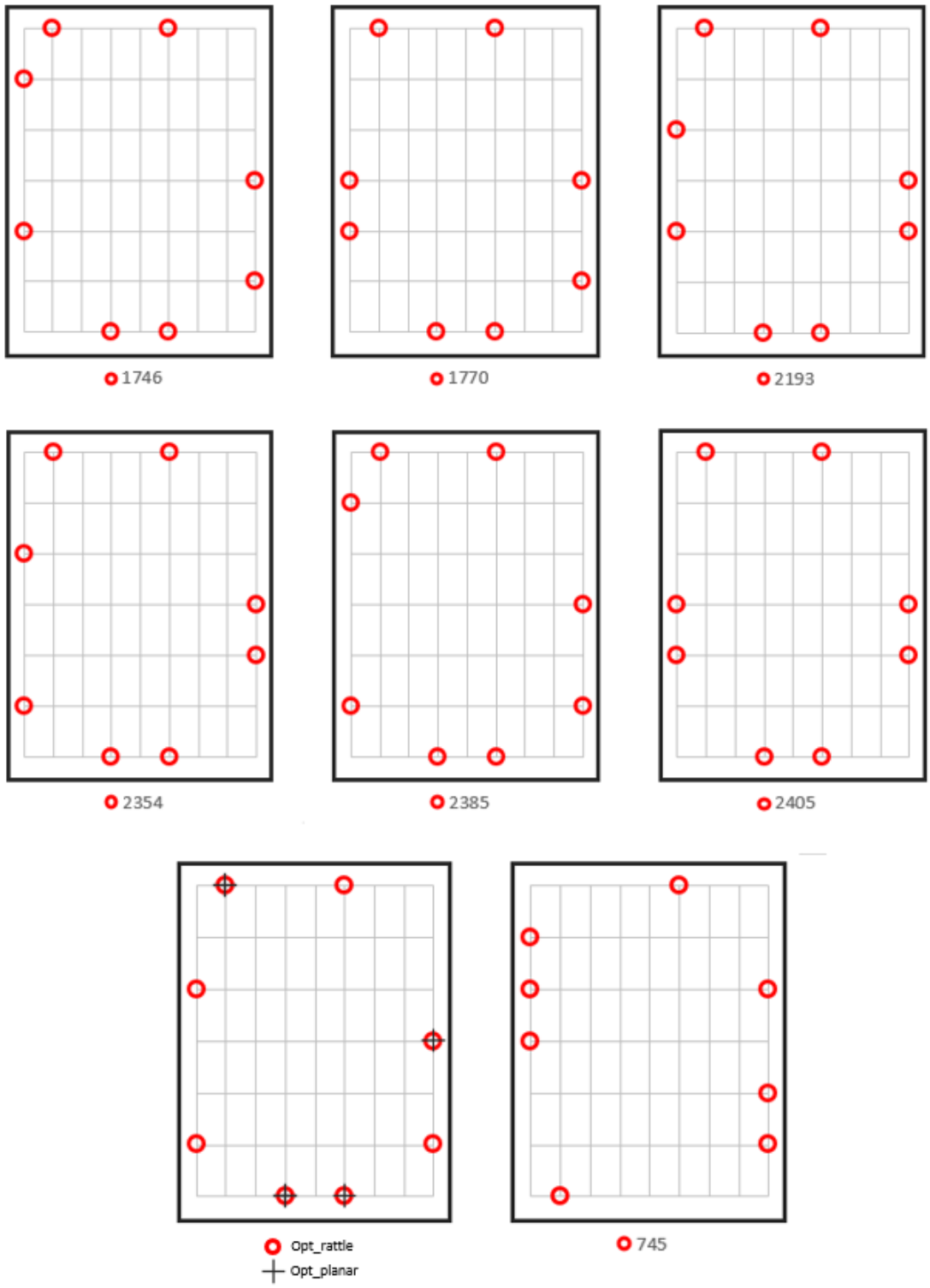

Figure 4.41: Schematic connection configuration for the designs that form the Pareto of Figure 4.37 in Configuration 12.

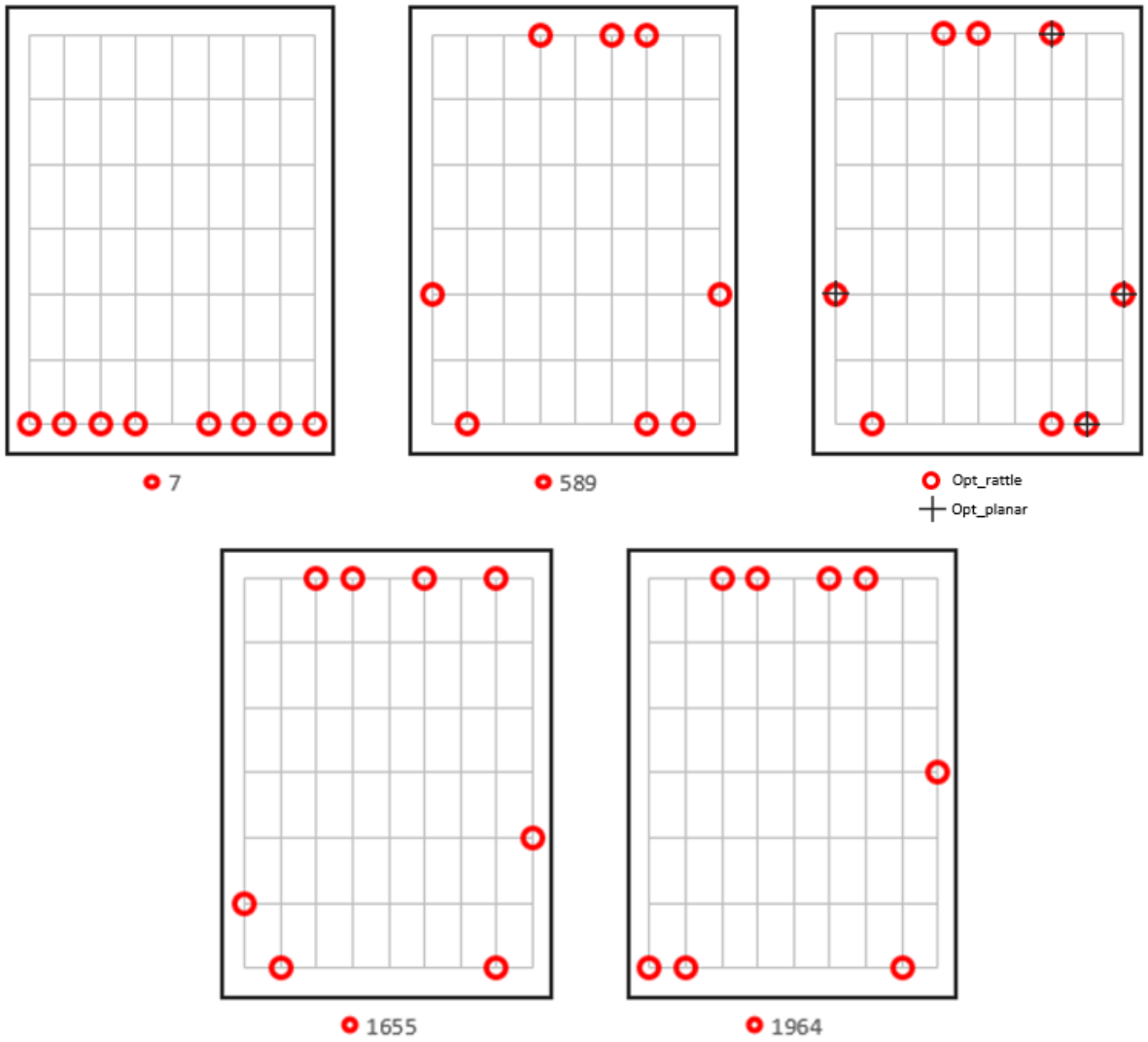

Figure 4.42: Schematic connection configuration for the designs that form the Pareto of Figure 4.39 in Configuration 12.

4.1.5.3 Multi-Disciplinary Optimisation

The results of the first stage MDO optimisation is shown in Figure 4.43 and the connection configuration in Figure 4.45. The results of the second stage planar attachment point optimisation is shown in Figure 4.44.

The configuration showed similar traits to configuration 10. All the optimisation results resulted in a more evenly spaced design with planar points also spaced out. Unlike configuration 10, configuration 12 had four planar attachment points. In the MDO result, the attachment points were spaced out whereas three of the four planar attachment points were clustered on one corner.

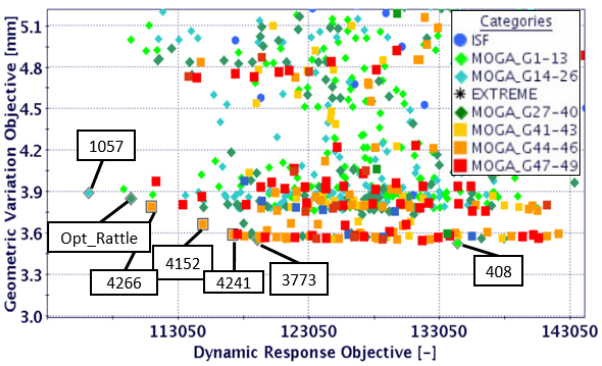

Figure 4.43: Scatter plot of objective function of Geometric Variation and Dynamic response for Configuration 12, MDO stage one optimisation

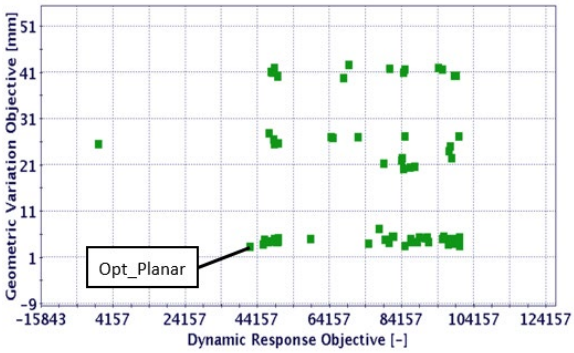

Figure 4.44: Scatter plot of objective function of Geometric Variation and Dynamic response for Configuration 12, MDO stage two optimisation

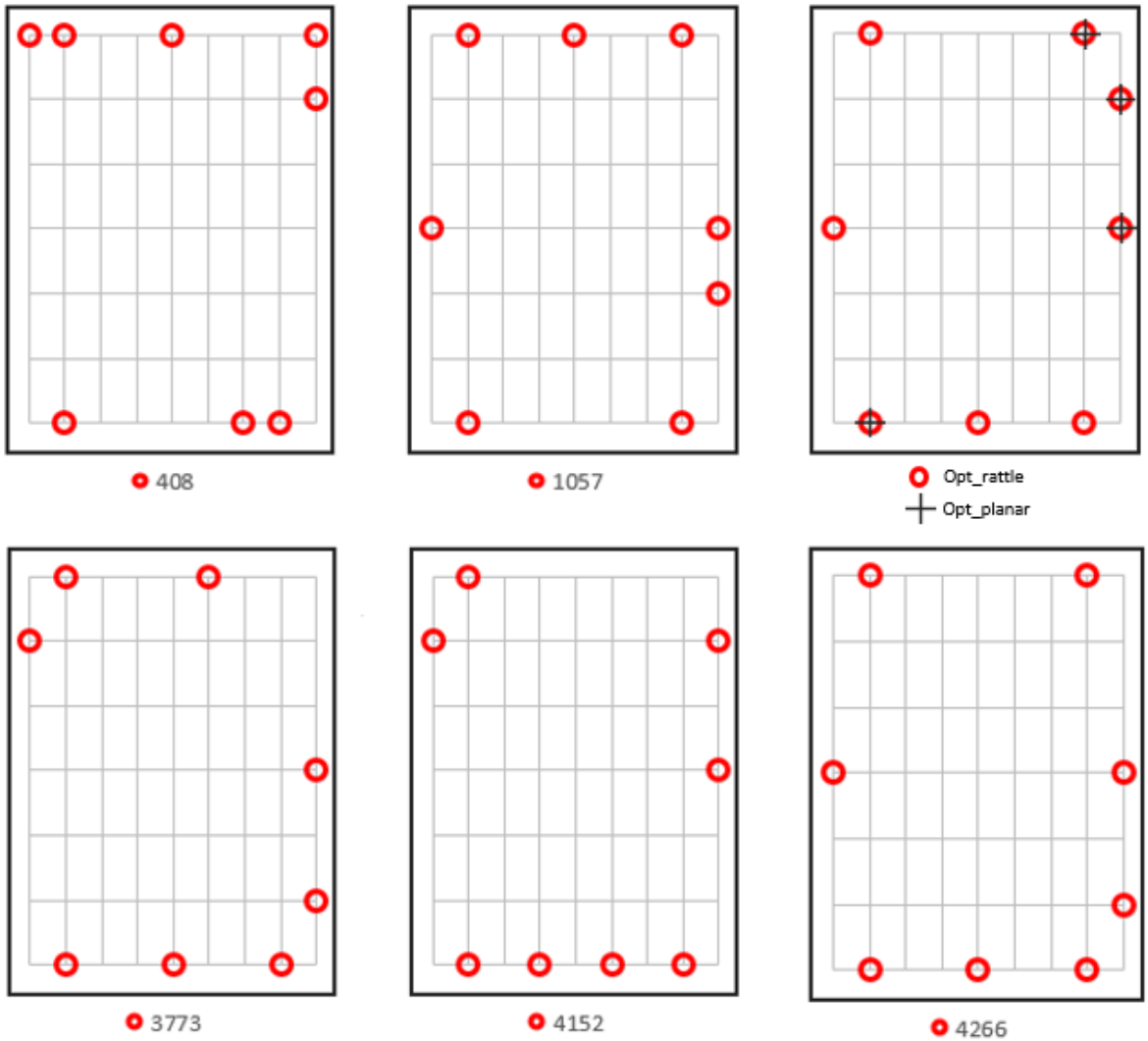

Figure 4.45: Schematic connection configuration for the designs that form the Pareto of Figure 4.43 in Configuration 12.

4.1.6 Configuration 13 (Structure – Structure)

This configuration involves assembly of two structures and hence is a heavy model. The optimisation method is the same except that the optimisation took longer than the previous configurations owing to its size.

4.1.6.1 Geometric Variation Optimisation

The results of the first stage optimisation in the form of a pareto is shown in Figure 4.46 and the connection configuration is shown in Figure 4.48. The second stage optimisation involved identification of the attachment points constrained in planar direction and the results is shown in Figure 4.47.

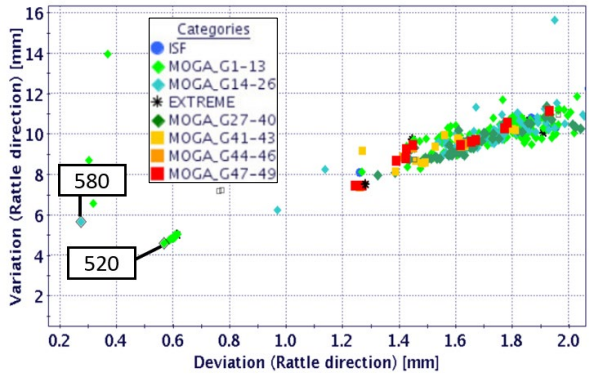

Figure 4.46: Scatter plot of objective function of Variation and Deviation for Configuration 13, Geometric Variation stage one optimisation

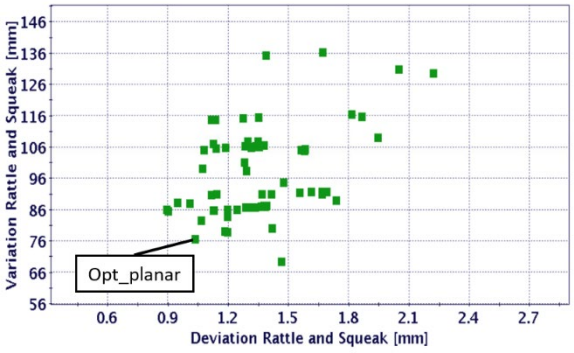

Figure 4.47: Scatter plot of objective function of Variation and Deviation for Configuration 13, Geometric Variation stage two optimisation

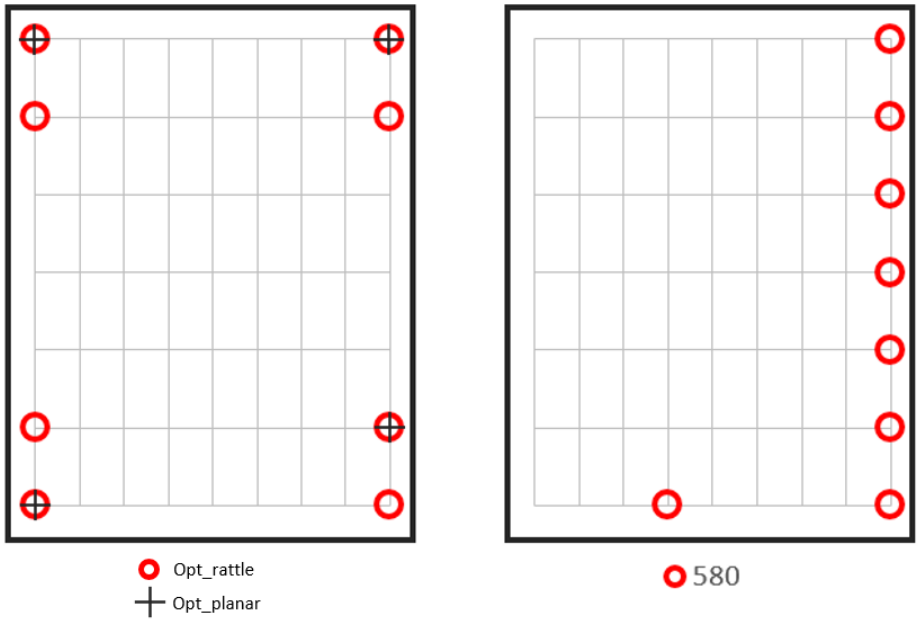

Figure 4.48: Schematic connection configuration for the designs that form the Pareto of Figure 4.48 in Configuration 13.

4.1.6.2 Dynamic Response Optimisation

For the Dynamic response optimisation, the results of the first stage optimisation in the form of a pareto is shown in Figure 4.49 and the connection configuration is shown in Figure 4.51. The pareto chart of the second stage optimisation is shown in Figure 4.50.

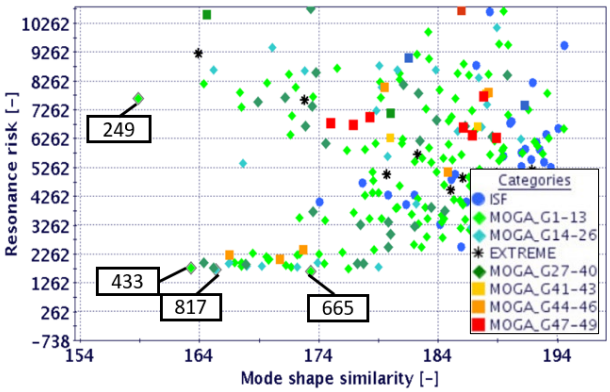

Figure 4.49: Scatter plot of objective function of Mode Shape Similarity and Resonance risk for Configuration 13, Dynamic response stage one optimisation

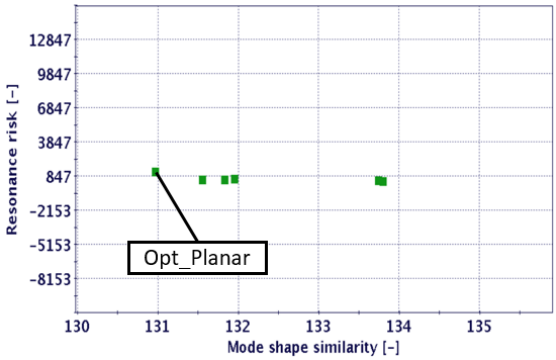

Figure 4.50: Scatter plot of objective function of Mode Shape Similarity and Resonance risk for Configuration 13, Dynamic response stage two optimisation

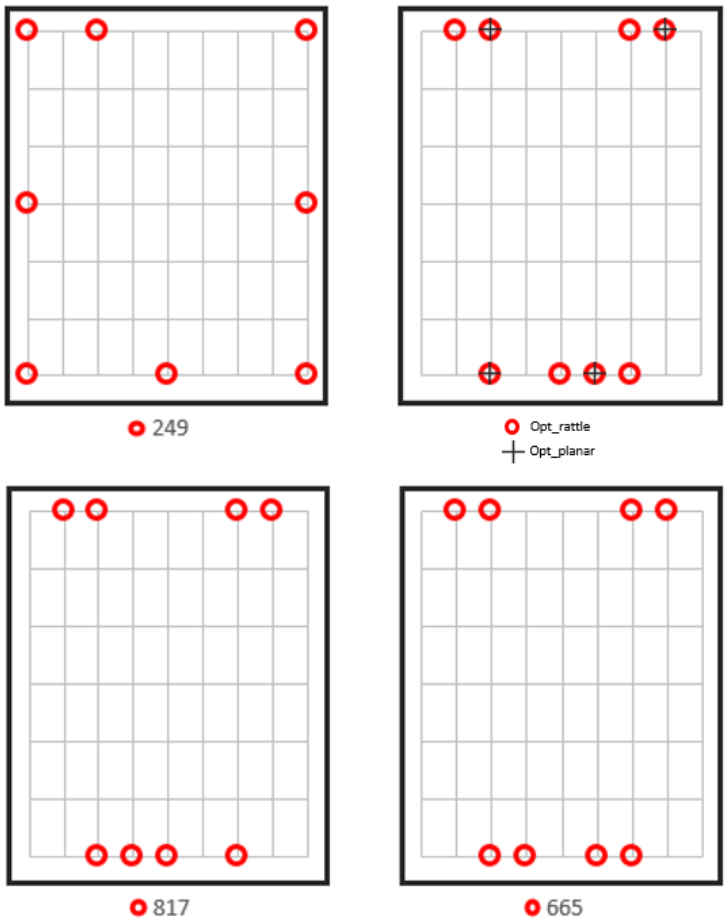

Figure 4.51: Schematic connection configuration for the designs that form the Pareto of Figure 4.49 in Configuration 13.

4.1.6.3 Multi-Disciplinary Optimisation

The results of the first stage MDO optimisation is shown in Figure 4.52 and the connection configuration in Figure 4.54. The results of the second stage planar attachment point optimisation is shown in Figure 4.53.

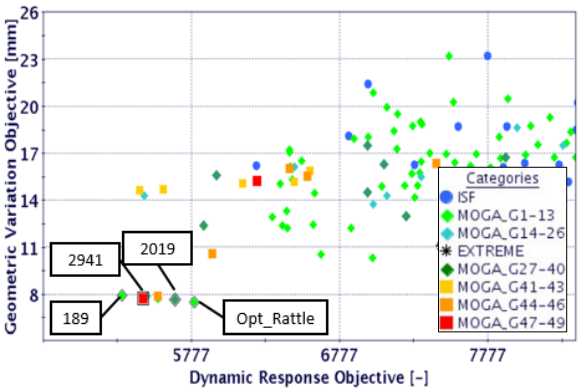

Figure 4.52: Scatter plot of objective function of Geometric Variation and Dynamic response for Configuration 13, MDO stage one optimisation

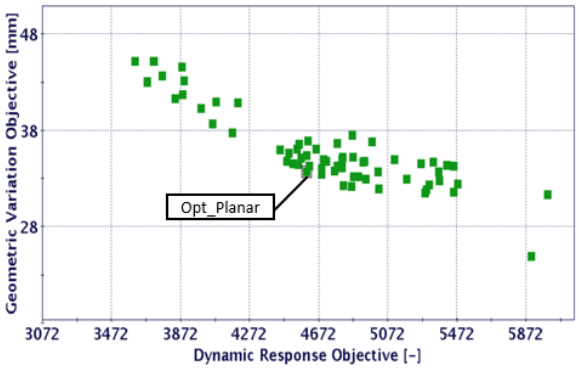

Figure 4.53: Scatter plot of objective function of Geometric Variation and Dynamic response for Configuration 13, MDO stage two optimisation

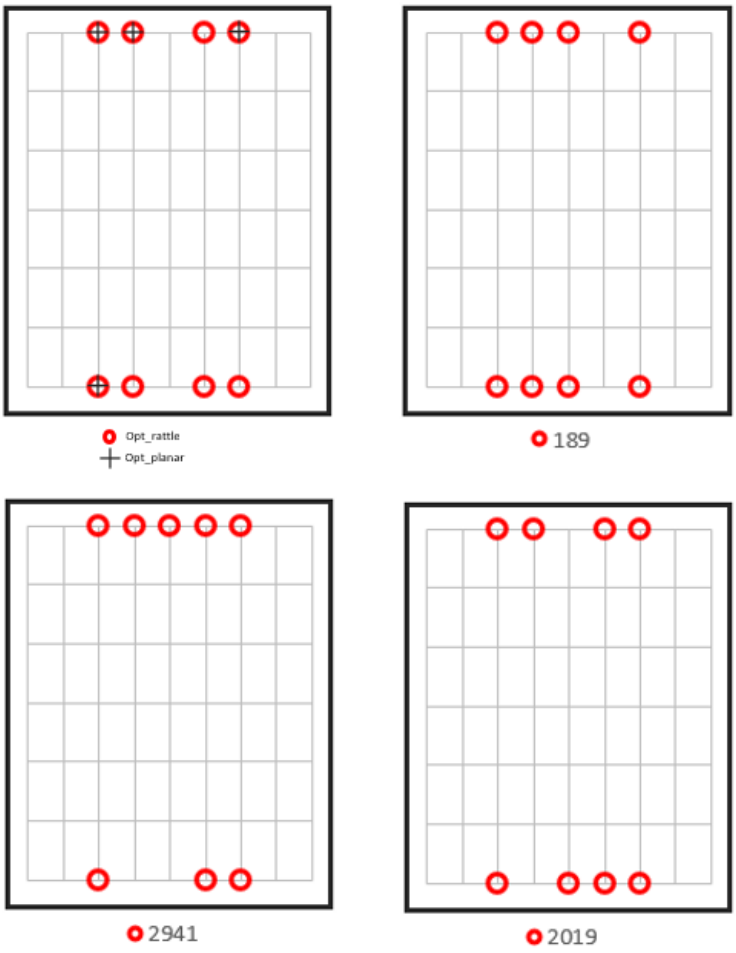

Figure 4.54: Schematic connection configuration for the designs that form the Pareto of Figure 4.52 in Configuration 13.

The optimum designs from the three optimisation were alike and accurately evenly spaced. The planar points were also evenly spread across the design. The reason for this phenomenon could be that both the components being attached to each other are structures with same dimensions and material.

4.1.7 Configuration 9 (Beam – Panel)

Configuration 9 is a special model where two beams attached to a panel is considered. These beams also hold a structure above them. This model represents a seat rail and involves four components in the assembly. The beams are independently attached to the panel and the structure is welded to the beams. A total of three attachment points holds each rail to the panel. Each rail has one attachment point that constraints in the planar direction. The left rail is constrained in planar X direction and the right rail is constrained in both planar X and planar Y direction.

A different optimisation approach was followed for this configuration. In the first phase of the optimisation, two attachment points in each rail were optimised for rattle direction. A dummy attachment point constrained in the planar direction was activated in each rail so that each rail will have three attachment points in total with 3 constraining in normal direction and 1 constraining in planar direction.

In the second phase of the optimisation, the optimum points from the rattle direction was activated and the optimisation was run for identifying the optimum point to be constrained in planar direction. The dummy planar attachment point was deactivated for this phase.

4.1.7.1 Geometric Variation Optimisation

The results of the first stage optimisation in the form of a pareto is shown in Figure 4.55 and the connection configuration is shown in Figure 4.57. The second stage optimisation involved identification of the attachment points constrained in planar direction and the results is shown in Figure 4.56.

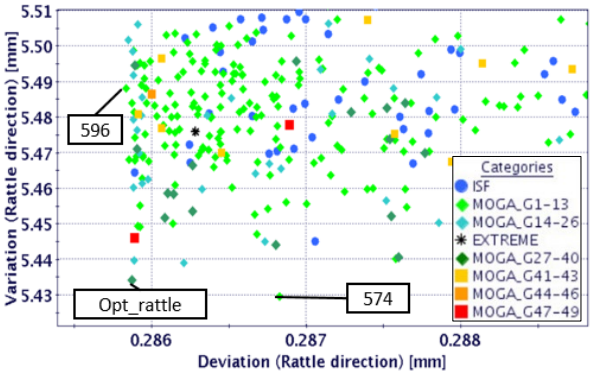

Figure 4.55: Scatter plot of objective function of Variation and Deviation for Configuration 9, Geometric Variation phase one optimisation

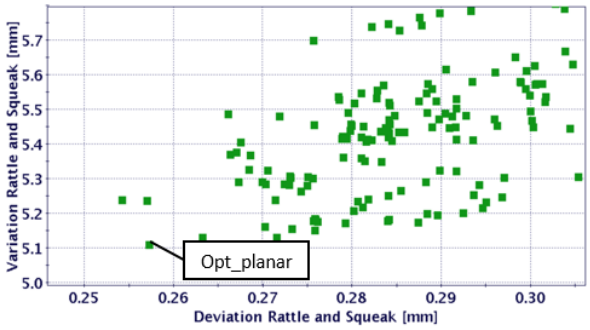

Figure 4.56: Scatter plot of objective function of Variation and Deviation for Configuration 9, Geometric Variation phase two optimisation

The Opt_rattle plot in Figure 4.57 shows the points that is constrained in planar X and both planar XY directions.

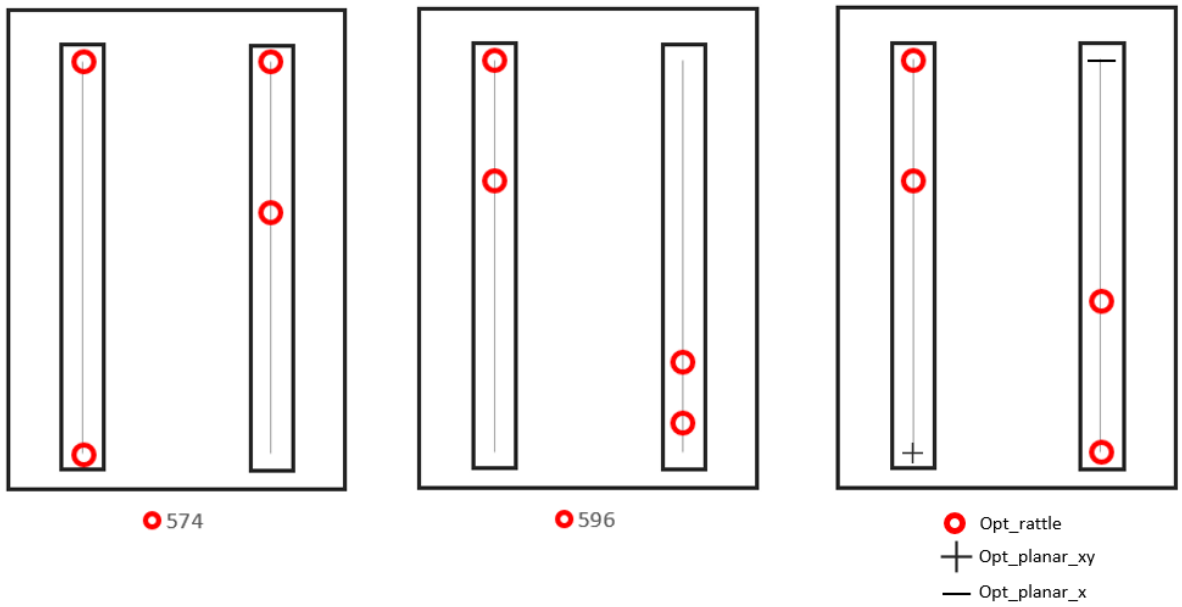

Figure 4.57: Schematic connection configuration for the designs that form the Pareto of Figure 4.55 in Configuration 9.

4.1.7.2 Dynamic Response Optimisation

For the Dynamic response optimisation, the results of the first stage optimisation in the form of a pareto is shown in Figure 4.58 and the connection configuration is shown in Figure 4.60. The pareto chart of the second stage optimisation is shown in Figure 4.59.

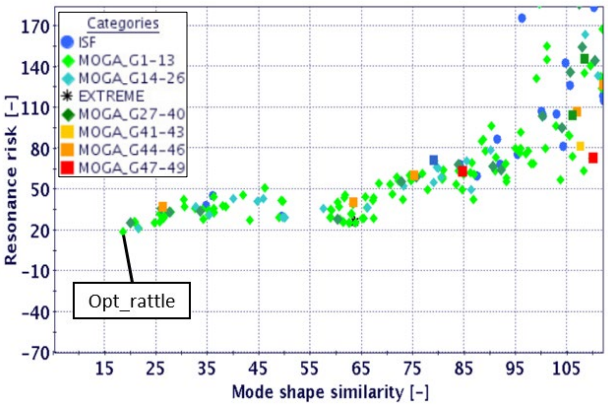

Figure 4.58: Scatter plot of objective function of Mode Shape Similarity and Resonance risk for Configuration 9, Dynamic response phase one optimisation

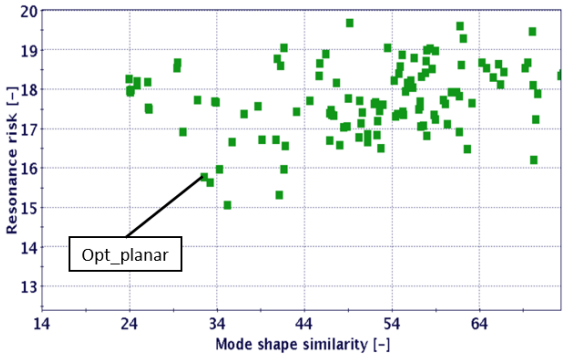

Figure 4.59: Scatter plot of objective function of Mode Shape Similarity and Resonance risk for Configuration 9, Dynamic response phase two optimisation

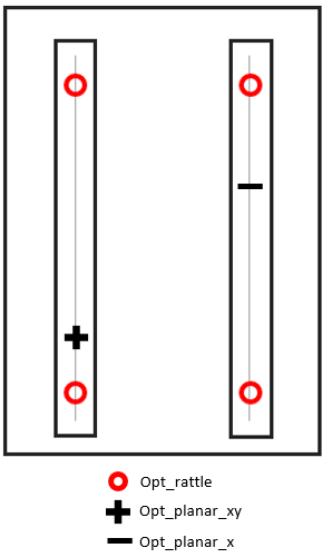

Figure 4.60: Schematic connection configuration for the designs that form the Pareto of Figure 4.58 in Configuration 9.

4.1.7.3 Multi-Disciplinary Optimisation

The results of the first stage MDO optimisation is shown in Figure 4.61 and the connection configuration in Figure 4.63.

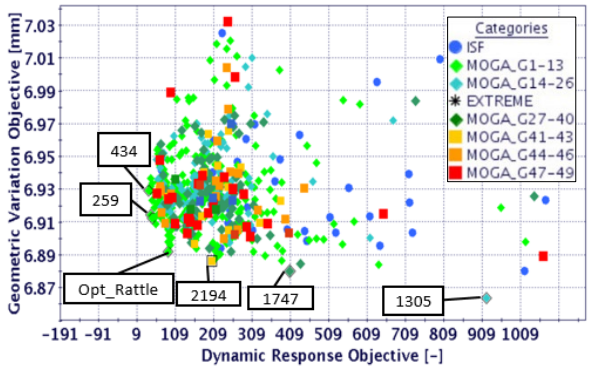

Figure 4.61: Scatter plot of objective function of Geometric Variation and Dynamic response for Configuration 9, MDO phase one optimisation

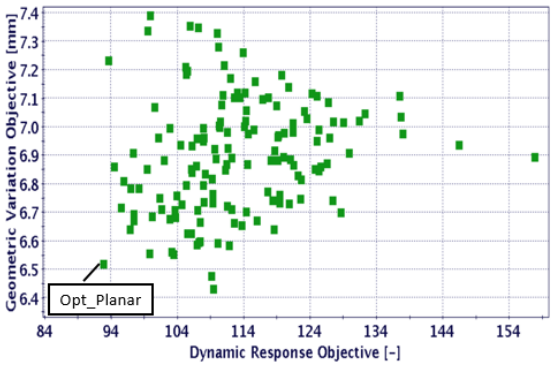

Figure 4.62: Scatter plot of objective function of Geometric Variation and Dynamic response for Configuration 9, MDO phase two optimisation

The results of the second stage planar attachment point optimisation is shown in Figure 4.62.

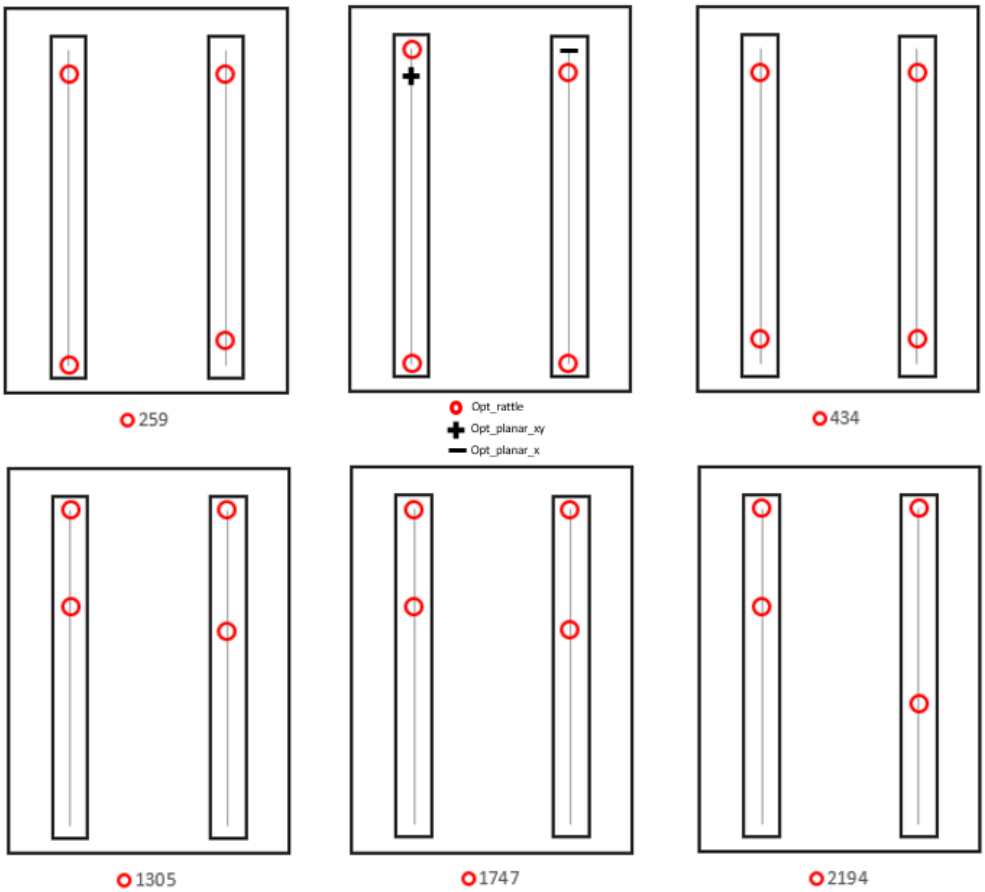

Figure 4.63: Schematic connection configuration for the designs that form the Pareto of Figure 4.61 in Configuration 9.

4.1.8 Configuration 14 (Panel – Panel)

Configuration 14 is also a special type of configuration where the two panels are not attached to each other. Instead, they are each attached to another neighbouring part and only the measure points between these panels are of interest. Hence, a modified two-stage optimisation approach was followed for this configuration.

For the first phase of optimisation, four attachment points in Instrument panel and two attachment points in the tunnel console are optimized with one dummy attachment point in the tunnel console. The attachment points in Instrument Panel and Tunnel Console are constrained in directions perpendicular to each other since the parts are perpendicular to each other.

For the second phase of optimisation, two out of the four chosen attachment points in the instrument panel is selected for a design and in addition to the two attachment points found in tunnel console, one more attachment point to be constrained in planar direction is found out. This point replaces the need of the dummy planar attachment point. The planar attachment point is constrained in the squeak plane of the tunnel console, but it contributes to rattle with the instrument panel.

4.1.8.1 Geometric Variation Optimisation

The results of the first stage optimisation in the form of a pareto is shown in Figure 4.64 and the connection configuration is shown in Figure 4.65.

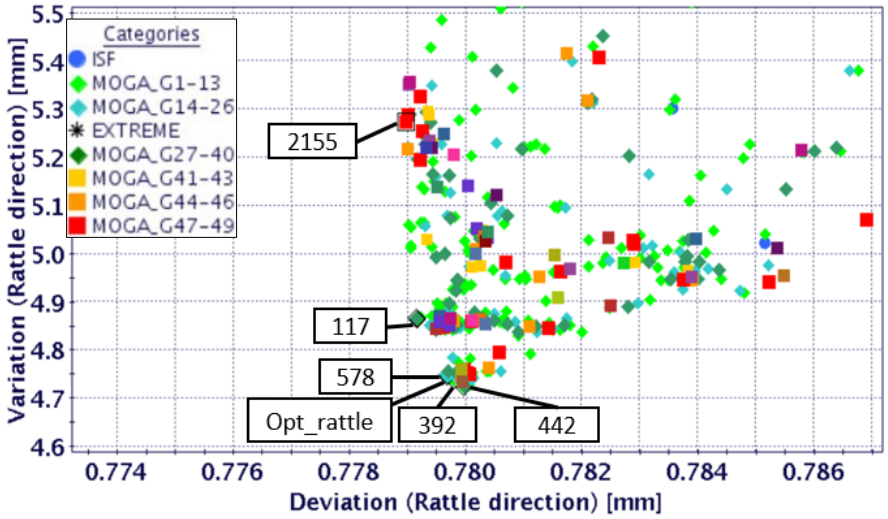

Figure 4.64: Scatter plot of objective function of Variation and Deviation for Configuration 14, Geometric Variation phase one optimisation

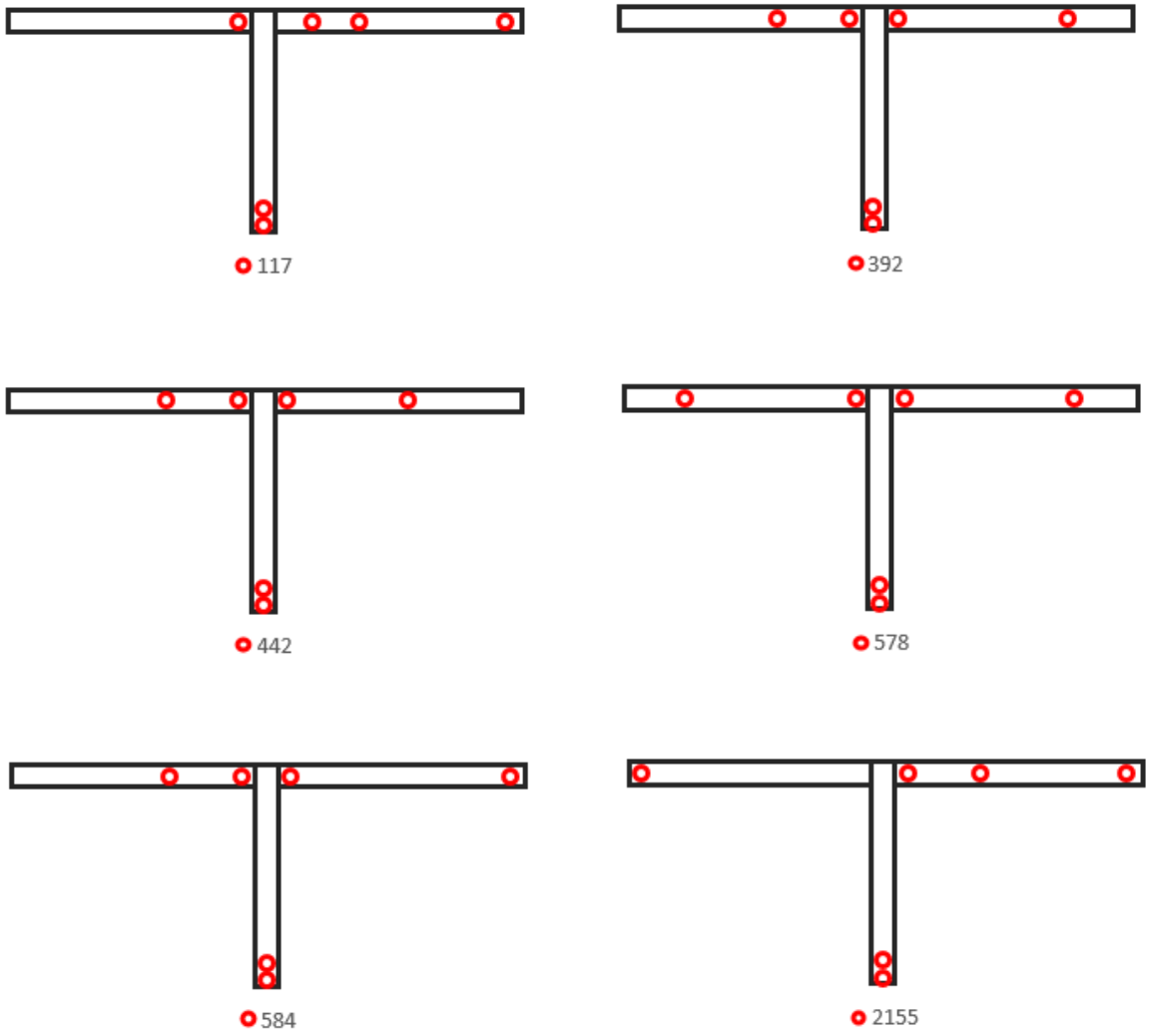

Figure 4.65: Schematic connection configuration for the designs that form the Pareto of Figure 4.64 in Configuration 14.

The second stage optimisation involved identification of the attachment points constrained in planar direction and the results is shown in Figure 4.66 and the final design is showed in the Figure 4.67.

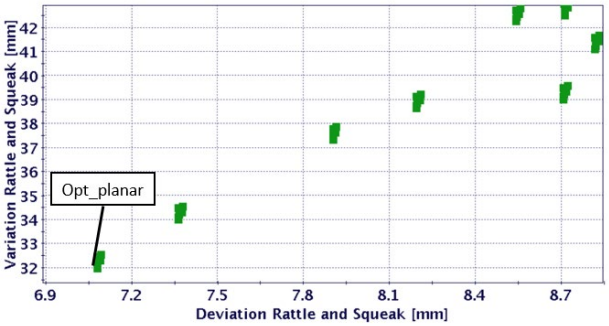

Figure 4.66: Scatter plot of objective function of Variation and Deviation for Configuration 14, Geometric Variation phase two optimisation

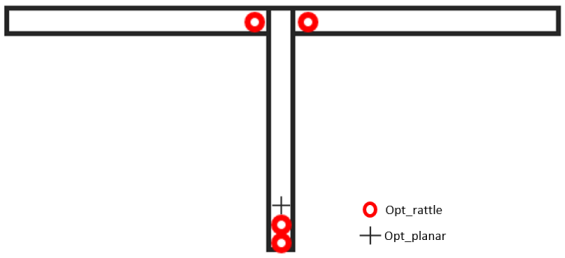

Figure 4.67: Schematic connection configuration of the final optimum design in Geometric variation of Configuration 14.

4.1.8.2 Dynamic Response Optimisation

The results of the first stage optimisation in the form of a pareto is shown in Figure 4.68 and the connection configuration is shown in Figure 4.69.

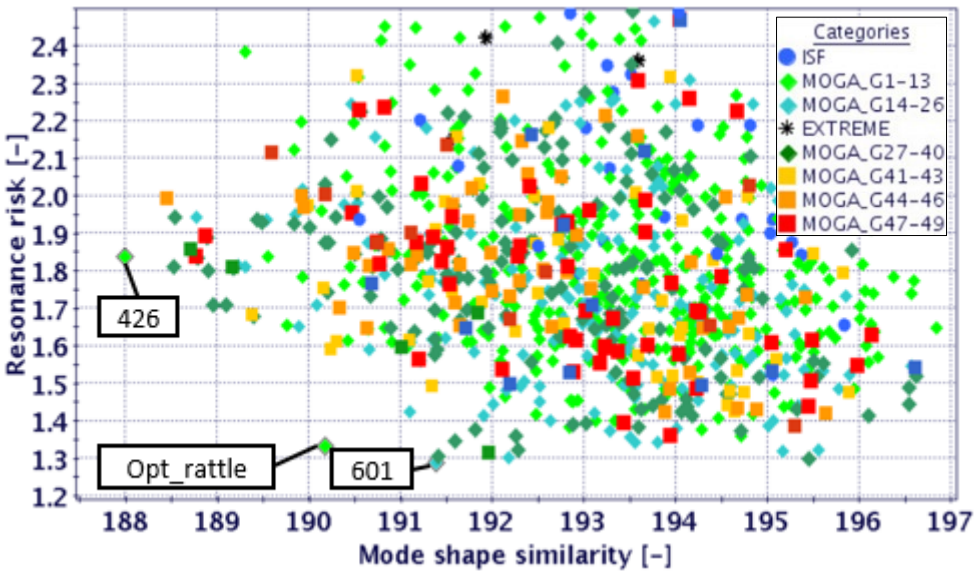

Figure 4.68: Scatter plot of objective function of Mode shape similarity and Resonance risk for Configuration 14, Dynamic Response phase one optimisation

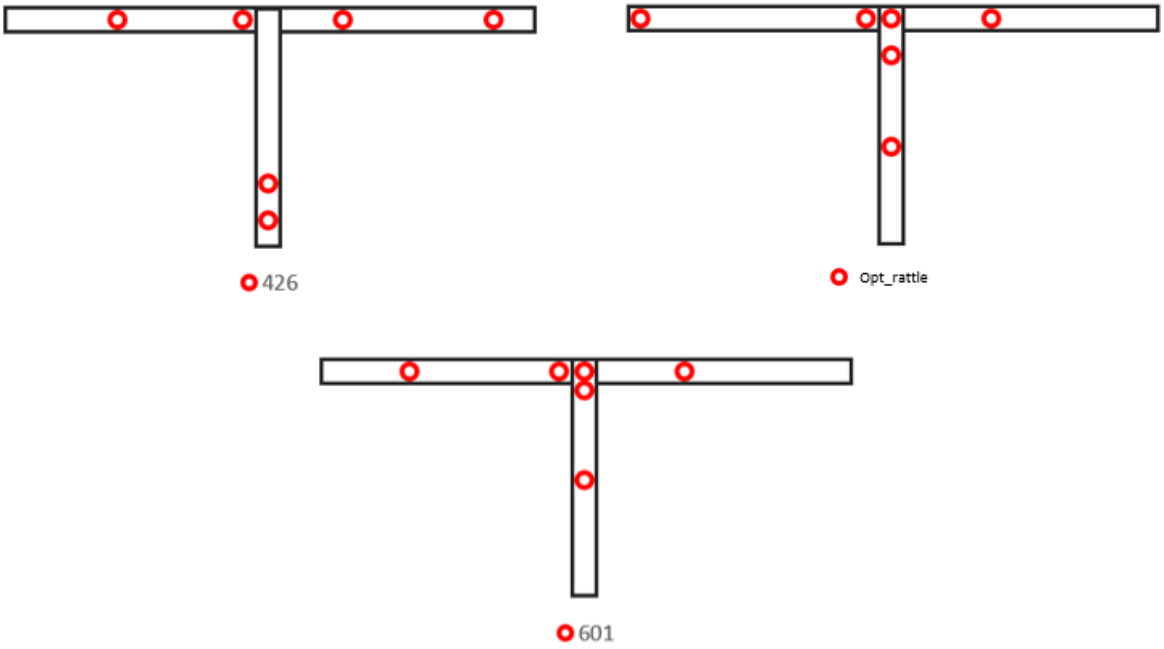

Figure 4.69: Schematic connection configuration for the designs that form the Pareto of Figure 4.68 in Configuration 14.

The second stage optimisation involved identification of the attachment points constrained in planar direction and the results is shown in Figure 4.70 and the final design is showed in the

Figure 4.71: Schematic connection configuration of the final optimum design in Dynamic Response of Configuration 14..

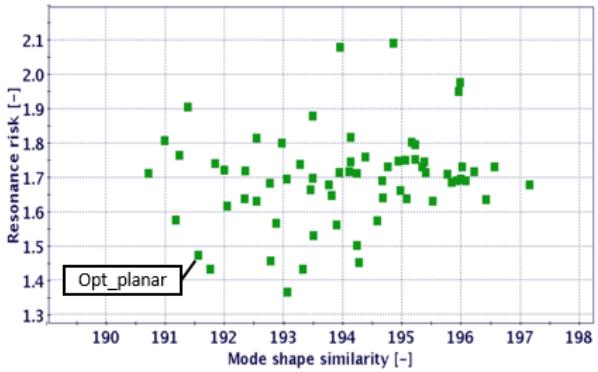

Figure 4.70: Scatter plot of objective function of Mode shape similarity and Resonance risk for Configuration 14, Dynamic Response phase two optimisation

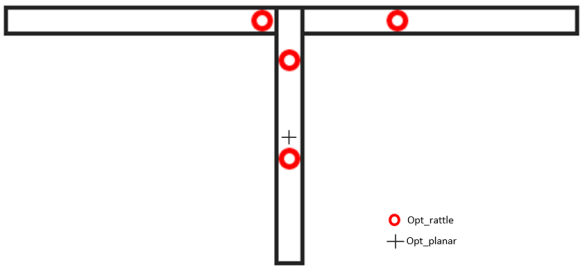

Figure 4.71: Schematic connection configuration of the final optimum design in Dynamic Response of Configuration 14.

4.1.8.3 Multi-Disciplinary Optimisation

The results of the first stage optimisation in the form of a pareto is shown in Figure 4.72 and the connection configuration is shown in Figure 4.73.

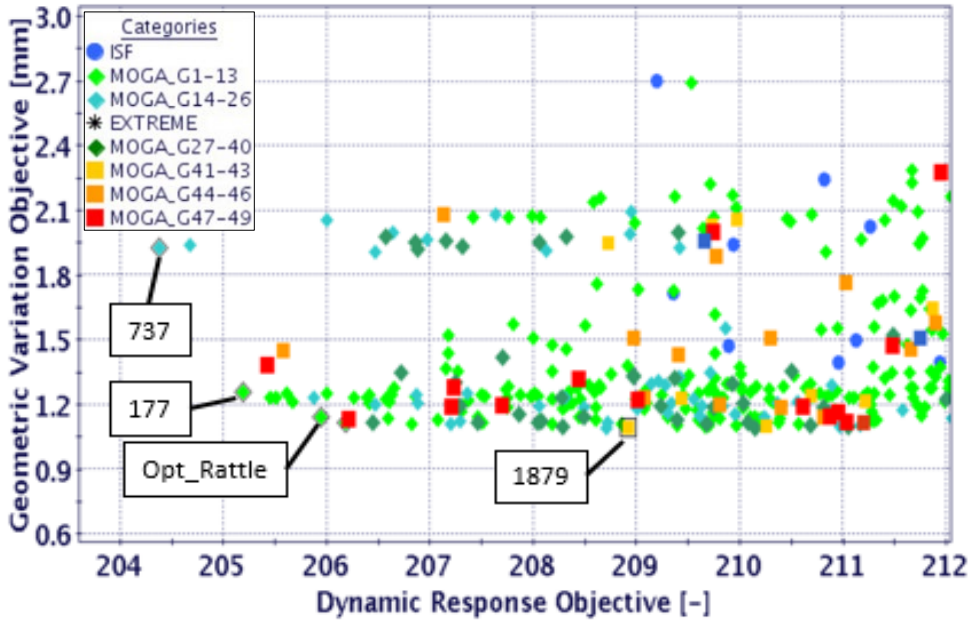

Figure 4.72: Scatter plot of objective function of Geometric Variation and Dynamic Response for Configuration 14, MDO phase one optimisation

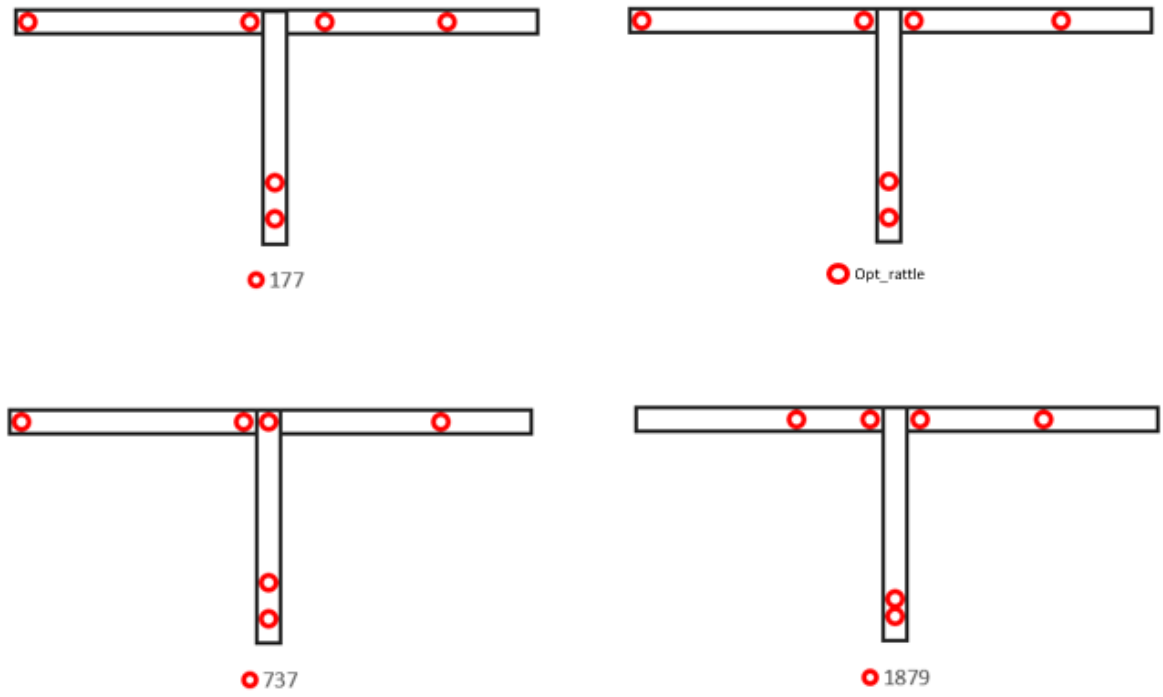

Figure 4.73: Schematic connection configuration for the designs that form the Pareto of Figure 4.72 in Configuration 14.

The second stage optimisation involved identification of the attachment points constrained in planar direction and the results is shown in Figure 4.74 and the final design is showed in the Figure 4.75.

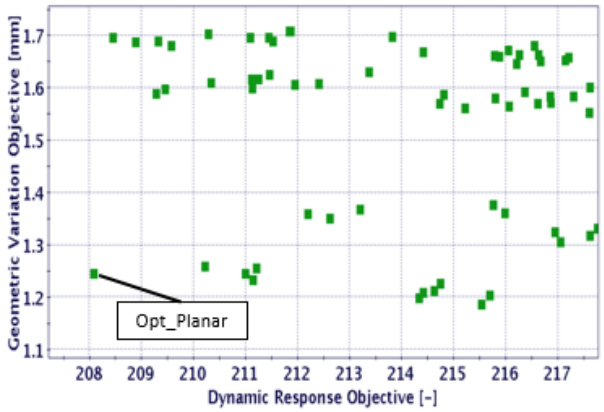

Figure 4.74: Scatter plot of objective function of Geometric Variation and Dynamic Response for Configuration 14, MDO phase two optimisation

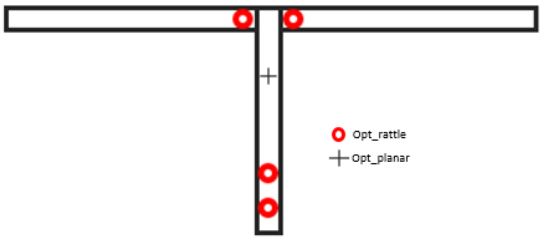

Figure 4.75: Schematic connection configuration of the final optimum design in MDO of Configuration 14.

4.2 Effect of number of fasteners

A study was performed to understand the effect of increasing the number of attachment points for a model. For this, configuration 10 and configuration 13 was chosen, and optimisation was run with 16 attachment points. The optimisation for rattle direction was run and the objectives were plotted to form a pareto. The optimum design from the pareto was represented in the form of a connection configuration. The optimum design with 16 points and 8 points for configuration 10 is shown in Figure 4.76 and for configuration 13 is shown in Figure 4.77.

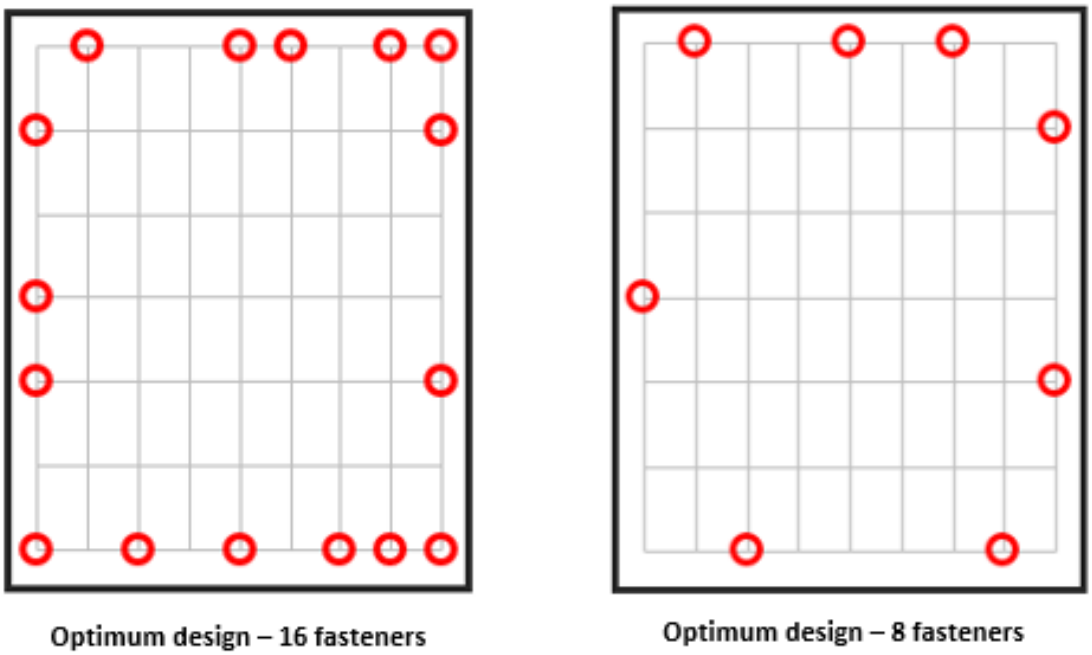

Figure 4.76: Comparison of the design between 16 attachment points and 8 attachment points in configuration 10.

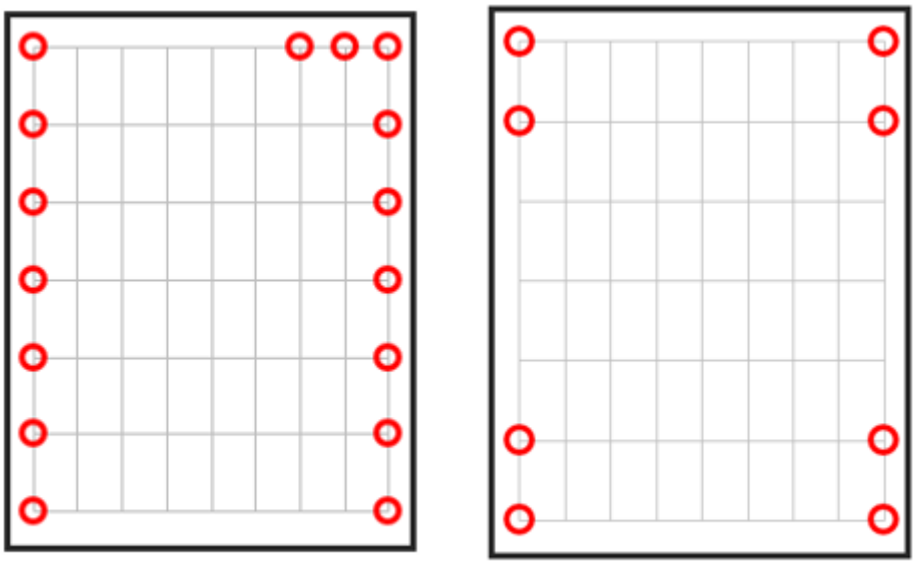

Figure 4.77: Comparison of the design between 16 attachment points and 8 attachment points in configuration 13.

The objective values for the optimum design in configuration 10 and configuration 13 is shown in Table 4.1 and Table 4.2 respectively.

Table 4.1: Table showing the objective values of the optimum design in Configuration 10

Model No.	Deviation Objective		Variation Objective	
	16 – point	8 – point	16 – point	8 – point
10	0.402	0.403	3.57	3.45

Table 4.2: : Table showing the objective values of the optimum design in Configuration 13

Model No.	Deviation Objective		Variation Objective	
	16 – point	8 – point	16 – point	8 – point
13	1.176	0.271	7.91	5.69

The designs that were generated followed the same trend and the optimizer added additional points closer to the existing points. The objective values also indicate that there is no improvement in the S&R behaviour by merely increasing the number of attachment points beyond certain level. In both the configurations, the points in the 8-point design featured in the 16-point design as well. These comparison proved that increasing the number of points does not make a difference in how the optimizer assigns the attachment points.

4.3 Effect of inclination of fasteners

A study was performed to understand the effect of having the attachment points inclined on the results. For the study, configurations 1-3 were selected and two models were created, one with attachment points that were normal in direction and the other model with attachment points at an angle. The angle of the attachment point varied between 10-40 degrees. The optimum results for the two cases for the configuration 1 are shown in Figure 4.78.

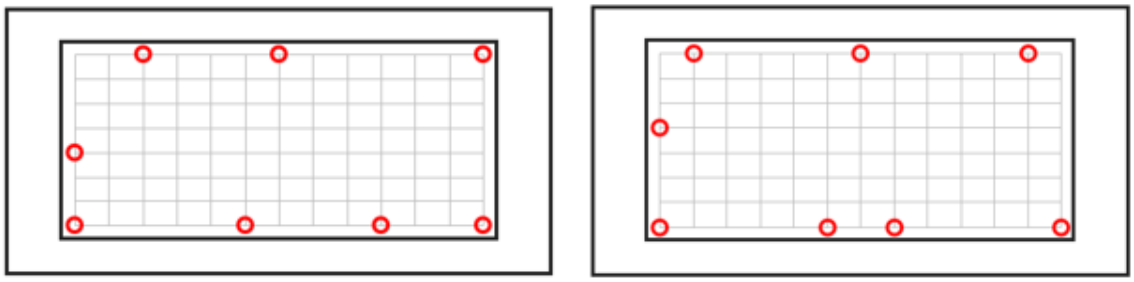

Figure 4.78: Connection configuration of designs generated using inclined attachment point (left) and straight attachment point (right) – Configuration 1

The results for the configuration 2 and configuration 3 are shown in Figure 4.79 and Figure 4.80.

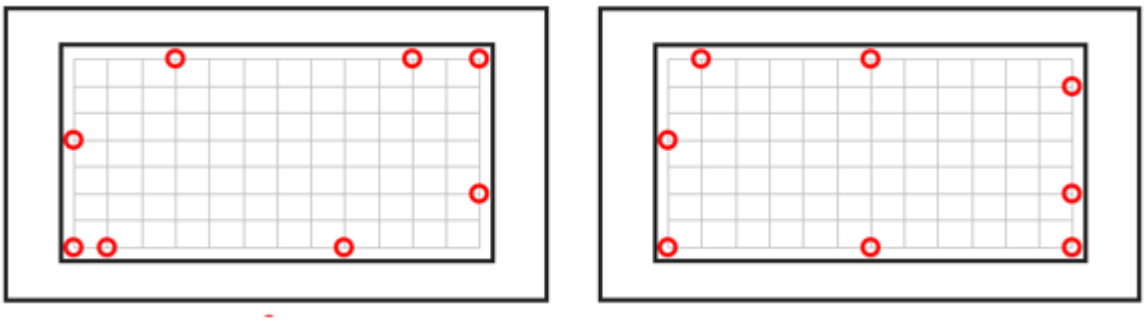

Figure 4.79: Connection configuration of designs generated using inclined attachment point (left) and straight attachment point (right) – Configuration 2

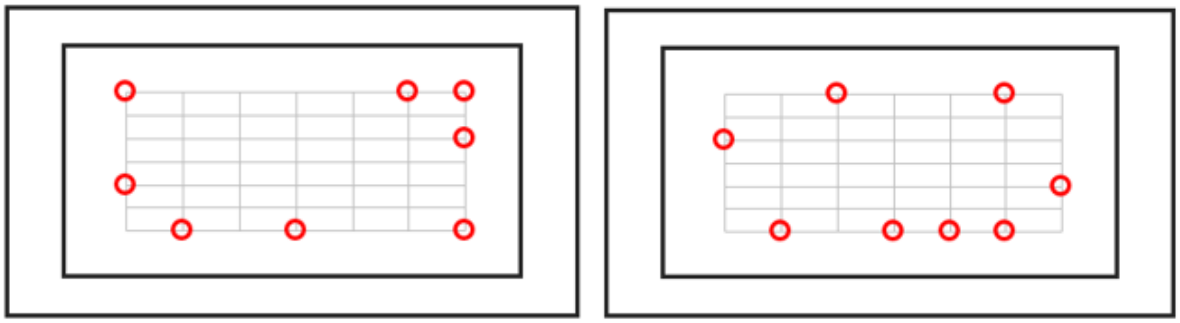

Figure 4.80: Connection configuration of designs generated using inclined attachment point (left) and straight attachment point (right) – Configuration 3

In all the configurations that were run, the same design had significant differences when the attachment points were inclined. The absolute mean of the differences for each configuration

is shown in Table 4.3: Table showing the difference in the objective values for each configuration.

Table 4.3: Table showing the difference in the objective values for each configuration

Model No.	Deviation Objective	Variation Objective
1	10%	25%
2	30%	45%
3	23%	50%

5. Industrial Cases

This chapter explains the results of the optimisation that was carried out with the industrial cases such as Instrument Panel – Deco Panel assembly and Side door assembly. The models were prepared in the work done by [12] during the Master thesis work done at VCC. These models were modified by including the objectives and constraints discussed in the Chapter 2. Single Disciplinary Optimisation for Geometric Variation for both the models: IP assembly and the Side door assembly has been performed by Bayani, M. et al [12] and the results could be seen in the conference proceedings [12].

5.1 Instrument Panel Assembly

Instrument Panel assembly has four fasteners in which 4 fasteners constrained in normal direction and 2 fasteners constrained in planar directions. The optimisation was run for this same number of fasteners as in the real assembly. The baseline design was included in the results plot facilitating easy comparison with the designs generated.

5.1.1 SDO – Dynamic response

The optimisation method proposed was applied to the IP Assembly model and the optimisation for Dynamic response was carried out. The optimisation ran for 50 generations and the results are shown in the Figure 5.1.

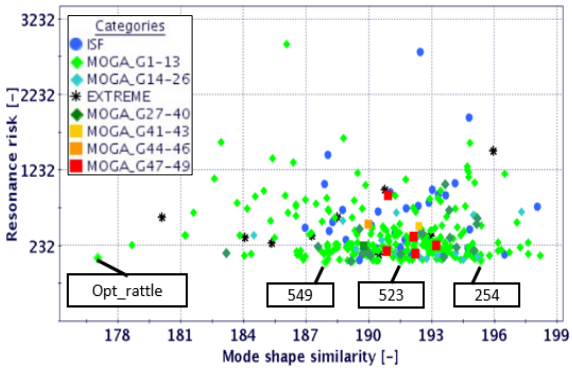

Figure 5.1: Scatter plot of objective function of Mode shape similarity and Resonance risk for the IP assembly, Dynamic response stage one optimisation

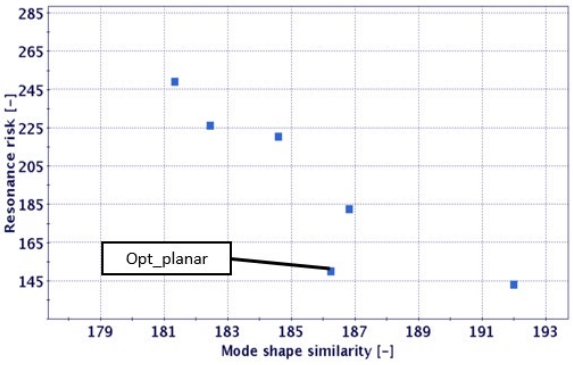

Figure 5.2: Scatter plot of objective function of Mode shape similarity and Resonance risk for the IP assembly, Dynamic response stage two optimisation

The extreme cases were far off from the pareto and the designs in the pareto also outperformed the baseline design. The connection configuration for the designs in the pareto front is shown in Figure 5.3. The baseline design is shown in grey solid circles in each plot. The design is shown in red circles and the optimum design from the first stage of optimisation is labelled as Opt_rattle in the Figure 5.3.

For the second stage of optimisation, the fasteners to be constrained in planar directions were identified in the optimum design from the first stage. This was done by running a full DOE considering the small size of the DOE. The result from the DOE study is shown in the Figure 5.2. The connection configuration for the planar fasteners is represented in the Opt_rattle design in Figure 5.3 with a black plus sign.

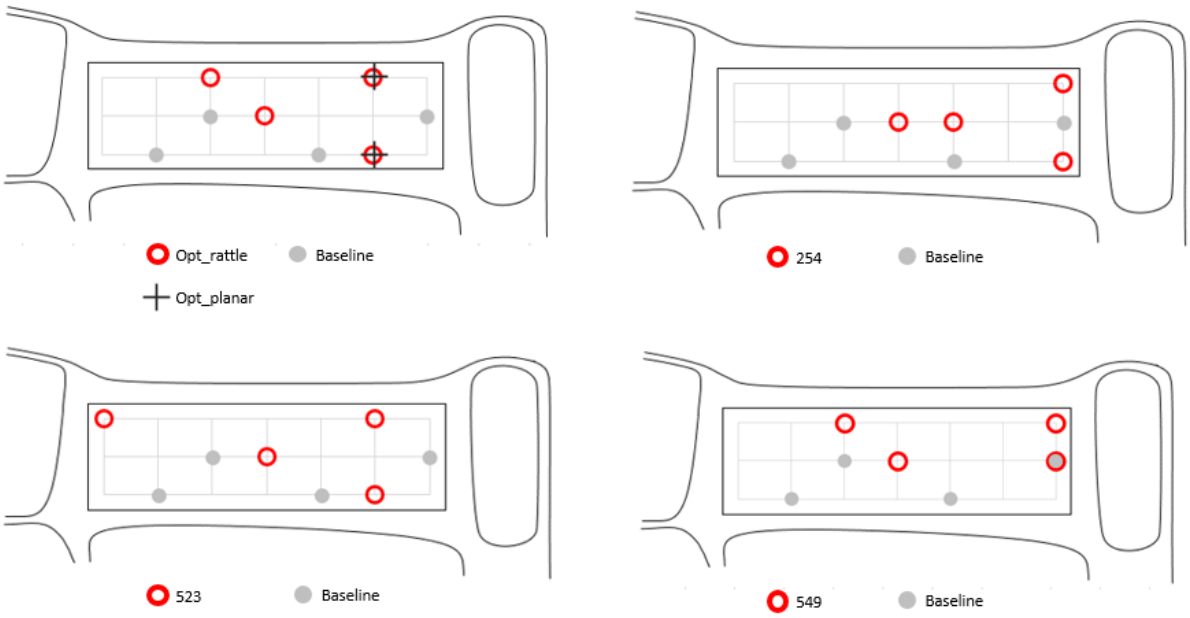

Figure 5.3: Schematic connection configuration for the designs that form the Pareto of Figure 5.1 in IP assembly

5.1.2 MDO – Geometric Variation and Dynamic response

For the MDO, the RD&T model developed by [17] was used for the Geometric variation. The model was improved by increasing the number of candidates making the design space bigger. The NASTRAN model was also updated accordingly, and the optimisation was run.

For the first stage of the optimisation, the optimum design in the rattle direction was found by activating two dummy fasteners and the result is represented in Figure 5.4. The connection configuration is shown in Figure 5.6.

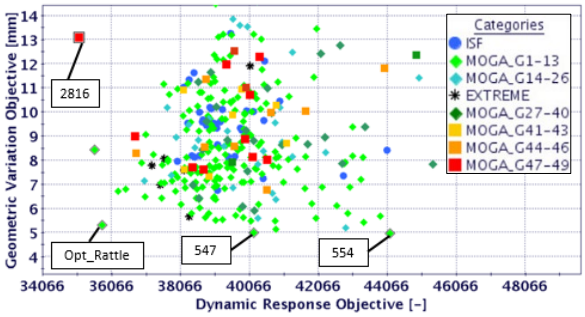

Figure 5.4: Scatter plot of objective function of Geometric variation objective and Dynamic response objective for the IP assembly, MDO stage one optimisation

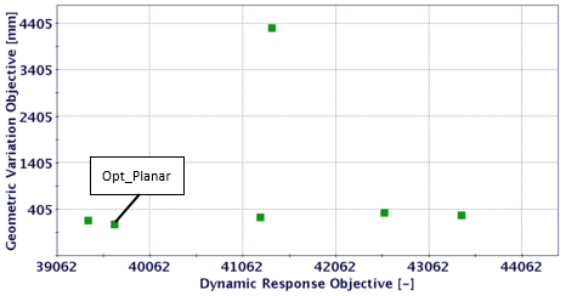

Figure 5.5: Scatter plot of objective function of Geometric variation objective and Dynamic response objective for the IP assembly, MDO stage two optimisation

In the second stage optimisation, the planar fasteners were identified, and the result is shown in Figure 5.5. The connection configuration is shown in the Opt_rattle plot in Figure 5.6.

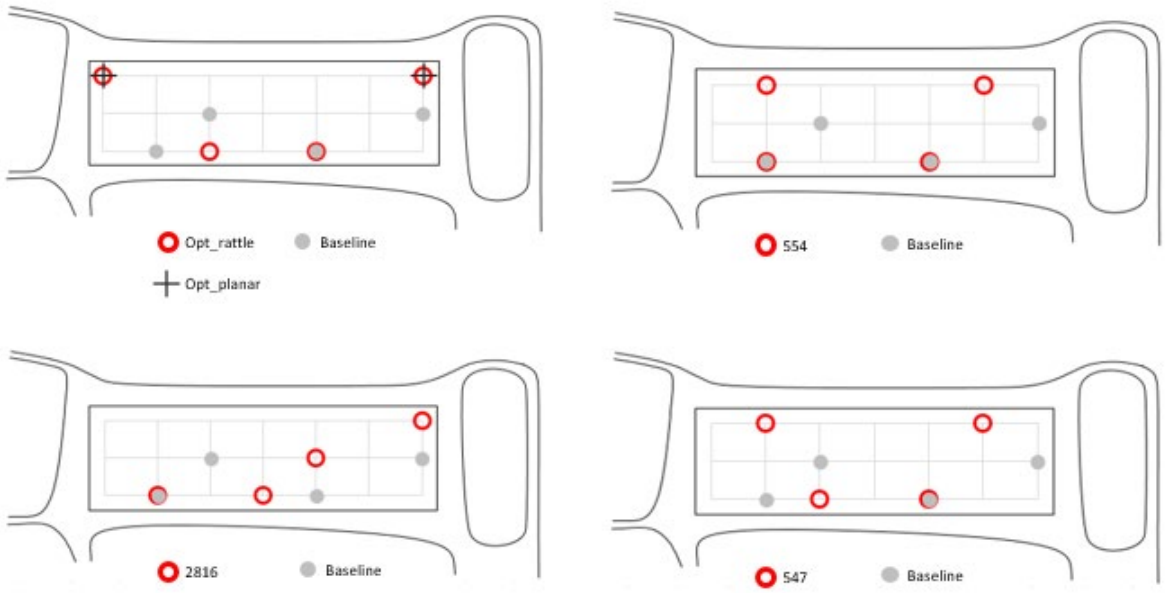

Figure 5.6: Schematic connection configuration for the designs that form the Pareto of Figure 5.4 in IP assembly

5.2 Side Door Assembly

Side door assembly is another model that was chosen for the industrial case. The model was prepared by [17] and it was modified with the updated constraints, objectives and methodology. The side door assembly has a total of 10 fasteners of which 10 constrained in the normal direction and 4 constrained in planar directions. The baseline design was used to compare the performance of the designs generated in the optimisation.

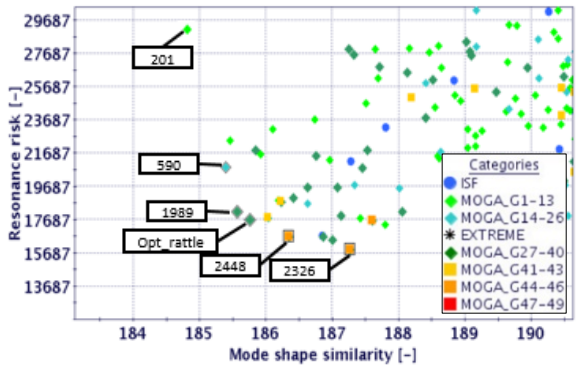

Figure 5.7: Scatter plot of objective function of Mode shape similarity and Resonance risk for the Side door assembly, Dynamic response stage one optimisation

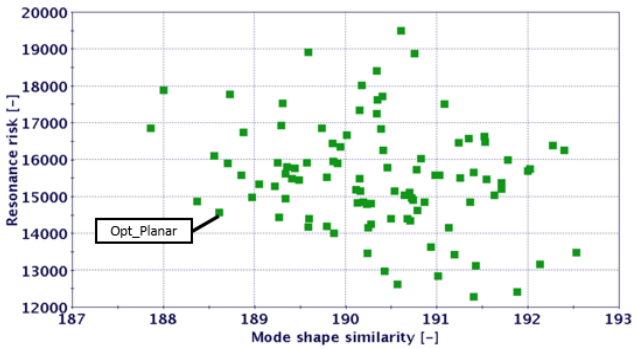

Figure 5.8: Scatter plot of objective function of Mode shape similarity and Resonance risk for the Side door assembly, Dynamic response stage two optimisation

5.2.1 SDO – Dynamic response

The optimisation method proposed was also applied to the Side door Assembly model and the optimisation in rattle direction was carried out. The optimisation ran for 50 generations and it was made sure that no designs in the pareto front was from the final 5 generations. the results are shown in the Figure 5.7.

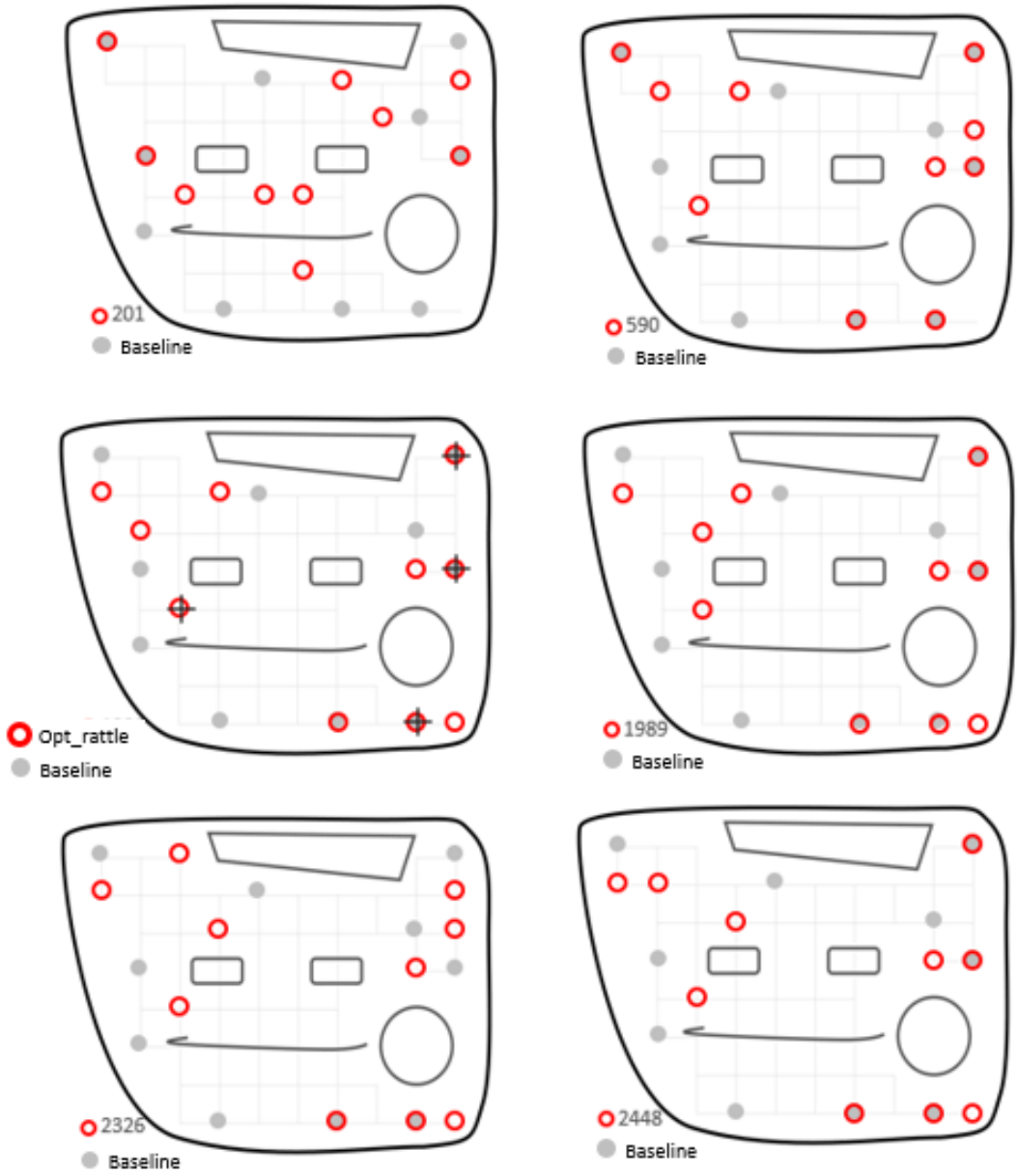

Figure 5.9: Schematic connection configuration for the designs that form the Pareto of Figure 5.7 in Side door assembly

As in the case of IP assembly, the extreme cases were far off from the pareto and the designs in the pareto outperformed the baseline design. The connection configuration for the designs in the pareto front is shown in Figure 5.9. The optimum design that was chosen in the first stage of optimisation is labelled as Opt_rattle in the Figure 5.9.

For the second stage of optimisation, the points in the optimum rattle design that must be constrained in planar direction was found by running a full DOE considering the small size of the DOE. The result from the DOE study is shown in the Figure 5.8. The connection configuration for the planar fasteners is represented in the Opt_rattle design in Figure 5.9 with a black plus sign.

5.2.2 MDO – Geometric Variation and Dynamic response

For the first stage of the optimisation, the optimum design in the rattle direction was found by activating two dummy fasteners and the result is represented in Figure 5.10. The connection configuration is shown in Figure 5.12. A multiplier to the Dynamic response and Geometric variation objective was added so that the values are normalized when summing them up.

In the second stage optimisation, the planar fasteners were identified, and the result is shown in Figure 5.11. The connection configuration is shown in the Opt_rattle plot in Figure 5.12.

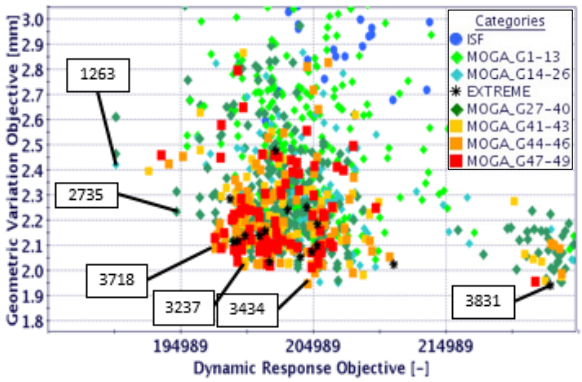

Figure 5.10: Scatter plot of objective function of Mode shape similarity and Resonance risk for the Side door assembly, MDO stage one optimisation

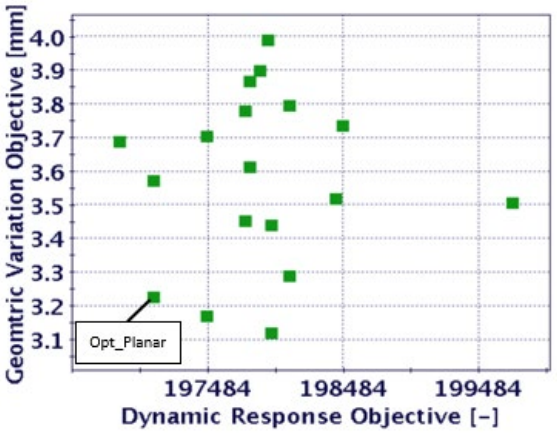

Figure 5.11: Scatter plot of objective function of Mode shape similarity and Resonance risk for the Side door assembly, MDO stage two optimisation

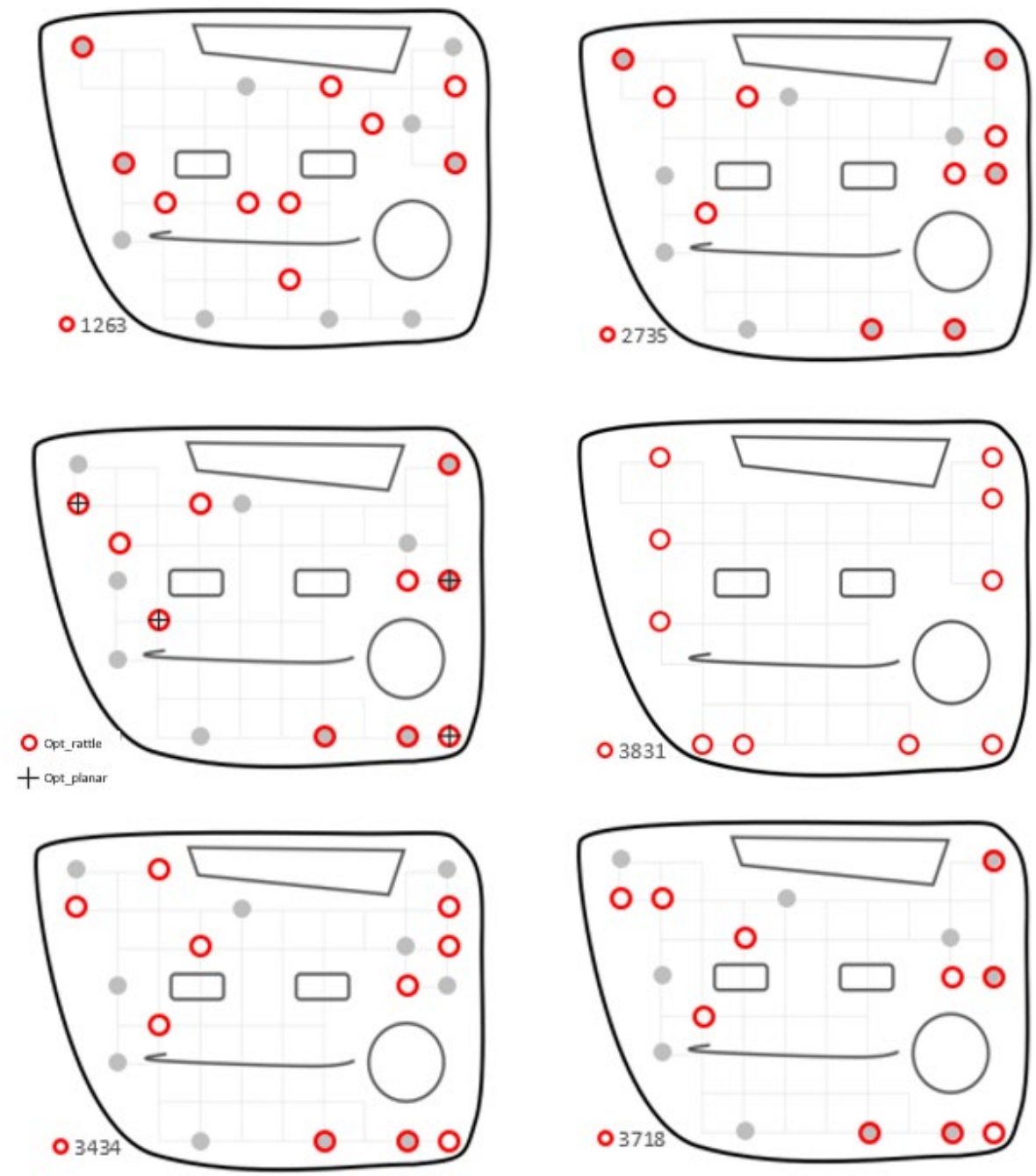

Figure 5.12: Schematic connection configuration for the designs that form the Pareto of Figure 5.10 in Side door assembly

6. Conclusion

6.1 Conclusion

The thesis work involved single and multi-disciplinary optimisation of selected simplified geometries and assembly models from industrial applications. The work intended to answer the research questions that were framed in Chapter 1.

RQ1 - With the aim of S&R prevention by geometric variation and dynamic response analyses, how different the results of a decoupled or multidisciplinary optimization are?

Results of the Single Disciplinary Optimisations (SDO) for Dynamic response and geometric variations proved that the direction of the result was not identical and took different directions to find the optimum design. A trade-off was needed to generate a design that behaves well with respect to both geometric variation and dynamic response thereby reducing the possibility of S&R. This answers the research question 1.

RQ2 - For different geometries (and assemblies), how the above difference varies? Can the findings be clustered for different types of geometries and attachment schemes?

Research question 2 was answered by comparing the results generated within different simplified models and there was no correlation between the different models and could not be grouped in categories. Although there were models that shared the base model, the results varied with the boundary conditions, number of attachment points and material of the components.

RQ3 - What would be the effect of having tolerances in the planar tolerances on measures in normal directions?

Research question 3 was framed since there was a two-stage optimisation methodology followed for the optimisation. In order to validate the results of the first stage where the designs were only optimized for rattle direction by using dummy fasteners in planar directions: The influence of these planar fasteners need to be validated and their influence on the results was estimated by a study that was explained in detail in Section 2.1.1.1.

In addition to the single disciplinary optimisation that was done for dynamic response and geometric variation, MDO between the two objectives was also done for the simplified geometries. The number of attachment points were also increased, and a comparison was made based on the number of attachment points. The angle in which the fastener was applied was also modified and the results were compared. The work also included real industrial applications to demonstrate how the methodology can also be implemented on complex industrial models.

6.2 Recommendations

The model selection involved a final selection of 14 simplified geometries out of which 8 was chosen for the optimisation. The methodology could be applied to the other geometries which involves different boundary conditions and curved geometries. The results of those geometries could be compared with the geometries chosen for this work.

Industrial cases like sunroofs, trunk door could be optimised for attachment points and could be correlated with the simplified geometry results.

This work involved optimisation with a specific number of attachments point in every model. An optimisation that could optimize for the number of attachment point could be done and the number of attachment point could be lowered.

A meta model could be created by training a response surface model with the designs available to make the optimisation faster. Different RSM algorithms could be used to create the meta models and compare them for accuracy.

The RD&T software found certain models such as the side door too big to handle and resulted in a longer time than expected for the results. An updated version of the software and a powerful machine would make the optimisation faster and more efficient.

A topometry optimisation to optimise the geometry of a component should be possible in RD&T. This work will be possible by making changes to the script that runs the RD&T simulation manually.

Bibliography

[1] M. Trapp and F. Chen, Automotive Buzz, Squeak and Rattle, Waltham, USA: Butterworth-Heinemann, 2012.

[2] R. Söderberg, L. Lindkvist and J. Carlson, "Virtual geometry assurance for effective product realization," in *1st Nordic Conference on Product Lifecycle Management - NordPLM'06*, Göteborg, 2006.

[3] K. Wärmefjord, R. Söderberg and L. Lindkvist , "Simulation of the effect of geometrical variation on assembly and holding forces," *Int. J. Product Development,* vol. 18, no. 1, pp. 88-108, 2013.

[4] K. Wärmefjord, R. S. Tabar and R. Söderberg, "A method for identification and sequence optimisation of geometry spot welds in a digital twin context," *Proceedings of the Institution of Mechanical Engineers, Part C: Journal of Mechanical Engineering Science,* vol. 233, no. 16, 2019.

[5] K. Wärmefjord, R. Söderberg and L. Lindkvist, "Strategies for Optimization of Spot Welding Sequence With Respect to Geometrical Variation in Sheet Metal Assemblies.," in *Proceedings of the ASME 2010 International Mechanical Engineering Congress and Exposition. Volume 3: Design and Manufacturing, Parts A and B.*, Vancouver, British Columbia, Canada, 2010.

[6] F. Alphonce and V. Wadenvik, "Possibility of Implementing Part Related Tolerances in Variation Simulation," Master Thesis, Chalmers University of Technology, Göteborg, 2015.

[7] J. Her, M. Lee, D. S.-R. Hsieh and P. Tsou, "Squeak and Rattle CAE Simulation Using FEA," in *Automotive Buzz, Squeak and Rattle*, Elsevier Ltd., 2012, pp. 179-201.

[8] F. Anselmet, "Identification of experimental resonance frequencies," in *Acoustics, aeroacoustics and vibrations*, NJ, Hoboken, NJ : John Wiley and Sons, Inc., 2016.

[9] N. Chaudhari, R. Mohammed and P. Raghavendran, "A Disciplined Approach to Minimize Rattle Issues in Automotive Glove Box Assembly," *SAE Technical Paper 2018-01-1481,* 2018.

[10] I. Benhayoun, F. Bonin, A. Milliet de Faverges and J. Masson, "Simulation and Optimization Driven Design Process for S&R Problematic - PSA Peugeot Citroën Application for Interior Assembly," *SAE Technical Paper 2017-01-1861,* 2017.

[11] *RD&T Technology, 2019. The Tool RD&T. RD&T Technology. Available at: http://rdnt.se/tool.html [Accessed February, 2020].*

[12] M. Bayani, L. Lindkvist, C. Wickman and R. Soderberg, “SQUEAK AND RATTLE PREVENTION BY GEOMETRIC VARIATION MANAGEMENT USING A TWO-STAGE EVOLUTIONARY OPTIMISATION APPROACH,” in *International Mechanical Engineering Congress and Exposition*, Portland, USA, 2020.

[13] *ESTECO modeFRONTIER User Guide, Ver 2017R4.*

[14] G. Cassio, *Optimization strategies - Volvo Tech Days (2019-05-22).*

[15] K. Deb, A. Bhattacharya, N. Chakraborti, P. Chakraborty, S. Das, J. Dutta, S. Gupta, A. Jain, V. Aggarwal, J. Branke, S. Louis and K. Tan, “Simulated Evolution and Learning,” in *8th International Conference, SEAL 2010*, Kanpur, India, 2010.

[16] S. Poles, E. Rigoni and T. Robic, “MOGA-II performance on noisy optimization problems,” in *Proc. Int. Conf. Bioinspired Optimization Methods Application (BIOMA '04)*, Ljubljana, Slovenia, 2004.

[17] D. Velmani Thanga Ratnam and S. Kulkarni, “Multidisciplinary Optimization of Geometric Variation and Modal Behaviour for Squeak and Rattle Prevention,” Master Thesis, Chalmers University of Technology, Gothenburg, Sweden, 2019.